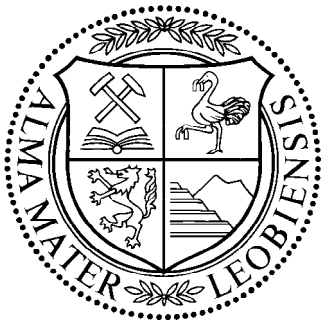

"Assessing the Influence of Commingled Production on the Performance of a Layered Reservoir"

A THESIS IN PARTIAL FULFILLMENT OF THE REQUIREMENTS FOR THE DEGREE OF

"MASTER OF SCIENCE"

SUBMITTED TO THE DEPARTMENT OF "NATURAL RESOURCES AND PETROLEUM ENGINEERING"

MONTANUNIVERSITÄT LEOBEN, AUSTRIA

Written by

Mohamed M. Gharsalla

Under supervision of

em.O.Univ.Prof. Dipl.-Ing. Dr.mont. Dr.h.c: Z. E. Heinemann

December 2009

Affidavit

I declare in lieu of oath that I did this work by myself using only literature cited at the end of this volume.

Mohamed M. Gharsalla

Leoben, December 2009


بِسْمِ اللَّهِ الرَّحْمَٰنِ الرَّحِيمِ
اقْرَأْ بِاسْمِ رَبِّكَ الَّذِي خَلَقَ ﴿١﴾ خَلَقَ الْإِنسَانَ مِنْ عَلَقٍ ﴿٢﴾ اقْرَأْ وَرَبُّكَ
الْأَكْرَمُ ﴿٣﴾ الَّذِي عَلَّمَ بِالْقَلَمِ ﴿٤﴾ عَلَّمَ الْإِنسَانَ مَا لَمْ يَعْلَمْ ﴿٥﴾

{ وَقُل رَّبِّ زِدْنِي عِلْمًا }

{ يَرْفَعِ اللَّهُ الَّذِينَ آمَنُوا مِنكُمْ وَالَّذِينَ أُوتُوا الْعِلْمَ دَرَجَاتٍ وَاللَّهُ بِمَا تَعْمَلُونَ خَبِيرٌ }

صدق الله العظيم

Dedication

Firstly, I truly thank my God for the guidance that led me over the right path to complete this effort. Secondly, I would like to dedicate this work to all members of my family for their help and assistance, especially to my wife who gives me great support and shares with me in both the sweet and difficult aspects of life.

Acknowledgments

I would like to express my deep gratitude to em.O. Univ. Prof. Dipl.-Ing. Dr.mont. Dr.h.c. Zoltán Heinemann for his support during my studies at Montanuniversität-Leoben and throughout the time I spent working on this thesis. He has made an enormous contribution to this study. Collaborating with him enabled me to gain a deeper understanding of reservoir engineering. Also I am grateful for the opportunity to attend some of his lectures.

I would also like to express my special appreciation to my friend, Dr. Andreas Harrer, for his endless and valuable help and advice during this thesis work.

I thank the Zueitina Oil Company for permission to use data from the Hakim field in my thesis work.

This project would not be completed without the support and backing of the staff of Heinemann Oil, especially my dear friend, Dr. Gabor Heinemann, CEO of the company.

Additionally, I would like to thank all members of the Petroleum Engineering Department at the Montanuniversität for providing a perfect environment that allowed me to accomplish my study and research.

Last but not the least, I would like to declare my special thanks and appreciation to my parents, wife, sisters, brothers and other family members whose moral support was very dear to me.

Kurzfassung

Einfluß der gekoppelten Förderung auf der Leistung getrennten Lagerstätten

Assessing the Influence of Commingled Production on the Performance of a Layered Reservoir"

MS Thesis

MONTANUNIVERSITÄT LEOBEN, AUSTRIA

von

Mohamed M. Gharsalla

In geschichteten Lagerstätten mit hydrodynamisch separierten, vertikal übereinander geordneten Lagerstättenteilen ist es wünschenswert, sowohl Produktion als auch Injektion für die einzelnen Zonen separat zu planen, um die Förderung aus jeder Zone zu optimieren. Dennoch werden vertikale Sonden, die alle Schichten durchteufen und aus allen Schichten gemischt produzieren, zur Förderung herangezogen, um Entwicklungskosten zu minimieren, vor allem wenn einige der einzelnen Schichten sehr dünn sind. Die heutigen Komplettierungstechnologien, z.B. die Verwendung von Zuflusskontrollventilen, ermöglichen es, die Produktion aus den einzelnen Zonen individuell zu planen und folglich zu optimieren.

Diese Diplomarbeit bewertet die Vorteile einer für jede separierte Lagerstätteneinheit optimierten Produktion und Injektion im Vergleich zur einfachen, gemischten Förderung für diesen Lagerstättentyp.

Die allgemeinen Ergebnisse wurden am Hakim Feld in Libyen angewendet.

Das Hakim Feld wird von der Zuetina Oil Company betrieben. Es befindet sich im südwestlichen Sirte Becken in der Konzession NC74A. Der Förderhorizont in diesem Feld ist der Facha Member der Gir Formation, der vorwiegend aus einer Dolomit/Kalkstein Sequenz besteht. Basierend auf den petrophysikalischen Eigenschaften wurde die Lagerstätte in 12 Schichten unterteilt. Diese Schichten weisen erstaunliche Unterschiede in Mächtigkeit, Porosität und Permeabilität auf. Zwei der Schichten werden als Zonen ohne Lagerstättenqualität klassifiziert und teilen die Lagerstätte in 3 individuelle Lagerstättenzonen. Seit Förderbeginn im Jahr 1985 wird das Feld sowohl mit gemischter Förderung als auch Wassereinpressung betrieben. Moderne Lagerstättensimulations-Software wurde verwendet, um die Vorteile von optimierter Produktion und Injektion jeder einzelnen Lagerstättenzone im Vergleich zur aktuell durchgeführten einfachen gemischten Förderung der einzelnen Zonen zu untersuchen.

Abstract

Assessing the Influence of Commingled Production on the Performance of a Layered Reservoir"

MS Thesis

MONTANUNIVERSITÄT LEOBEN, AUSTRIA

Mohamed M. Gharsalla

In layered reservoirs with hydrodynamically separated, vertically stacked reservoir units, it is desirable in order to optimize recovery to design both, production and injection for each unit separately. Especially if some units are relatively thin, vertical wells penetrating all units, producing commingled are used in order to minimize development costs. Today's smart completion technologies, including inflow control valves, provide means to design and hence optimize production from individual zones.

This master thesis assesses the benefits of production and injection methods customized for each separated reservoir unit for such a reservoir as compared with simple commingled production.

The general findings were applied to the Libyan Hakim field located in the Southwest Sirte Basin in the Concession NC74A. This field is operated by Zueitina Oil Company, and the productive horizon is a dolomite/limestone sequence classified as the Facha Member of the Gir formation. Based on remarkable variations in thickness, porosity, permeability and other characteristics, this reservoir has been divided into 12 layers. Two of these are not considered part of the reservoir, hydrodynamically separating it into three separate zones. Since the start of continuous production in 1985, the field is operated by both commingled production as well as water injection.

State of the art reservoir simulation software was used to investigate the benefits of optimized production and injection for each reservoir unit as compared with the current commingled production.

Table of Contents

List of Figures

List of Tables

Chapter 1

1 Introduction

1.1 Motivation of the work

The ambition of the candidate was to combine his personal professional development with the interests of his company and the interest of the Petroleum Industry of his home country. Manny oil fields in Libya have complicated geological structure, with numerous pools separated partly or completely by non-reservoir formations or impermeable interbeddings. Some of theses pools are small, containing OOIP in the magnitude of some tens of million STB only, and therefore can not be developed with independent well patterns. These pools must be produced commingled; conventionally by opening the layers in the wells without separation or using intelligent well technology. Numerous publications exist presenting the advantage of different intelligent well technologies but none of these techniques found application within the candidate's company so far. The reason of that is manifold, but the main burden is that no feasibility studies were made under real Libyan conditions. The candidate believed that the best way to persuade the Libyan industry about the advantage of the intelligent well technology is to conduct an investigation for a field which already was operated in conventional way and to show which would be the advantages by using intelligent well technology under realistic conditions. The author has chosen the Hakim field as target of his examination, considering also that OMV is one of the owners of the asset, taking benefit from the author efforts, too.

1.2 Scope of work

The fundamental decision was to conduct the investigation as a case study. The author believed that a general appraisal using artificial models will not be enough. All field cases are different so general statements are no suitable basis for operative decisions. A careful individual investigation must be conducted in all field cases, considering all specific circumstances. Therefore a case study, giving also an example how the investigation should be performed, can give more help to future applications.

The scope of work was two folds. At first a realistic dynamic reservoir model had to be build. This includes the careful examination of the static geological model, the production history, gathering and quality check all PVT and SCAL data and then conducting a history match. Without a verified simulation model it would not be possible to satisfactorily show the advantages of intelligent well technology. If a dynamic reservoir model fails to reproduce the conventional production process, any modeling of improved technology and calculated possible improvement of the production can not be seen to be reliable. Secondly the author tries to design a general applicable workflow for future field investigations.

1.3 Outline of the work

Chapter 2 gives a short overview about the today technology of intelligent well completion and discusses the advantages in a general approach.

Chapter 3 is devoted to the description of the Hakim field, starting with the regional geology and ending up in the volumetric estimation of the OOIP. This chapter is a summary from older studies, where the author eliminates some contradictions.

Chapter 4 describes the dynamic simulation model which was build and history matched by the author parallel but independently from ongoing company internal works.

Chapter 5 presents the investigations regarding the possible advantages of intelligent well technologies.

Chapter 6 provides a short summary about the whole workflow and gives conclusions and recommendations

In **Chapter 7,** a list of symbols and abbreviations used in this research are provided.

Chapter 8 provides the list of references to the literature used for this thesis work.

Chapter 2

2 Intelligent Well Completion Techniques for Multi-Pool Reservoirs

Intelligent well completions are focused on the delivery and management of increased production flexibility,

Intelligent Well systems Technology (IWsT) delivers the ability to install, operate, monitor and control completions without the need for conventional interventions.

Commingled production is the simultaneous production of hydrocarbons from multiple reservoirs or pools through a single production conduit in the well bore.

2.1 A Technical Challenge

Oil and gas producers and service companies have long been committed to recovering more hydrocarbons from fewer wells. This presents a significant challenge and most in our industry will agree that innovative application of technology is key to addressing it. Today, however, the challenge is even more daunting: to produce more complex hydrocarbon resources economically while continuing to increase ultimate recovery. In the past, a well's longevity could be prolonged by plugging it back and recompleting it in a shallower pay zone, continuing until all zones had watered out and the well was abandoned. However, engineers realized that in spite of their best attempts, recovery factors averaged only 30%, and often their response was to drill more wells. Engineers sought new ways to improve recovery while drilling fewer wells using geophysical and reservoir information to guide well placement.

More accurate, higher-resolution data reduce interpretation ambiguities and decision-making risks, and advances in drilling technology allowed wells to be steered into the most prolific portions of the reservoir. Most significantly, the shift from analog to digital data recording enabled integration of information from separate sources. This integration improved knowledge and allowed full field simulation, which in turn resulted in better reservoir understanding and more efficient field development plans.

Over time, several techniques have been employed to maximize early production and optimize financial returns. However, in the current environment, production rates alone do not define a good project. Economically improving recovery is perceived as more difficult to achieve than just increasing production. Recovery is highly dependent on completion technology and reservoir management. Completion technology and reservoir management are more likely to succeed when applied on a field-wide basis, and they both require substantial upfront engineering and investment. Despite the technical challenges, increasing recovery economically is essential to bringing the industry to a new level of success.

2.2 Intelligent Well Completions

As we encounter more complex reservoirs, that require multiple-zone completions, it is critical to have the capability to modify the downhole completion as production parameters change over the life of the well. The types of completions that can be modified to improve recovery are intelligent completion combinations of downhole sensors and actuators, plus the software and systems integration to monitor and control individual sections of a well remotely.

“An intelligent well is a well with the ability to control the production flow by a down-hole choke. This is managed through real time monitoring and control of the producing zones using installed Inflow Control Valves (ICV) and an optimized sensor distribution for data acquisition and down-hole fluid production measurement. It also has the ability to shut off a water/gas producing zone at the wellbore. It produces single or multiple zones into one wellbore, leading to commingled production from different zones and lateral bores.”[19]

Intelligent completions are focused on the delivery and management of increased production flexibility. Advances in drilling technology now allow several reservoirs to be intersected by one wellbore and well designs routinely include several laterals to achieve maximum reservoir contact.

Intelligent Well systems Technology (IWsT) delivers the ability to install, operate, monitor and control completions without the need for conventional interventions. Multi-zone intelligent-well completions contain appropriate monitoring devices located between zonal isolation packers; Figure 2-1 illustrate the conventional wells compared to intelligent well completion.

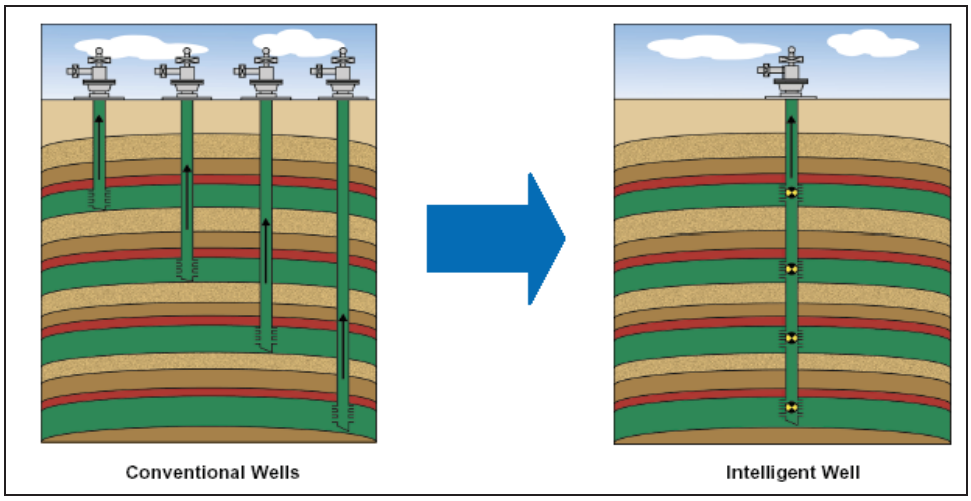

Figure 2-1: Sketch of Conventional and Intelligent Completion (Baker Hughes[10])

Intelligent completions have proven to be an efficient reservoir management tool, with rapid deployment in various reservoir environments. Criteria have been established for the use of inflow control valves (ICVs) and different downhole sensors.

At the heart of intelligent wells are surface–actuated downhole valves, used to regulate flow from individual zones or laterals, and permanent downhole temperature and pressure sensors. Today, downhole control valves range from those with simple on-off controls to hydraulically actuated and electrically controlled infinitely variable-setting chokes. These innovations permit engineers to design valves that can be remotely adjusted within a range of cross -sectional flow areas matched to a zone's production profile.

While the initial objective of using intelligent well technology to extend well life was effective, this was not the most efficient use of the technology. Instead, the technology's true promise, the industry has come to understand, is best realized when intelligent wells are used as a tool for maximizing recovery. This change in intelligent well objective from intervention avoidance to reservoir management has been greatly enhanced by the emergence of robust downhole permanent pressure and temperature sensors capable of functioning in harsh environments for extended periods of time.

Data from these intelligent completions are also used to continually enhance and update production models and simulations, perform and interpret production tests on individual zones and laterals, predict sand and water encroachment, and measure flow rate and water cut. Figure 2-2 illustrates a three-zone intelligent well.

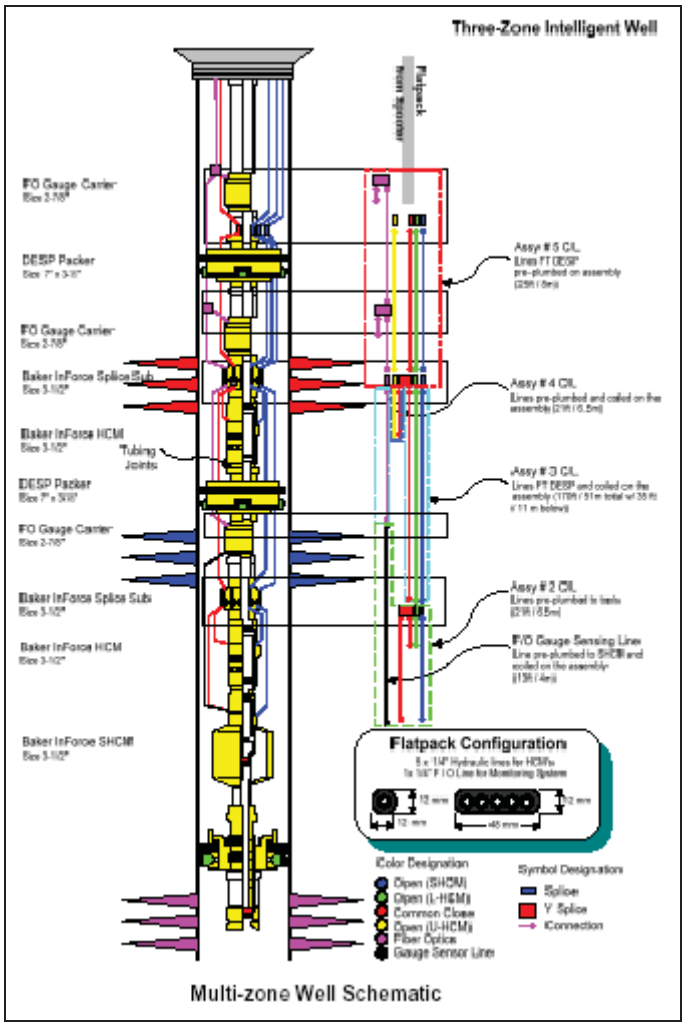

Figure 2-2: Example of an Intelligent Well penetrating three Zones (Baker Hughes[10])

The advantages of reservoir monitoring and control for reservoir management aspects are obvious. For example, since wells seldom cross only a single hydrocarbon-bearing zone, completion engineers are often forced to decide between commingling production from multiple zones or producing each zone sequentially. Historically, producing more than one zone at a time has been an option only if the zones are of compatible pressure and fluid composition, and no regulatory concerns exist. Two, three, and sometimes four perforated intervals also can be produced at the same time through completions in which each zone is mechanically isolated from the others and flowed to the surface through separate production strings.

Sequential production typically requires flowing one zone to its economic limit before plugging and abandoning it in order to move up the hole to complete the next zone.

This cycle is then repeated until all zones have been depleted. In almost all cases, this strategy leaves behind considerable reserves and results in poor production profiles because of extended periods of depletion within each zone.

In contrast, using intelligent completions in a sequential production scheme, which involves opening and closing each zone remotely from the surface, improves production by eliminating both intervention costs and poor production profiles. Variable setting valves can also be used to eliminate sequential production in favour of commingling by managing flow from high-pressure zones to prevent cross flow.

While intelligent completions can be effective in layered reservoirs, for obvious reasons they are decidedly more efficient when the shale zone separating the sands is continuous and the seal impermeable. Therefore, within the same layered reservoir, some wells crossing reliably sealed layers are well-served by intelligent completions.

One set of mathematical models developed for candidate screening uses reservoir simulation and well simulation techniques to generate a comparative model of the benefits of intelligent completions. Scenarios are created to generate variance in reservoir performance affecting the timing of events requiring intervention, reservoir monitoring, or reservoir management and are often driven by geological uncertainty and reservoir heterogeneity.

In heterogeneous channel reservoirs, the benefits of intelligent completions depend on well performance, which in turn, depends on well placement with respect to the permeability of the formation and connectivity of the channels. This is because the effectiveness of flow control valves depends on choking, which is a function of high deliverability. By their nature, however, the majority of heterogeneous reservoirs benefit from intelligent completions since their varying permeabilities and porosities tend to create just the kind of fluid front that variable -setting valves can best exploit.

2.2.1 Commingled Production

Commingled production from two or more productive horizons is the ideal method to accelerate production from a single well. Furthermore, marginal reservoirs, which are destined to be uneconomic with dedicated production, could become viable for production.

The application of intelligent completions for such commingled wells improves not only the production and recovery optimization for each individual reservoir, but also maximizes the value of the well.

One of the parameters that has to be known is the contribution from each completion to the well production. Any optimization technique has to base its calculations on the contribution and tries to improve the objective function. This function may be to maximize oil recovery, for example.

2.2.2 Benefits from Intelligent Well Technology

A series of generic reservoir types have been built based on property distributions derived from field data. They were tested to determine the added value from Intelligent Well system Techniques (IWsT) compared to standard well completions. Situations in which Intelligent Well system Techniques proved particularly successful have been identified. Results show that Intelligent Well system Techniques can control uneven, invading fluid-fronts that develop along the length of the well bore due to permeability differences, reservoir compartmentalization or different strength aquifer/gas cap supports.

Recovery improves and water production is reduced with the correct choice of ICVs (Down-hole Interval Control Valves) for the number, positions and lengths of zones being controlled. However, the degree of improvement is dependent on reservoir type and differs from one reservoir model to another. Intelligent Completions, by commingling stacked pay, manages the (possibly tilted) oil rims with different thickness in multiple fault blocks from a single well bore. Figure 2-3 and Figure 2-4 illustrate the commingled production from separate sands using an intelligent well.

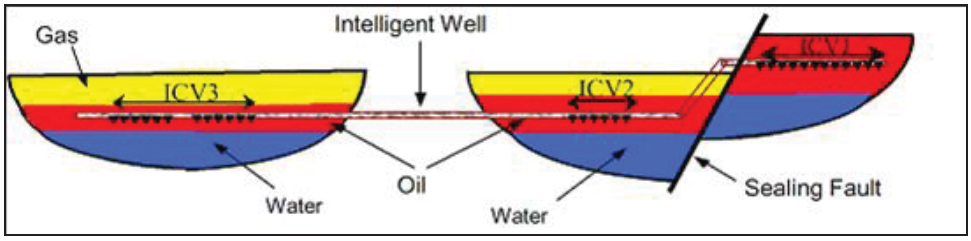

Figure 2-3: Commingled production from several sands (Farhad Ebadi et al[19])

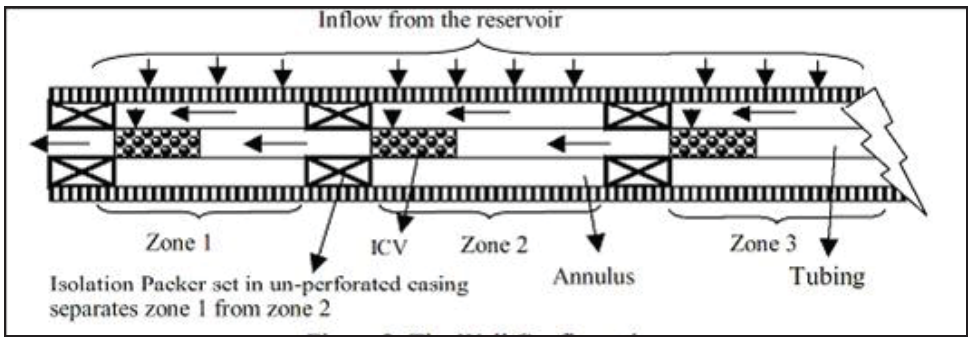

Figure 2-4: Completion sketch for commingled production (Farhad Ebadi et al[19])

Intelligent completion techniques are gaining popularity because of their reservoir monitoring and well / field performance management capabilities while minimizing the requirement for well interventions. Intelligent Well system Techniques can decrease the risk and uncertainty associated with the production of complicated reservoirs.

Reservoir management objectives include increasing production and reserves, maximizing recovery, and minimizing capital and operating costs while reducing risk. It involves taking decisions and predicting their future consequences; hence the need to model the reservoir's future behaviour. This requires skills in reservoir characterization, reservoir performance, well performance and field development.

A key issue in the reservoir management process is geological uncertainty. Intelligent Well system Techniques, operating at or near real-time, enables high quality, well surveillance, interpretation and reaction in a continuous feedback loop. The ultimate goal for this continuous monitoring of the reservoir is to implement a more proactive style of reservoir management technique.

Identifying the type of reservoir where the Intelligent Well system Techniques can be applied is an important step in evaluating its application. Knowing where to apply this technology begins with reservoir characterization- a crucial stage in reservoir management.

The artificial lift system is also part of the control devices. For example, the production rate can be reduced to avoid coning and to establish production below the critical rates at the first signs of breakthrough.

Finally Intelligent Well system Technique has been shown to be capable of managing geological variability and thus coping with geological uncertainty in a wide range of reservoirs. It can also control uneven invading fluid-fronts that develop along the length of the wellbore because of permeability differences, reservoir compartmentalization or different strengths of aquifer/gas cap support.

The following figures give a clearer view of commingled completion.

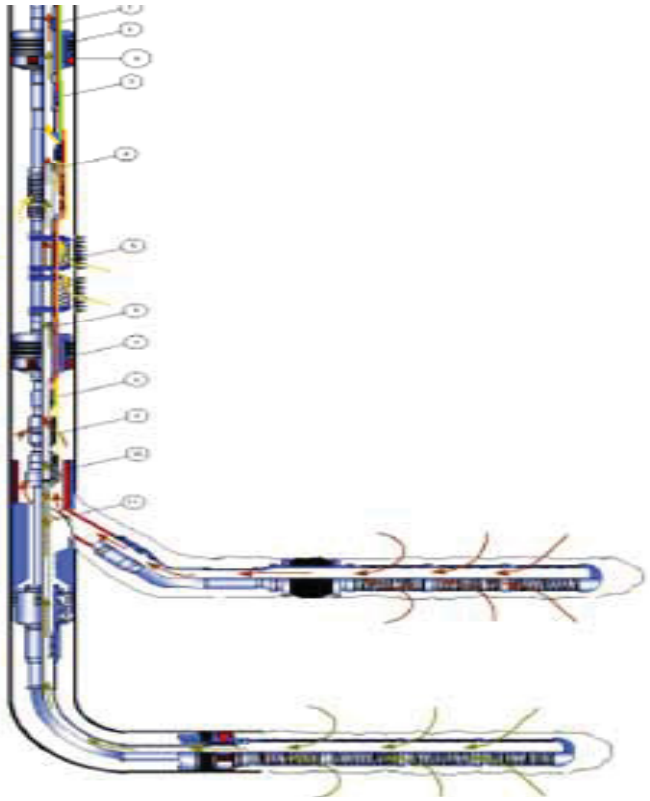

Figure 2-5: Multilateral Flow Control (Timo Jokela[34])

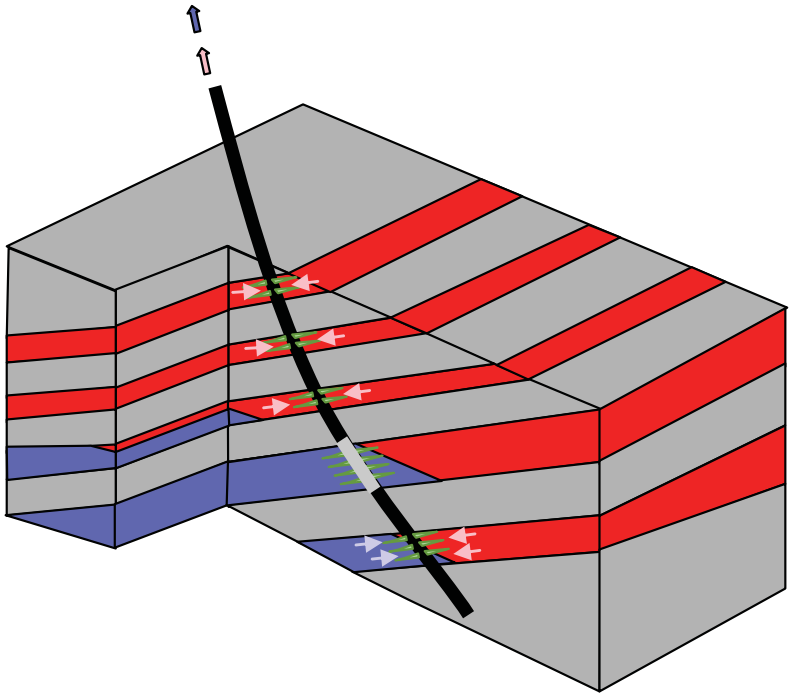

Figure 2-6: Intelligent Well Technology adds value by Accelerating Production via Controlled Commingling of Stacked Pay. (Carlos Glandt[15])

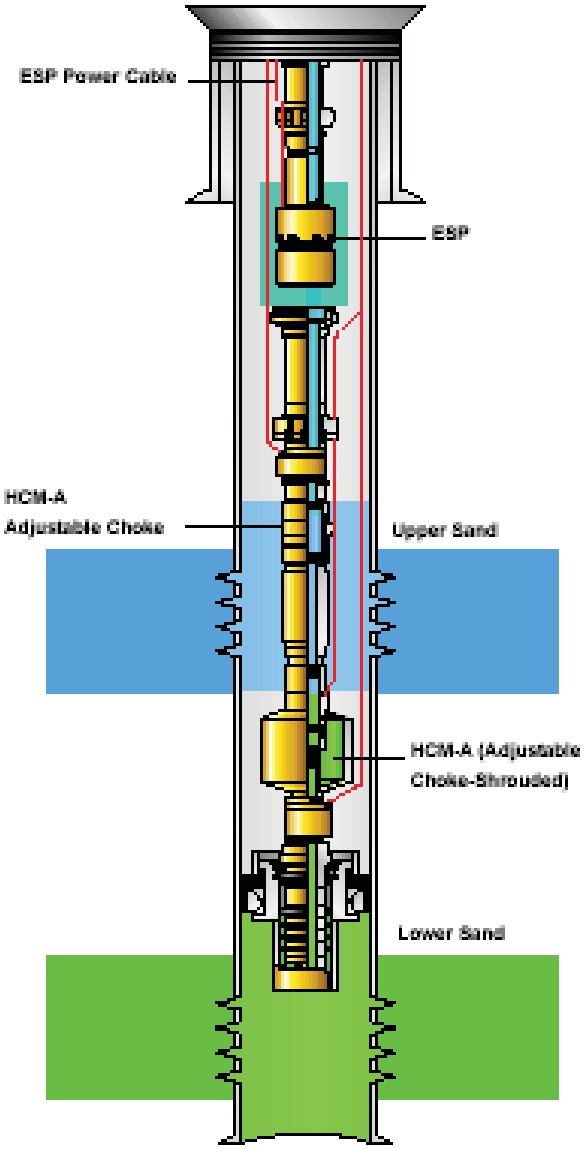

Figure 2-7: intelligent completion with commingled production from two zones with adjustable chokes and artificial lift provided by electric submersible pump.(Dr. Guy Vachon[18])

Chapter 3

3 Description of the Hakim Field

3.1 Historical Background

This chapter discusses the geological setting and petroleum history of the area of interest where the Hakim oil field that is author's study subject is located

3.1.1 Regional Geological of Libya

Libya occupies an area of some 1.8 million sq. kms with a 1800 km shoreline along the southern margin of the Mediterranean Sea. The country is the repository of some 50 billion barrels of in place oil reserves entrapped in Paleozoic, Mesozoic and Tertiary sediments. Structurally Libya is part of the Mediterranean foreland formed by the North African shield, and has a sedimentary section that has been subjected to transgressions and regressions since the early Paleozoic. There are five major sedimentary basins which are; the Sirt Basin, Murzaq Basin, Kufra Basin, Ghadamis Basin and Tripolitania Basin of which the most important is Sirte Basin, Figure 3-1 presents the location of major Sedimentary Basins of Libya. The evolution of sedimentary basins of Libya was controlled by tectonic movement that included:

- A compressional early Paleozoic Pan-African event
- The Hercynian Orogeny
- Extension related to Cretaceous, middle Tertiary and Holocene events starting with the southern Tethys and evolving into the Meditterranean

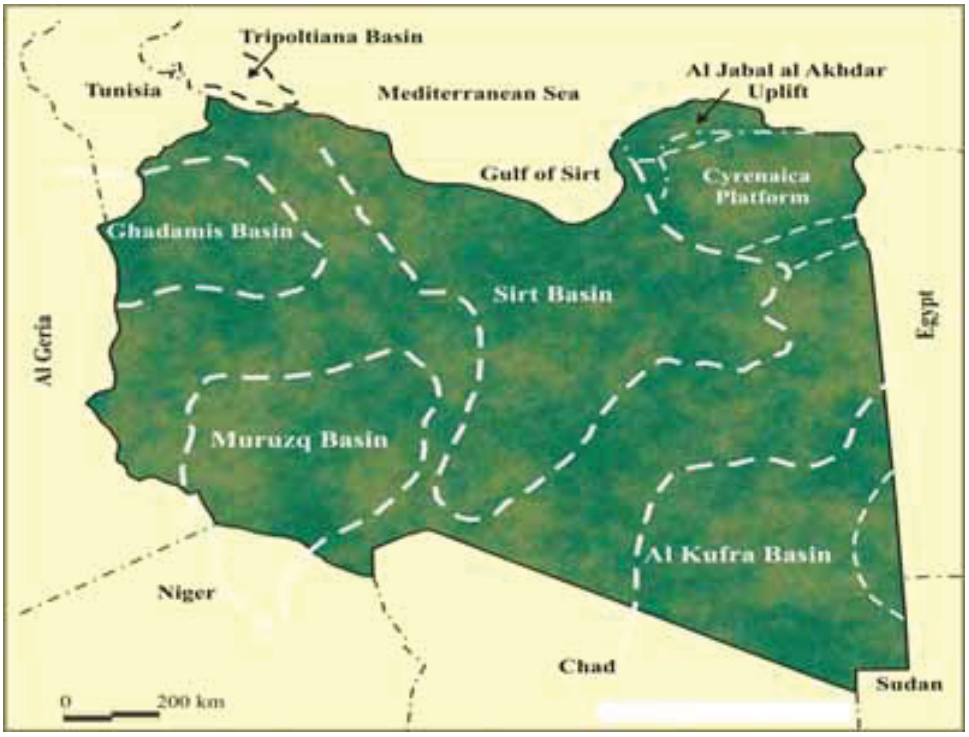

Figure 3-1 Location of major Sedimentary Basins of Libya (Hassan S. Hassan[26])

3.1.2 Geological History of Sirte Basin

The Sirt basin, is the youngest of the Libyan basins. It has the largest petroleum reserves in Libya and is ranked 13th among the world's petroleum basins Which contains some sixteen giant oil fields and considered to be the most prolific oil basin in north Africa.. The basin's recoverable reserves are about 45 billion barrels of oil and 33 trillion cubic feet of gas. Generally the origin of the Sirt Basin is attributed to the collapse of the Sirt Arch during latest Jurassic to Early Cretaceous times. In the Early Paleozoic the basin was the site of siliciclastic deposition, and clastics accumulated all over North Africa. In the Cretaceous and Tertiary, large quantities of organic-rich shales and other terrigenous clastic materials accumulated in the basinal area.

The two principal source rocks in the Sirt Province are the Upper Cretaceous Rachmat Shale and Sirt Shale. Hydrocarbon distribution of the Sirt Basin has been controlled by the major tectonic elements. This is particularly true of reservoirs related to Cretaceous and Eocene to Miocene rift structures, Figure 3-2 presents

the East-West cross section of sirte Basin. These reservoirs in Sirt Basin are composed of 58% of clastic, mostly is of Mesozoic age and 42% of carbonate rocks mostly of Tertiary age.

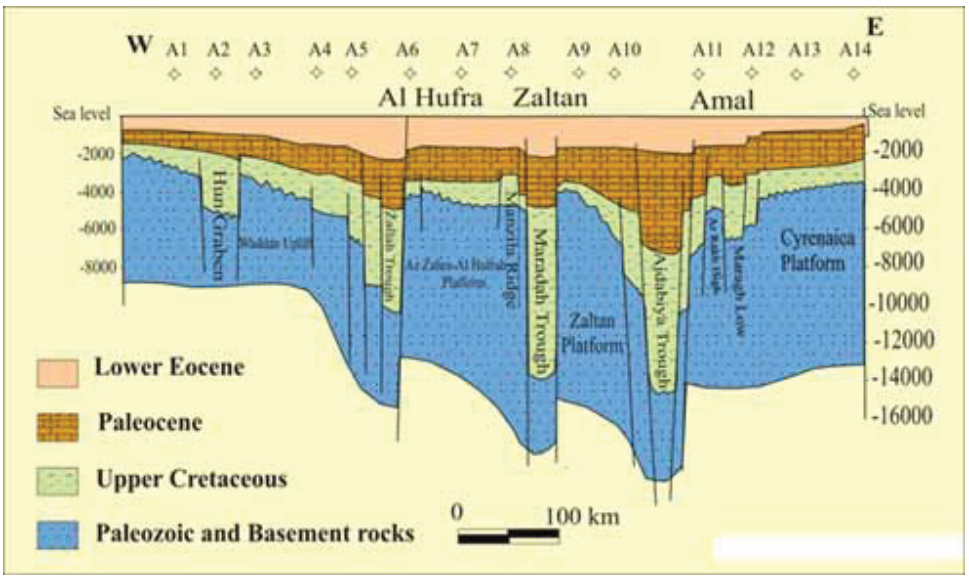

Figure 3-2 East-West cross section of sirte Basin (Roohi M.[31])

Generalized stratigraphic correlation chart of the Sirt Basin study areas: south Ajdabiya trough, Maradah graben, and south Zallah trough–Tumayam trough. The main reservoir and source intervals are indicated on the chart below, Figure 3-3.

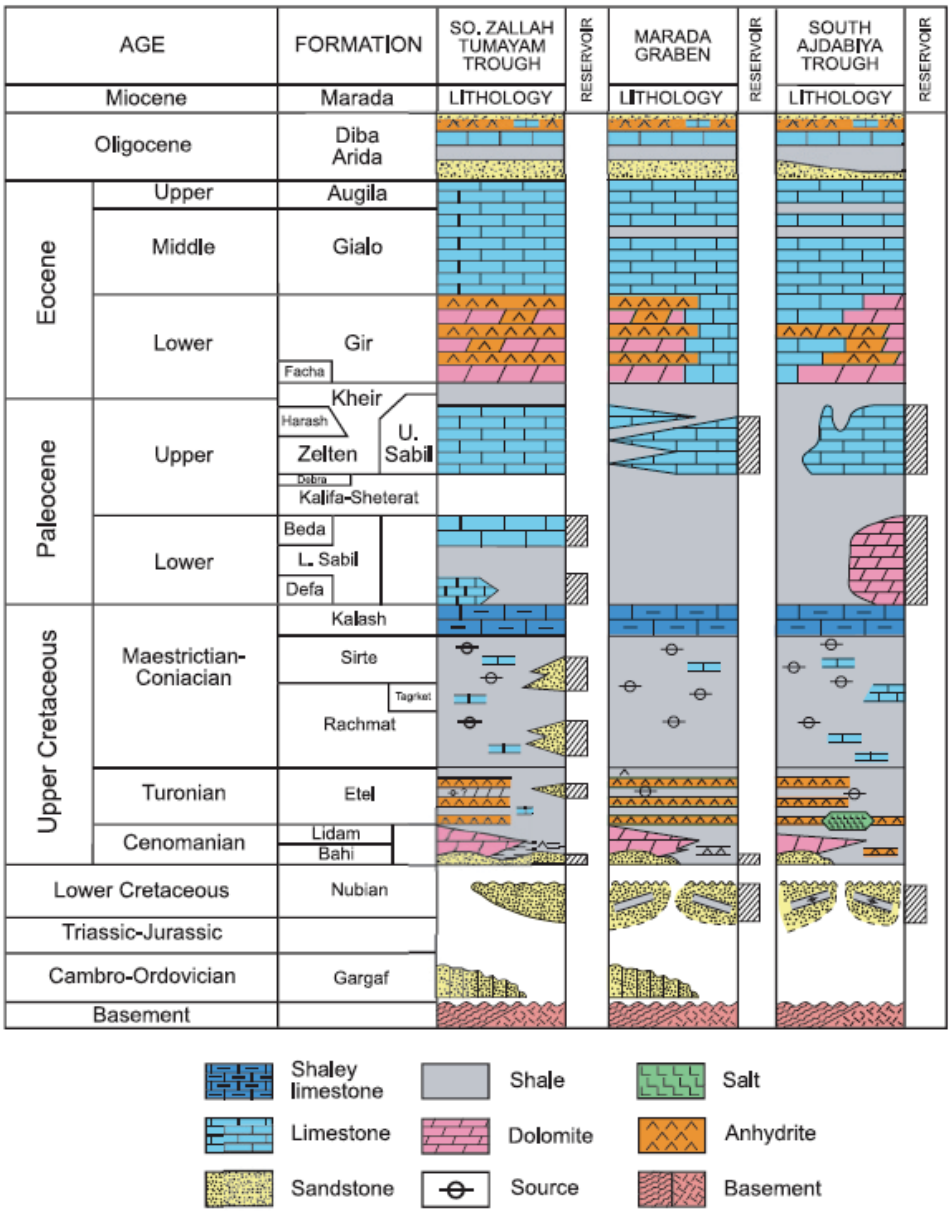

Figure 3-3 Stratigraphic Column (Rusk, D. C.[32])

3.1.3 Petroleum Exploration History of Libya

Active exploration in Libya started in 1953. The first well was drilled in 1956 in western Fezzan, and the first oil was struck in 1957. In September 1961 production started, and by 1965, Libya was the world's sixth-largest exporter of oil. By the end of 1969, Libya's production reached 15.4% of OPEC's total and 7.5% of the world's total. In 1969 a major oil field was discovered at Sarir, which is well to the southeast of the Sirt Basin fields. Minor fields were discovered located in northwestern Tripolitania. New discovereis were drilled in the Ghadamis sedimentary basin (400 kilometers southwest of Tripoli) in 1974 and in the offshore fields 30 kilometers northwest of Tripoli in 1977.

In 2007, the Sirte Basin Province contains approximately 80% of Libya's total proven oil reserves (41.5 billion barrels as of January 2007) and accounted for roughly 90% of the country's total oil output, which was 1.80 million bpd in 2006. Over twenty-three large oil fields and sixteen giant oil fields occur in the province. Libya's onshore oil has historically been discovered mainly within the confines of three major geological trends occurring in the Sirte Basin.

3.2 Introduction of Hakim Oil Field

The Hakim field is located in the southwest Sirte Basin, approximately 580km South-East of Tripoli, Figure 3-4 presents the location of Hakim field. It was discovered in 1978 and is located in the Concession NC74A. The field is divided into two sectors by faults, north and south Hakim. To date, a total of 21 wells have been drilled in Hakim, 18 of them are located in the South, 3 in North Hakim. Currently, there are 2 producers and 1 injector in North Hakim, and 11 producers, 4 injectors, 2 abandoned wells and 1 cathodic protection well in South Hakim. Two wells, A20 and A21 have been drilled only recently and made significant changes to the structure map of the field.

The reservoir fluids for North and South Hakim differ substantially. The formation volume factor for the south is 1.265 RB/STB, for the north it is 2.24 RB/STB. The

GOR for the south is 274 SCF/STB compared to 1719 SCF/STB for the North.

Oil production commenced in 1985 in the form of Long Term Testing, continuous production started in mid 1987, at the same time water injection was initiated. The cumulative oil production in July 2007 was 24.6 MMSTB, the oil rate was 2500 STB/day and the water cut was 75%.

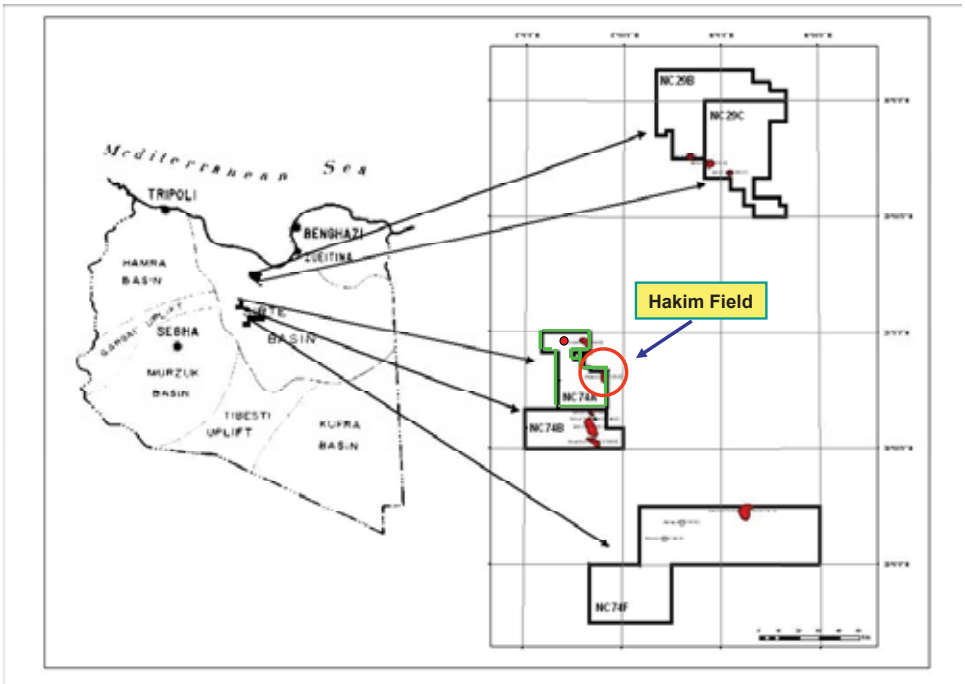

Figure 3-4: Location of Hakim field (Zueitina Oil Company[38])

3.3 Static Model of the Hakim Field

The static model was built by experts of consulting oil company and the author was part of the team who built this model, represented Zueitina Oil Company to following up and contributed in this study of Hakim field and to achieve an adequate static model which can be used it to build a reliable simulation model. .

3.3.1 Faults and Structural Segments

Faults in Hakim Field divide the field into three main structural sections, the North

Hakim pool, the South Hakim pool and an intervening graben. The North Hakim pool is bounded to the southwest by a linear, northwest trending steeply dipping extensional fault with a displacement of approximately 500 meters. The footwall of this major extensional fault forms the structural trap for the North Hakim pool, whose seal towards the south is provided by this fault and which is dip closed towards the north.

The fault bounding the North Hakim pool is the northeastern boundary of a graben that is approximately 1200 meters wide and contains only minor hydrocarbon volumes. The graben is confined to the southwest by another major extensional fault, which splits into two segments which apparently are not connected. Towards the southwest, the Hakim South pool is bounded by another major normal fault with a displacement of up to 700 ft, which traverses the field approximately 200 meters southwest of A20. The structural configuration of these three main fault blocks is shown in Figure 3-5.

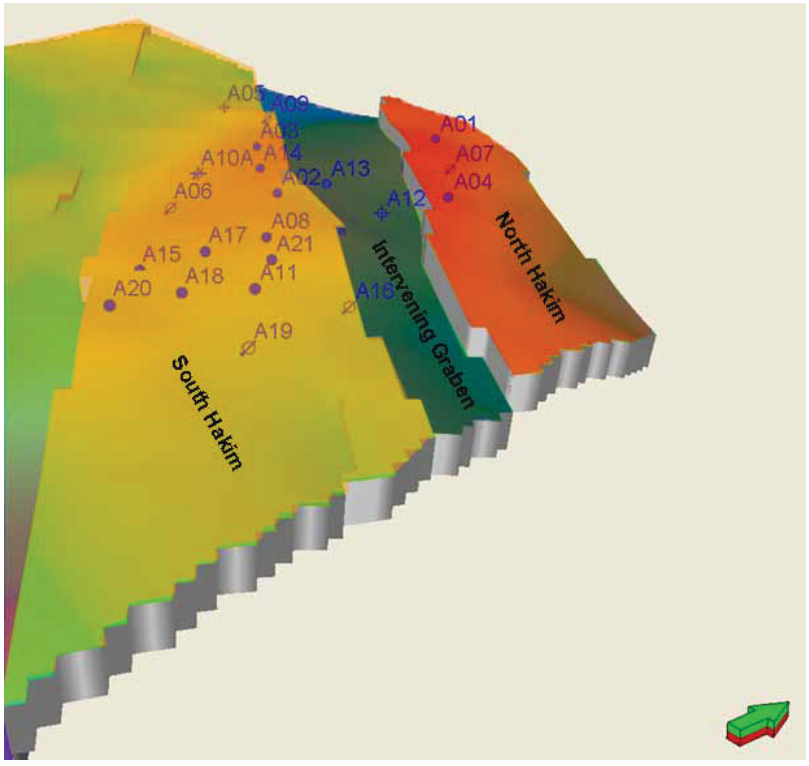

Figure 3-5: Main structural segments in the Hakim Field. North Hakim pool is shaded red, intervening graben is shaded blue and South Hakim pool is shaded orange[24]

3.3.2 Reservoir Zonation

Establishing a reservoir zonation for the Hakim Field is relatively uncomplicated, as the Facha member was deposited in a shallow marine or inner shelf environment, resulting in very good lateral continuity of log signatures within the well field. The main challenge to well correlation is the degree of dolomitization, which varies spatially and results in slightly different log responses.

The Facha Member was divided into six zones named Facha A (top) to Facha F (bottom), which were sub-divided into a different number of subzones. The Facha F is the oldest reservoir unit of the Facha Member and conformably overlies the Kheir Formation. The basal limestone facies has been preserved in most of the South Hakim pool. Towards the northeast, there is a trend of stronger dolomitization.

The top of the Facha F as interpreted from logs is the top of a layer approximately three feet thick with no porosity and permeability. The Facha F was divided into five subzones called Facha F1 (top) to Facha F5 (bottom). A well correlation panel showing the subdivision of the Facha F is shown in Figure 3-6.

Reservoir quality in Facha F is generally poor. Facha F3 to Facha F5 are generally tight, except for thin layers which locally have porosity and permeability. Porosity increases towards the top of the zone; porosities in the Facha F1 and Facha F2 vary laterally, but on average is around 10%. Permeability is poor throughout the entire Facha F and on average less than 1 mD.

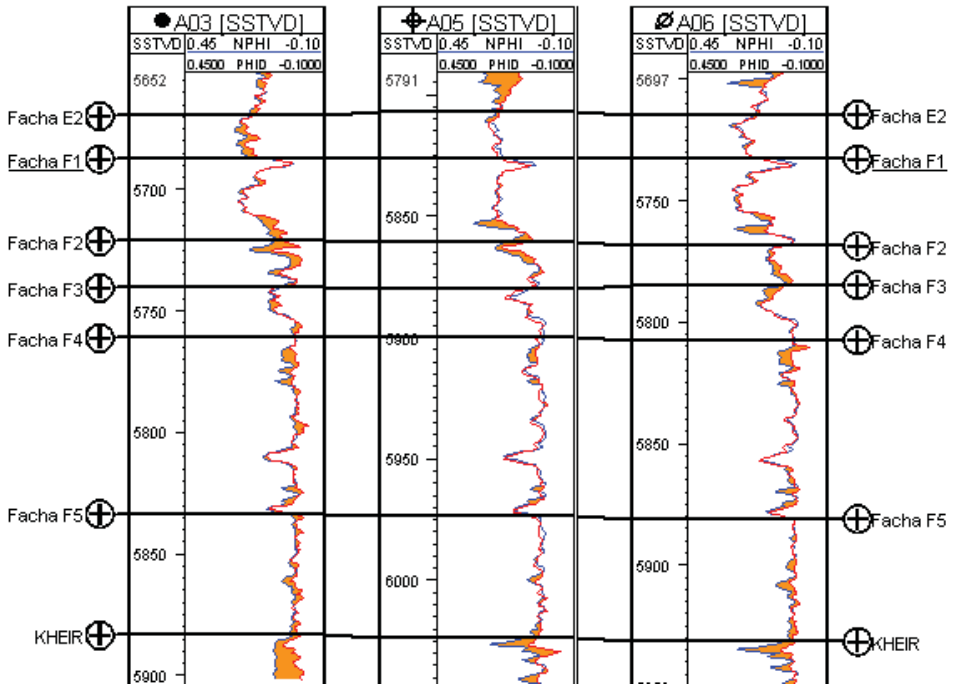

Figure 3-6: Well correlation panel showing the subdivision of the Facha F into subzones F1 to F5[24]

Facha F is conformably overlain by Facha E, a transition zone from the basal limestone facies to the dolomitic facies near the top of the reservoir section. This is reflected in the core descriptions where the Facha E has been divided into two subzones. Facha E1 on top and Facha E2 at the bottom. The contact between zones E1 and E2 in the South Hakim Pool is the contact between the basal limestone facies and the transition zone to the dolomitic facies on top.

In the South Hakim Pool, the rock matrix in Facha E2 is almost pure limestone, whereas in the Facha E1, the proportion of limestone is only between 60 to 70%. The average porosity in the Facha E is moderate, about porosity of 16% and the average permeability is 4 mD. Facha E is overlain by Facha D, a tight layer with an average thickness of 13 ft.

Facha C is the best reservoir unit in the Hakim Field and has been almost entirely dolomitized. It consists of locally argillaceous dolomite packstone, wackstone and grainstone, divided into five subunits.

Facha A and Facha B each consist of a thinly developed dolomite layer on top of a laterally persistent anhydrite zone. The dolomites of the Facha A and Facha B are therefore not in communication with the reservoir units below them.

3.3.3 Construction of the 3–D Structural Model

The project boundary is a polygon having a width of approximately 10 km in the east-west direction and a length of 9 km in the north-south direction, encompassing an area of about 90 km^2. A map of well locations in the Hakim Field and the extent of the project area is shown in Figure 3-7.

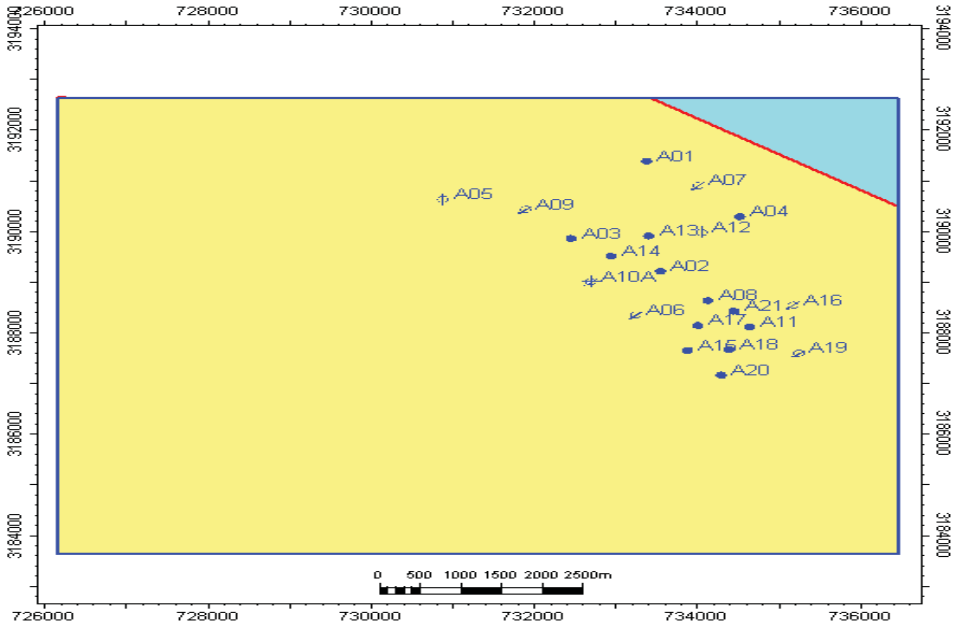

Figure 3-7: Extent of the project area (blue polygon) compared to area covered by 3–D seismic survey (red polygon) [24]

3.3.3.1 Fault Modeling

Fault modeling is the process of constructing a representative fault model based on interpretations from a seismic survey. Faults interpreted in the Hakim Field are steeply dipping normal faults. Because the thickness of the Facha Member is limited, the lateral component of the fault planes within the reservoir is small and varies between 10 to 30 meters.

Figure 3-8 shows the fault model for the Hakim Field. To illustrate that the modeled faults are at the correct locations, a coherency attribute is shown on the top of the Fach surface.

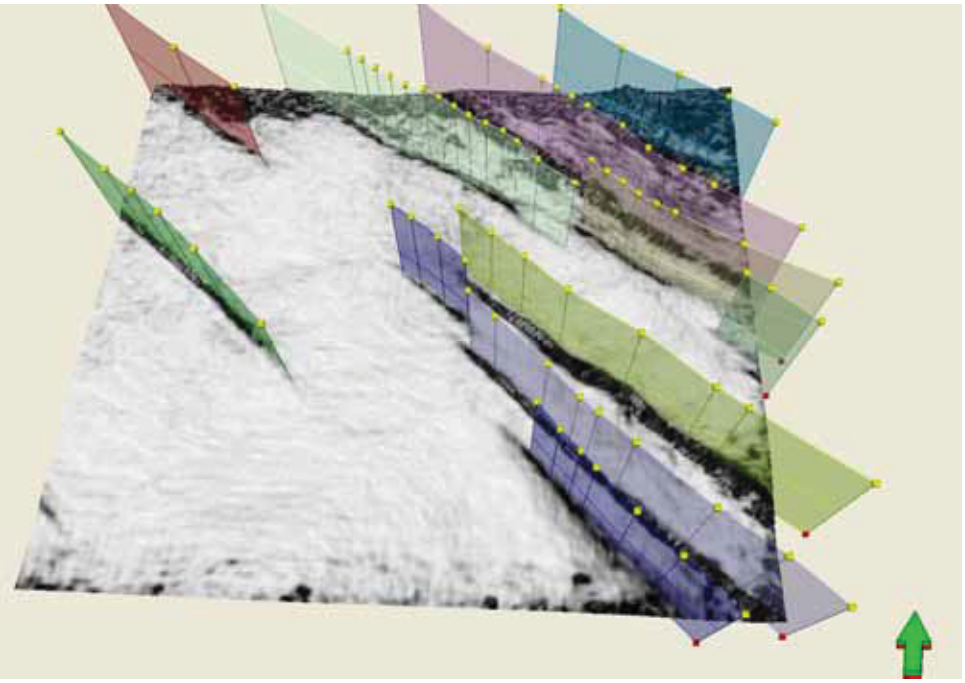

Figure 3-8: Fault model of the Hakim Field. Surface shows the coherency attribute on the depth-converted top Facha surface[24]

3.3.3.2 Grid Generation

The selection of appropriate grid parameters is governed mainly by the requirements of dynamic simulation. The most important parameter is the horizontal grid resolution. For accurate results in dynamic simulation, blocks containing wells must be separated by at least three or four grid blocks. For wells that are very close to each other, no two wells may be located in the same grid block. Faults should be separated by several grid blocks. Additionally, the geological grid should be orthogonal to allow accurate discretization of the flow equations in dynamic simulation. If the resulting inaccuracies can be assumed negligible, faults may be approximated as zig-zag surfaces in order to preserve orthogonal grid block geometry.

Grids with different sizes of grid blocks were constructed and tested for applicability; it was found that all modeling requirements could be met using a horizontal grid resolution of 100 x 100 meters. To align the grid with the main fault direction, the grid was rotated by 55 degrees counter clock wise. A 3-D view of the mid skeleton grid generated for geological modeling of the Hakim Field is shown in Figure 3-9.

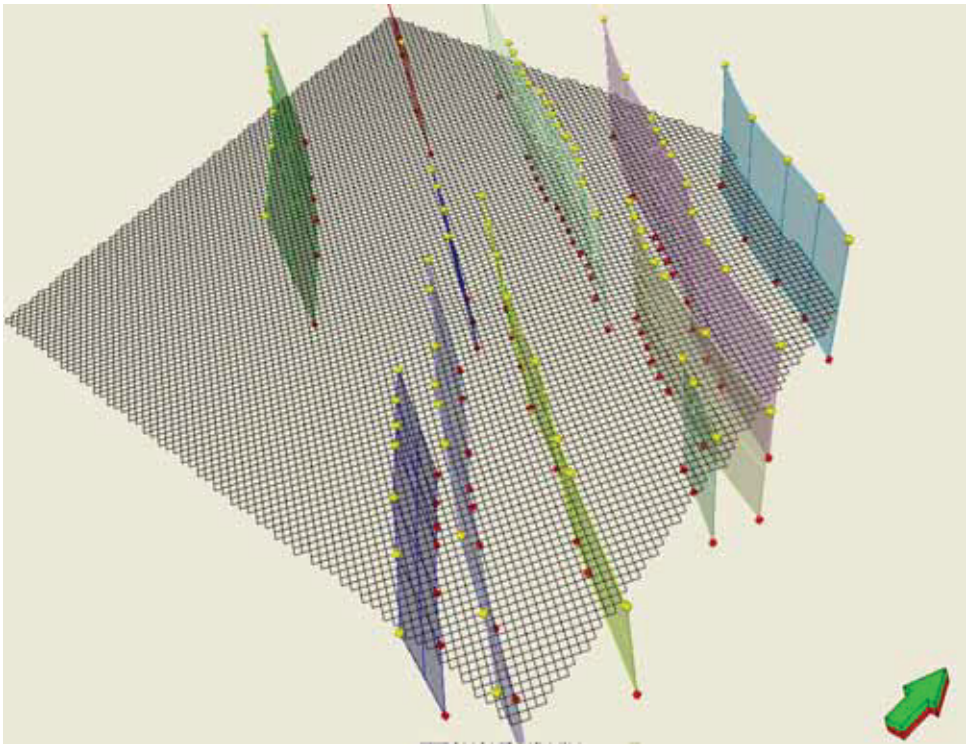

Figure 3-9: 3-D view of the mid skeleton grid and the fault model[24]

3.3.3.3 Horizon and Zonation Modeling

The objective of horizon modeling is to generate gridded surfaces based on seismic interpretations of stratigraphic horizons. The depth converted surfaces of top Facha and top Kheir were used to constrain the top and base of the geological model.

A 3-D view of the reservoir model after inserting the zones and horizons is shown in Figure 3-10 and Figure 3-11.

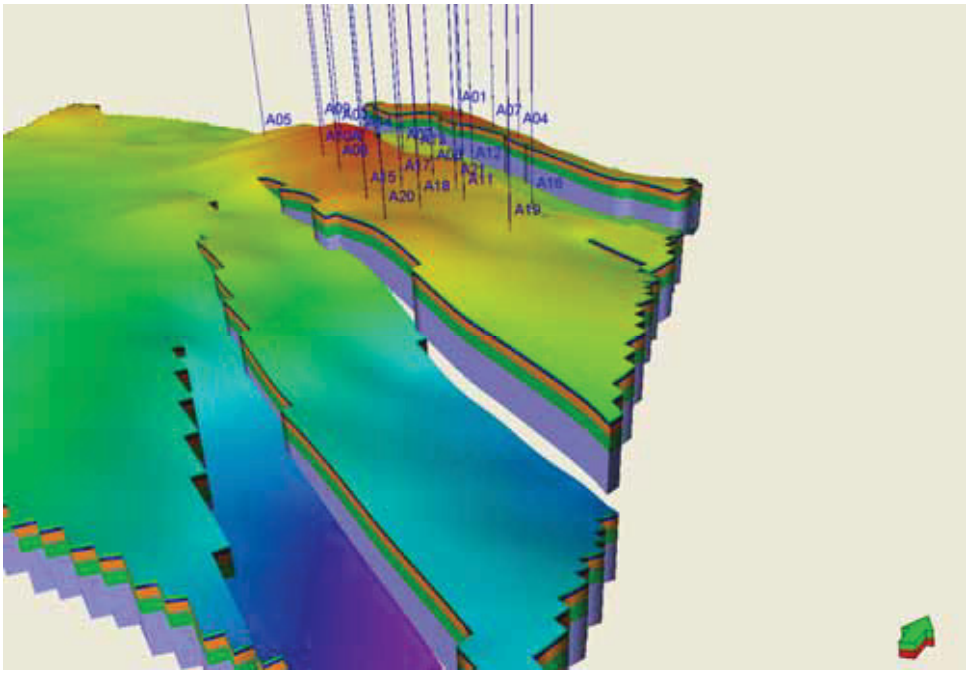

Figure 3-10: 3D view of the structural model showing the reservoir zonation of the Facha member[24]

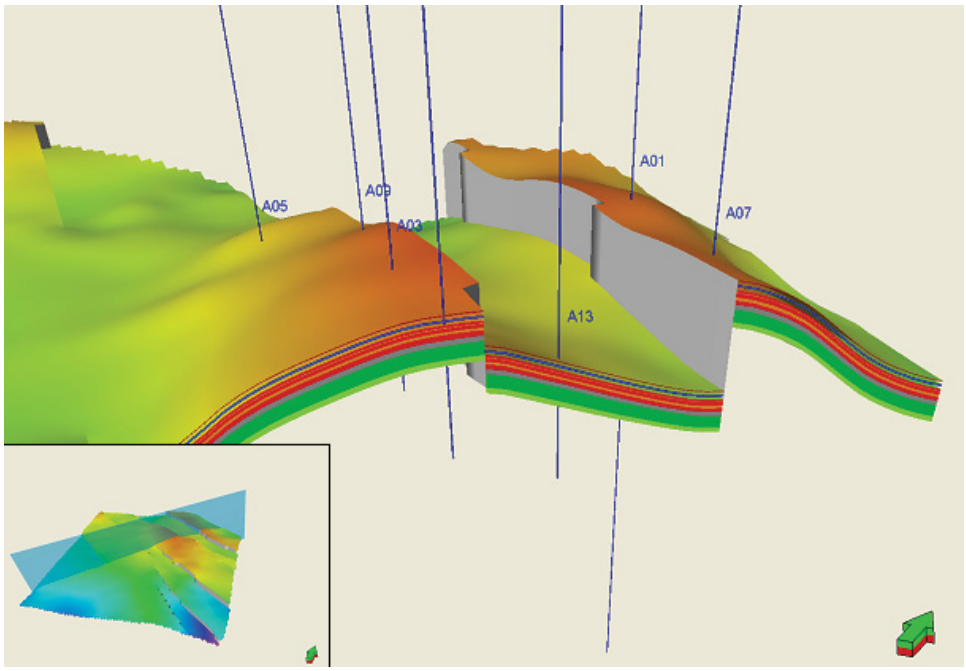

Figure 3-11: Cross section through the structural model showing the main reservoir units Facha E to Facha A[24]

3.3.3.4 Porosity and Permeability

The geocellular grid was populated with values of porosity, permeability and water saturation. A 3-D view of the resulting property model is shown in Figure 3-12 and Figure 3-13.

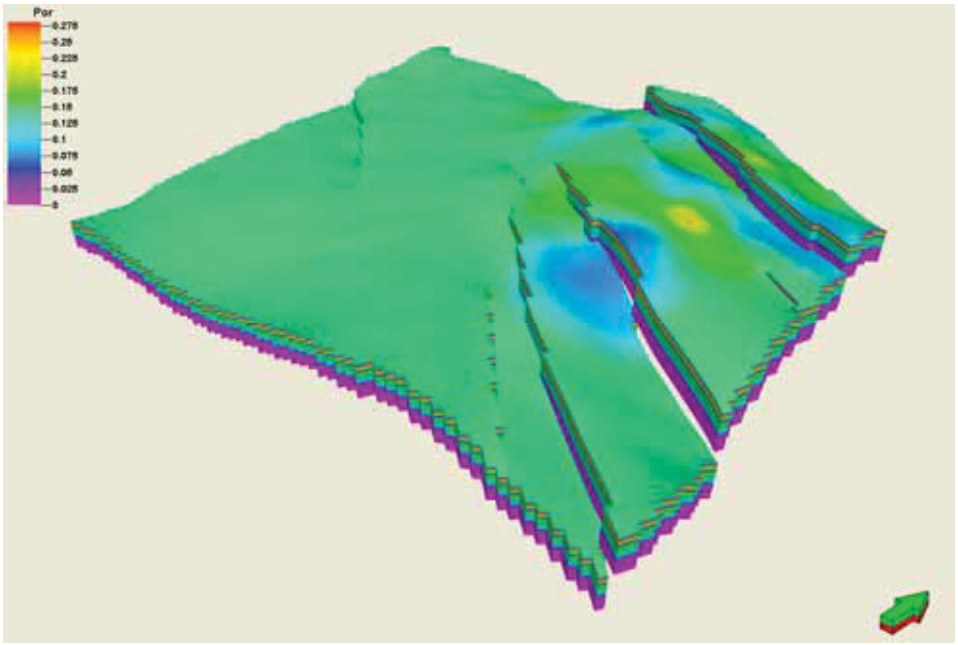

Figure 3-12: 3-D view of the porosity model generated for the Facha Member[24]

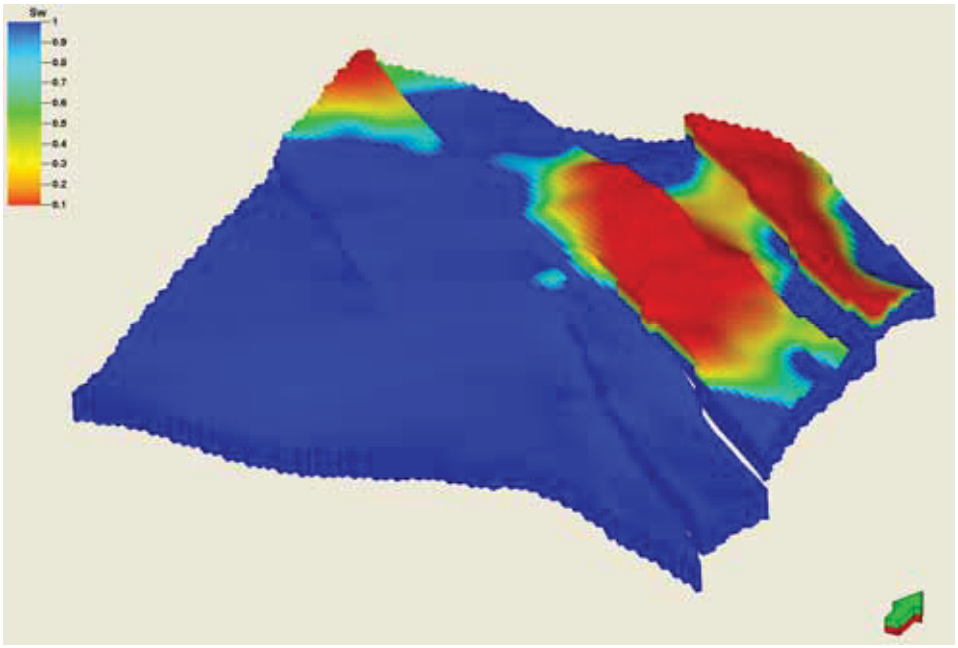

Figure 3-13: 3-D view of water saturation model[24]

The irreducible water saturation in the Hakim Field shows a pronounced trend of increasing saturation from the northeast to the southwest. The regional trend map is shown in Figure 3-14. The final water saturation model was then calculated by using the sum of the irreducible water saturation model and a model obtained from the saturation height curve. The resulting 3-D property model is shown in Figure 3-15.

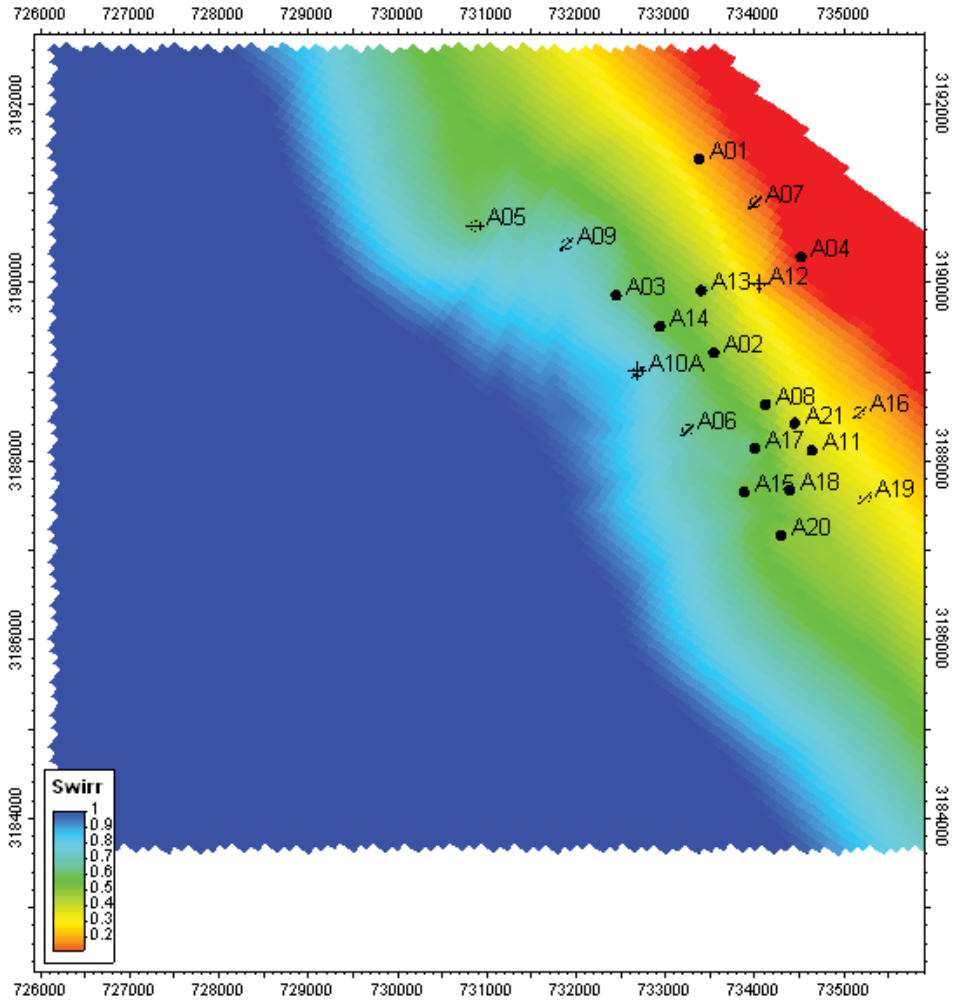

Figure 3-14: Regional trend of irreducible water saturation in the Facha Member[24]

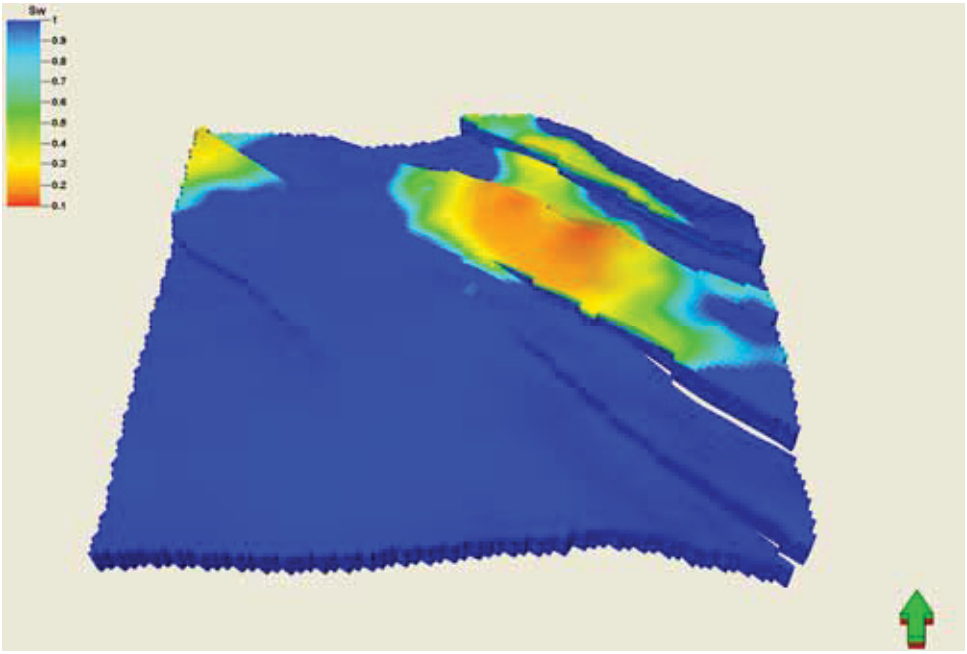

Figure 3-15: 3-D view of the water saturation model established for the Hakim Field. [24]

3.3.4 Estimation of STOIP

The original oil in place (STOIP) is estimated from the parameterized geological model. An initial formation volume factor (Boi) of 1.26 was used. Based on these parameters (without a water saturation cutoff) the STOIP was determined to be 150.5 million stb, of which 136.7 million stb are located in the South Hakim Pool and the remaining 13.7 million stb are located in North Hakim.

Chapter 4

4 Dynamic Reservoir Model

Based on the Geological model conducted and the data available, the author created a dynamic reservoir model. The simulation model covered the area of interest within the Hakim field and was history matched by the author.

4.1 Fluid Characterization for Hakim Field

4.1.1 Oil and Gas Properties

Sample from well A08 was used for PVT characterization and the corresponding report provides the results of a comprehensive reservoir fluid study carried out in November 1983 using subsurface samples collected from the subject well. The laboratory measurements included differential liberation experiments, a series of separator tests and compositional data until C_{32+}.

The saturation pressure of this fluid was measured to be 655 psia at the reservoir temperature of 190°F. Comparison of this value to the reservoir pressure measured prior to sampling (2700 psig at 6650 ft) indicated that the fluid existed in a highly undersaturated condition.

During differential depletion the fluid evolved 672 scf of gas per bbl of residual oil. The accompanying formation volume factor was measured to be 1.582 bbl of saturated fluid per barrel of residual oil. Viscosity was measured from pressures exceeding reservoir pressure to atmospheric pressure. It varied from a minimum of 0.37 cp at the saturation pressure to a maximum of 1.35 cp at atmospheric pressure. The measured gas properties are the incremental gas gravity and the compressibility factor. No gas viscosity was measured which had to be therefore calculated.

Two separator tests were performed, test A two-staged and test B three-staged, to determine the effect of changes in surface separation pressure upon the produced fluid. Table 4-1 shows the measured fluid composition.

Table 4-1: Composition of sample from well A08

Component	Wt. %	Mol. %
N2	0.30	1.20
H2S	-	-
CO2	0.05	0.13
C1	1.26	8.81
C2	1.98	7.38
C3	4.21	10.70
iC4	1.89	3.65
nC4	3.65	7.04
iC5	2.92	4.54
nC5	2.62	4.07
C6	4.73	6.30
C7	6.72	7.83
C8	7.91	8.27
C9	5.99	5.54
C10	4.97	4.15
C11	3.74	2.85
C12	3.32	2.31
C13	2.96	1.89
C14	2.76	1.62
C15	2.89	1.57
C16	2.22	1.12
C17	1.83	0.86
C18	1.73	0.77
C19	1.35	0.57

Component	Wt. %	Mol. %
C20	0.95	0.39
C21	0.79	0.30
C22	0.61	0.22
C23	0.47	0.17
C24	0.40	0.14
C25	0.35	0.11
C26	0.25	0.08
C27	0.24	0.07
C28	0.24	0.07
C29	0.29	0.08
C30	0.31	0.08
C31	0.35	0.09
C32+	22.75	5.03

* Average Molecular Weight of C32+ fraction: 505

Standard laboratory tests are carried out on the basis of two different thermodynamic processes being under way at the same time. These are the flash equilibrium separation of liquid and vapor in the surface traps during production and the differential equilibrium separation of liquid and vapor in the reservoir during pressure decline. As a consequence PVT reports give both flash and differential data and it is necessary to shift between both data types. The flash data from the separator test, e.g. the GOR or the Formation Volume Factor, always refer to stock tank oil (STO), the differential data from the Differential Liberation Experiment to the so-called Residual Oil. These two values will not be the same because the processes for obtaining them are different. The residual oil results from a series of flashes at reservoir temperature, the STO from a generally one-or two-stage flash at low pressure and temperature. The quantities of the released gas and the final liquid will be different, as well as the gravities of the products. Consequently, the corresponding data, such as the solution gas and the formation volume factor will be different for both experiments. For engineering purposes,

the GOR and the Formation Volume Factors are always referred to the STO basis; therefore, the differential data need to be "flash-converted" before using it for simulation input.

No detailed information was given on actual separator conditions at this time of production. Separator tests for the A08 fluid were conducted at a series of pressures and temperatures. The second separator test (test B) was used as the basis for flash-conversion assuming the following separator conditions:

First Stage:	120 psia and 100 F
Second stage:	35 psia and 100 F
Third stage (Stock tank):	15 psia and 60F

For this test the total measured GOR is 274 BBL/STB and the oil formation volume factor 1.265 at bubble point. These data were used for flash conversion of DLE Bo and Rs. Figure 4-1 and Figure 4-2 show comparisons of the measured differential data (in red) and the converted flash data (black). The flash data are the ones that have to be used for simulation input.

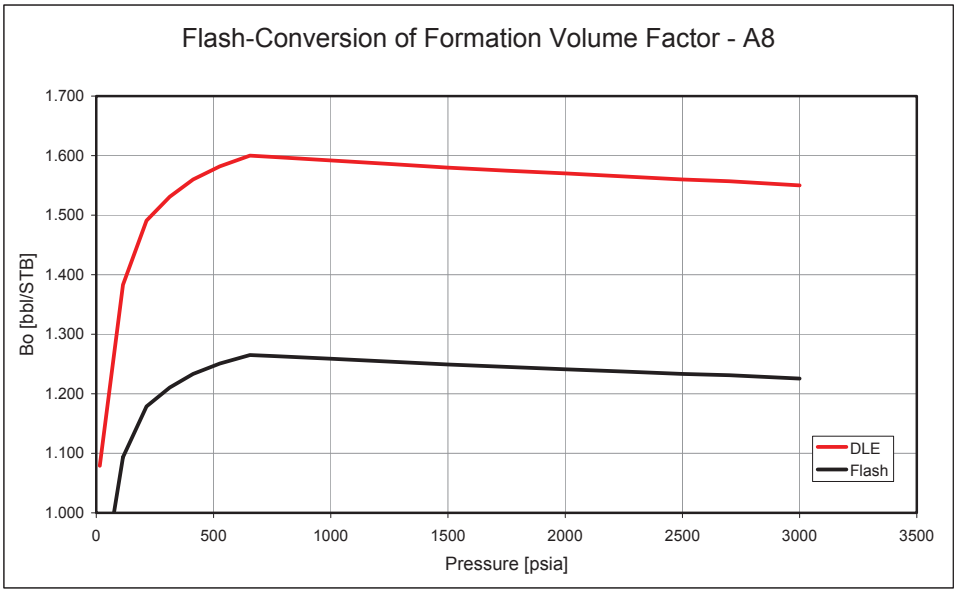

Figure 4-1: Flash conversion of differential FVF

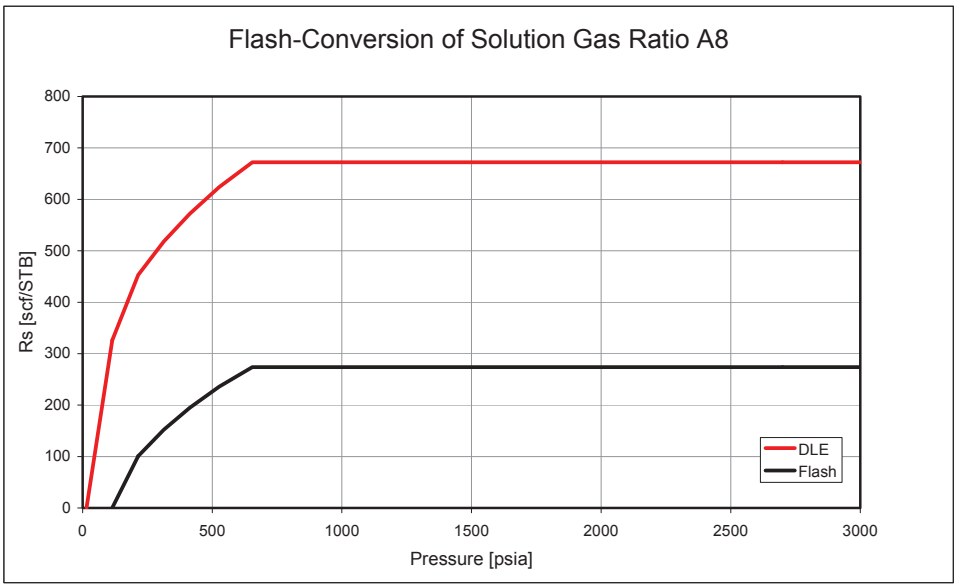

Figure 4-2: Flash conversion of differential GOR

Figure 4-3 and Figure 4-4 show the oil viscosity and the gas properties (the red curve displays the gas viscosity and the black curve the gas Z-Factor). Gas viscosities are very rarely measured because the laboratories are lacking the required equipment and also in this case it had to be calculated instead using the Lee-Gonzales correlation. It is given by:

$$\mu_g = A_1 \times 10^{-4} \exp\left(A_2 \rho_g^{A_3}\right), \qquad \text{Equation 4-1}$$

where

$$A_1 = \frac{\left(9.379 + 0.01607 M_g\right) T^{1.5}}{209.2 + 19.26 M_g + T}, \qquad \text{Equation 4-2}$$

$$A_2 = 3.448 + \left(\frac{986.4}{T}\right) + 0.01009 M_g, \qquad \text{Equation 4-3}$$

and

$$A_3 = 2.447 - 0.2224 A_2. \qquad \text{Equation 4-4}$$

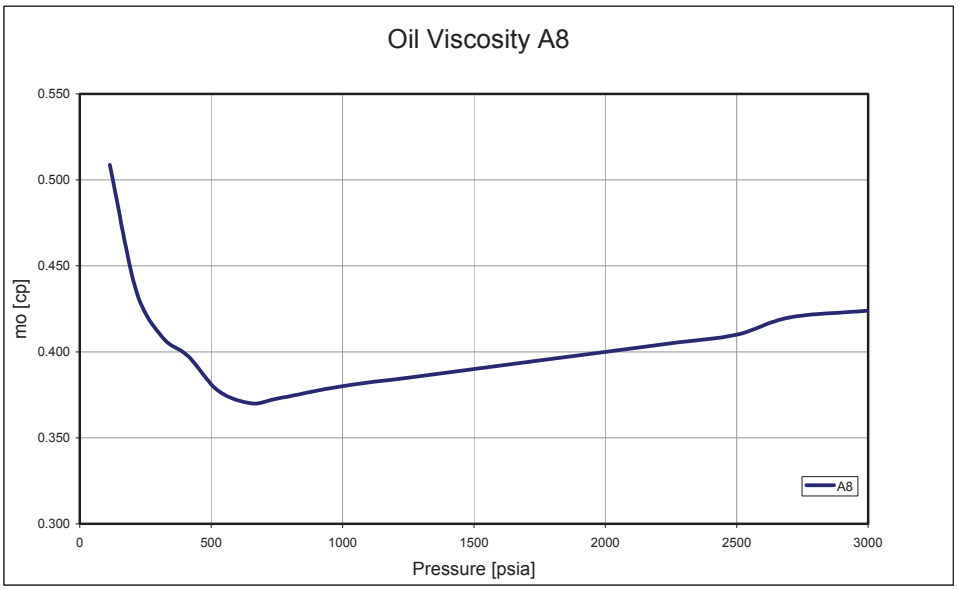

Figure 4-3: Oil viscosity for Hakim Field

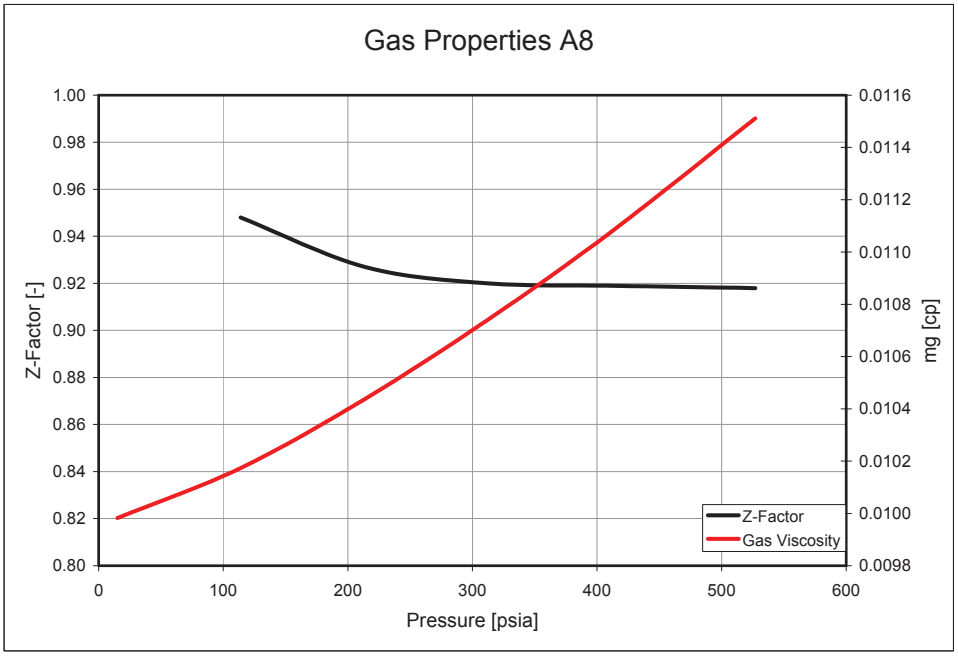

Figure 4-4: Gas properties for Hakim Field

4.1.2 Calculation of Average Water Properties

There have been a large number of studies on the physical properties of brines in the last three decades, and several such correlations exist in literature. The chosen correlations recommended by McCain *(McCain, 1990)* were used to calculate

reference values for the water properties at a reference pressure of 2700 psia and the reservoir temperature of 190 F, assumed an average salinity of 115,000 mg/l. The results presented in the following table 2-2:

Table 4-2: Water properties South Hakim

Specific gravity	1.082	-
Compressibility	2.55E-06	/psi
Viscosity	0.558	cp
Formation Volume Factor	1.031	rb/STB

4.2 Special Core Analysis

The objective of special core analysis is to obtain detailed information about multi-phase flow behaviour. Probably, the most prominent SCAL tests are two-phase or three-phase displacement experiments in the formation rock sample from which basic reservoir engineering properties are determined. SCAL gives information about the distribution of hydrocarbons in the reservoir (capillary pressure data), residual oil and multiphase flow characteristics (relative permeability) and wettability. Additionally, SCAL tests also include the measurements of electrical (formation factor and resistivity index) and mechanical properties.

4.2.1 Wettability

Four wettability measurements performed on four core samples were available. According to the classification of the Hakim wettability the tested samples cover a wettability range from water-wet to oil-wet.

4.2.2 Electrical Measurements: Resistivity Index

An indicator for the wettability of a reservoir rock is the saturation exponent *n* in Archie's water saturation equation which relates the resistivity index *RI* to the water saturation *Sw*.

In water-wet reservoirs and cleaned cores the Archie saturation exponent *n* typically has a value of about 2. In native-state, non water-wet cores and reservoirs the saturation exponent *n* is generally greater than 2, in oil wet rocks can reach values of up to 10.

As the saturation exponent depends on the wettability of the reservoir it must be measured at reservoir wetting conditions (native- or restored cores), otherwise invalid values will be derived. Exceptions are reservoirs that are known to be strongly water-wet where measurements performed on cleaned-state cores would yield representative results. The derived saturation exponent is in the proximity of 2.

4.2.3 Relative Permeabilities

Seven water-oil relative permeability and six gas-oil relative permeability measurements were performed and considered reliable for a detailed assessment of relative permeability characteristics.

The derived results were taken as basis for derivation of relative permeability functions for Hakim field. Figure 3-15 shows the normalized average relative permeability curve for the zones C1, C2, C3 and E1

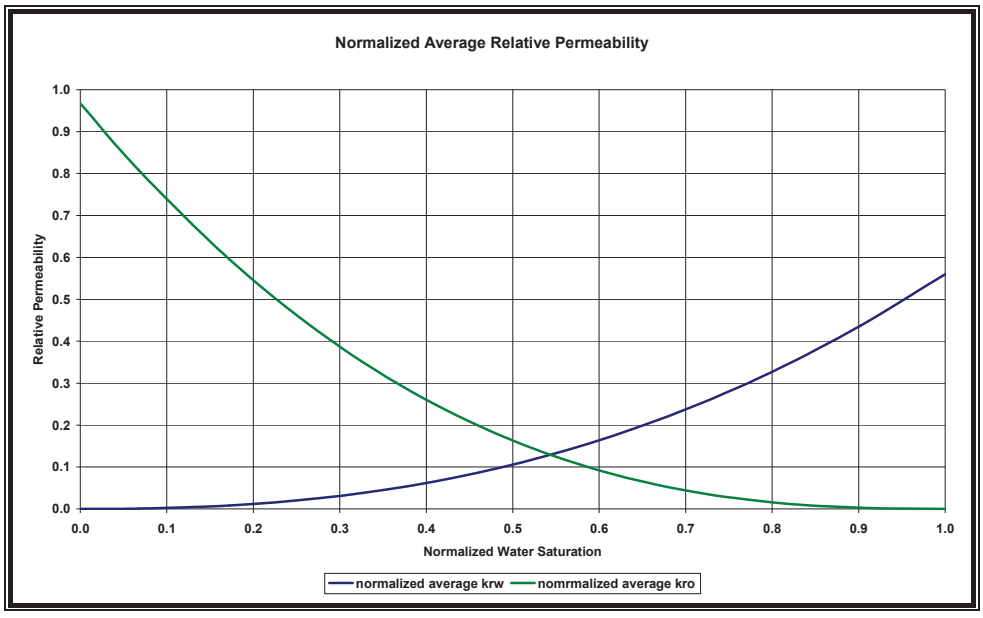

Figure 4-5: Normalized average relative permeability

4.2.4 Capillary Pressure

The capillary pressure samples were taken in reservoir zones B, C1, C2, C3, E1, E2 and F, a normalized average capillary pressure curve was applicable in simulation. This is illustrated in Figure 4-6. The de-normalized capillary pressure curve, applying the derived average irreducible water saturation for zones C and E in relative permeability analysis (11.8 %) and derived average oil saturation (40 %), is shown Figure 4-7. Both curves are given in tabular form in Table 4-3.

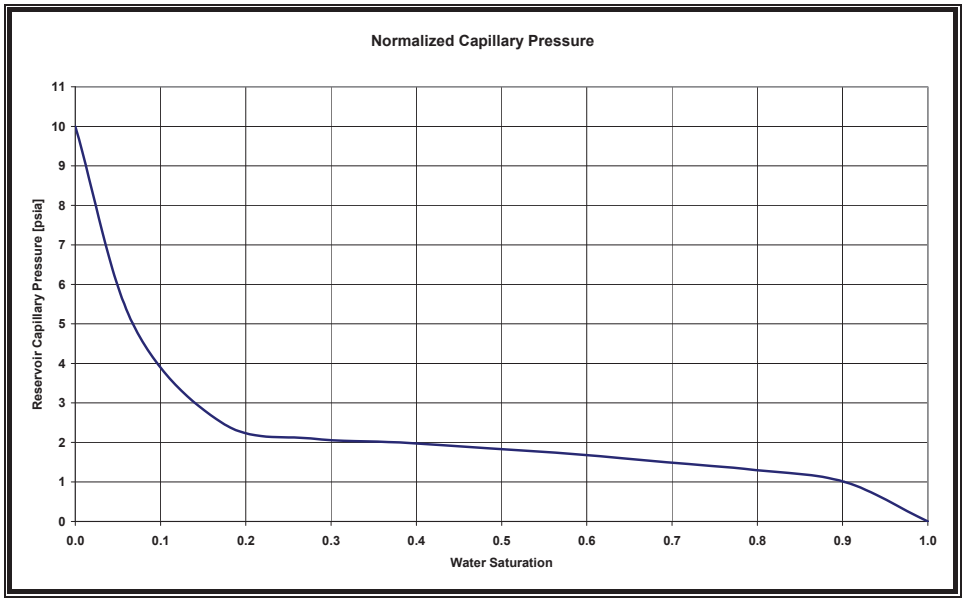

Figure 4-6: Normalized average capillary pressure

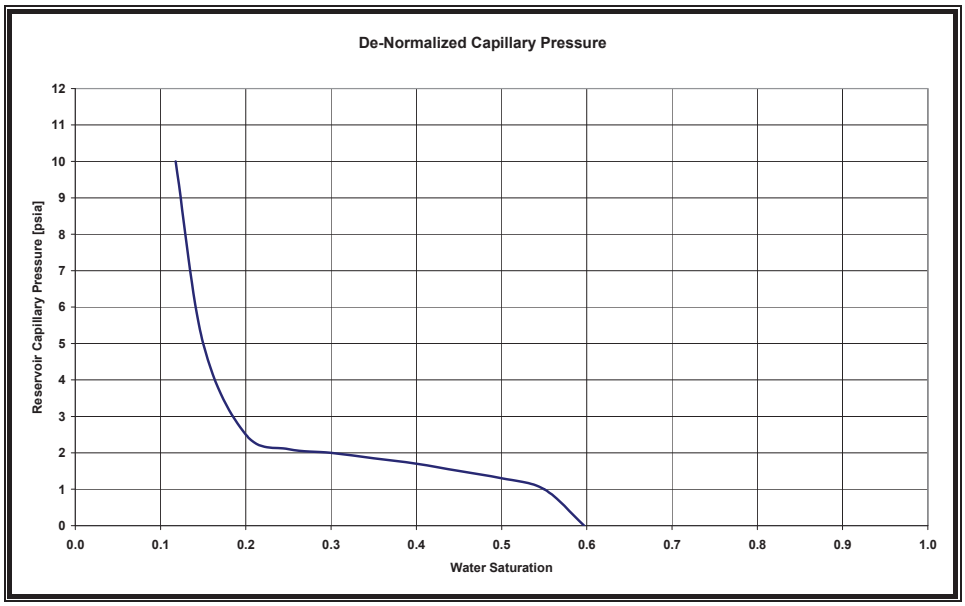

Figure 4-7: De-normalized average capillary pressure

Table 4-3: Average capillary pressure

Sw	Swn	Pc [psia]
0.1177	0.0000	10
0.1500	0.0675	5
0.2000	0.1718	2.5
0.2500	0.2762	2.1
0.3000	0.3805	2
0.3500	0.4849	1.85
0.4000	0.5892	1.7
0.4500	0.6936	1.5
0.5000	0.7979	1.3
0.5500	0.9023	1
0.5968	1.0000	0

4.3 Production Data

4.3.1 Field Production

The hydrocarbon accumulation in the Hakim field is divided into North Hakim and South Hakim, based upon a fault traversing the field.

A total of 21 wells have been drilled in Hakim field throughout its history. 3 wells are located in North Hakim (A1, A4, A7) and 18 wells are located in South Hakim (A2, A3, A5, A6, A8, A9, A10, A11, A12, A13, A14, A15, A16, A17, A18, A19, A20, A21).

Figure 4-8 shows the historical oil and gas production and the water cut between January 1985 and March 2008. The historical water injection is shown in Figure 4-9.

The continuous oil production started in June 1987 with an average oil rate of 2000 STB/day from nine wells. Water injection started at the same time as the continuous production. In summer 1988 the average oil rate increased significantly to about 6000 STB/day as water injection commenced in two injection wells and an additional producer started oil production. An average rate of 6000 STB/day was kept until 1992, including peak oil production of 6660 STB/day in 1991. After

1992 the average oil production decreased continuously. In 1994 the average rate increased due to the start of oil production from two new additional wells. In 2004 two further oil producers commenced production leading to an increased rate.

Table 4-4 summarizes the cumulative production and injection data for Hakim. In total 28.9 MM STB of oil have been produced in the period January 1985 to March 2008, the gas production amounts to 13.5 MM MSCF and the water production to 46.4 MM STB.

Table 4-4: Production/Injection summary Hakim

	cum oil prod STB	cum gas prod MSCF	cum water prod STB	cum water inj STB
North	3.58E+06	5.57E+06	6.56E+06	9.47E+06
South	2.53E+07	7.95E+06	3.99E+07	5.41E+07
SUM	2.89E+07	1.35E+07	4.64E+07	6.35E+07

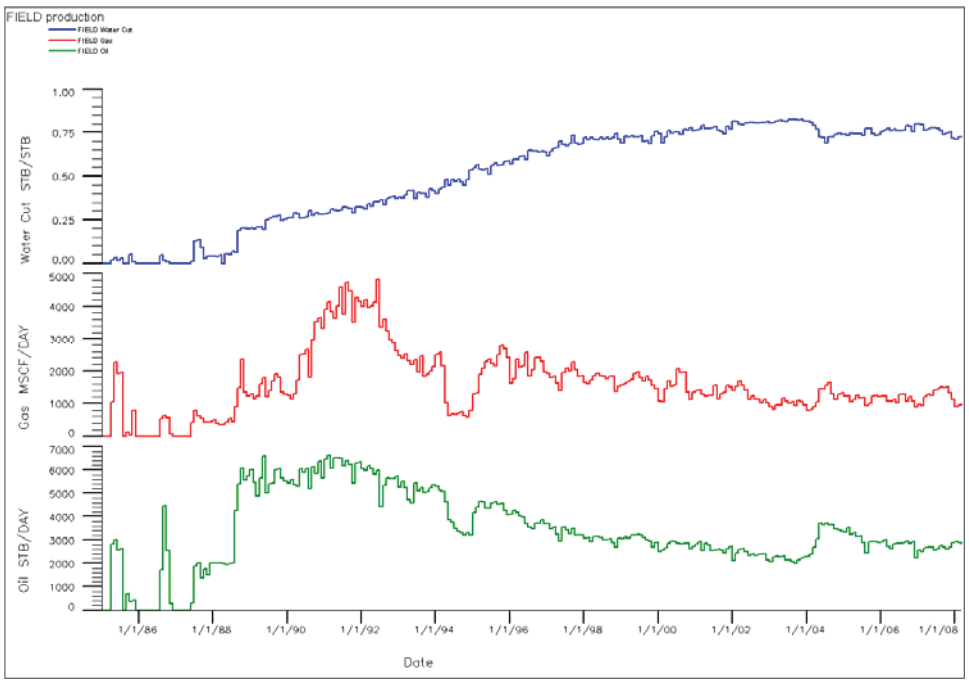

Figure 4-8: Historical field production (January 1985-March 2008): oil (green), gas (red) and water cut (blue)

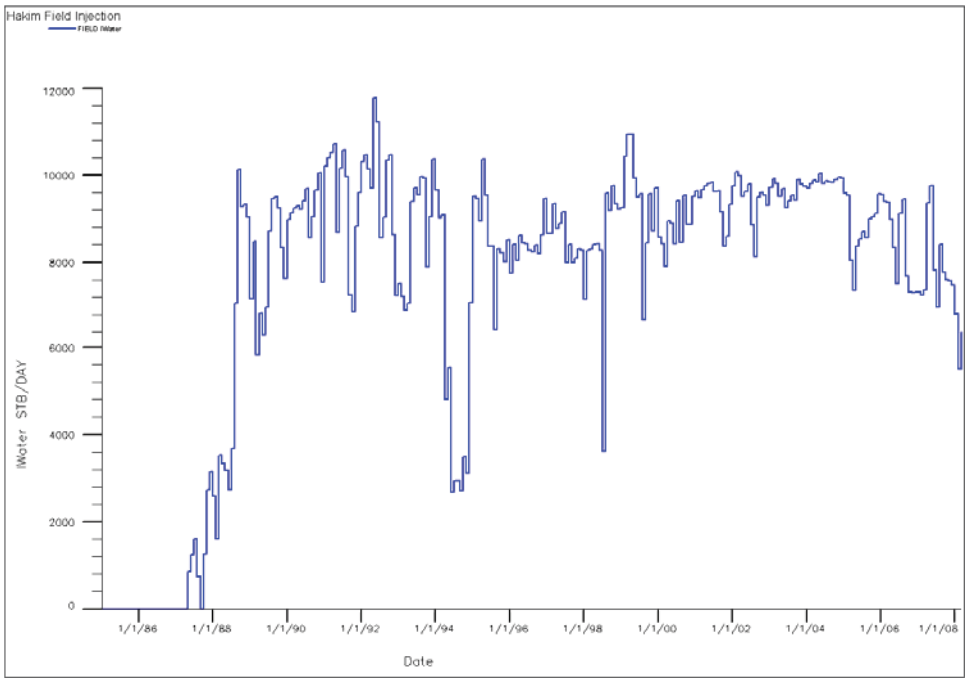

Figure 4-9: Historical field water injection (January 1985-March 2008)

4.3.2 Production Histories of Selected Wells

One crucial part of this thesis work was to analyze the production history of wells in the Hakim field, by the Author. His focus was put on gathering all relevant information on each well which is needed later on for history matching. Such information includes e.g. re-completions and workovers, casing leaks or other reported problems, interference with neighbouring producers as well as all specific events in the field's life which can be related to the recorded oil and water production and for instance explain long shut-in periods, unnatural water cuts or sudden changes in oil production.

Anticipating the following detailed well descriptions, a few issues were often observed and seem to be characteristic for Hakim field:

- All wells are producing on artificial lift. ESP pumps were installed either from the start or shortly after continuous production commenced. The free-flowing wells could not sustain production due to low pressure.
- All ESP installations encountered periodical problems and/or failure. Numerous workovers were necessary due to either stiff or locked pumps where debris and salt scales were believed to have been the

major factor in causing these pump failures. Debris and salt scales caused corrosion, overheating and pump failure due to the poor thermal conductivity of the scale material, as evidenced in seized or stuck motor and pump shafts and completely plugged off pump intake and discharge. Another extensively encountered reason for pump failure was problems in power supply caused by e.g. cable failure.

- Water production is a major issue for the depletion of Hakim field. Several wells are close to abandonment and some were converted to water injectors due to high water cuts.
- The high water production leads to salt creep in several wells. Salt creep forms inside the casing and leads to casing deformation. In order to prevent further casing deformation scab liners were run to isolate the damaged section of the casing.
- Stimulation by acidizing was conducted in several wells in order to increase the productivity/injectivity.

A poor cement bond was reported for all Hakim wells. Exceeding of formation fracture pressure during stimulation of the wells may have lead to vertical fractures in the cement bond allowing the underlying water to flow up to higher perforated intervals.

4.3.2.1 Well A2

Production from this well started in April 1985, the continuous production commenced in July 1987. In September 1988 the peak production of 1665 STB/day was achieved, afterwards the production rate decreased continuously. Since 2002 the production rate has settled down at a stable level of approximately 200 STB/day. The water cut increased steadily starting from the mid nineties and achieved its maximum of 92 % in August 2005. Figure 4-10 shows the production and workover history of well A2. The green line represents the daily oil production, the red line shows the daily gas production and the blue line illustrates the water cut. Workovers performed are marked with red circles.

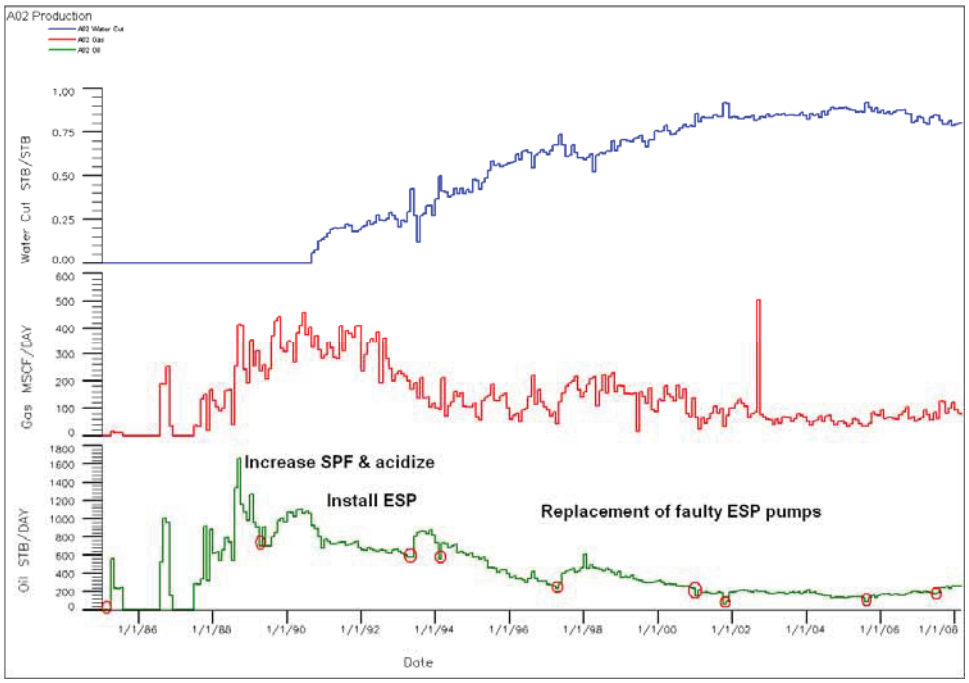

Figure 4-10: Well A2: production and workover history

4.3.2.2 Well A3

Production from this well started in April 1985, the continuous production commenced in October 1988. In January 1989 the peak production of 1051 STB/day was achieved, afterwards the production rate decreased continuously. Since 2002 the production rate has settled down at a stable level of approximately 100 STB/day. The water cut increased steadily starting from the start of continuous production and achieved its maximum of 97.4 % in March 2000. Figure 4-11 shows the production and workover history of well A3. The green line represents the daily oil production, the red line shows the daily gas production and the blue line illustrates the water cut. Workovers performed are marked with red circles.

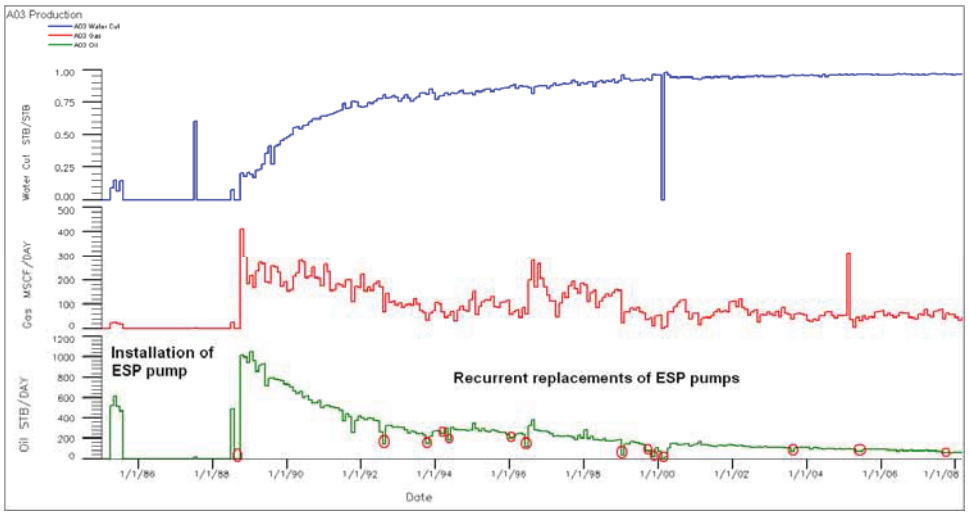

Figure 4-11: Well A3: production and workover history

4.3.2.3 Well A8

The well started to produce in April 1985, continuous production commenced in November 1987. The maximum oil rate of 1246 STB/day was achieved in September 1988. Starting from 1994 the production rate decreased continuously. The first water showed up in the beginning of 1989. The water cut increased continuously from this date and the maximum water cut of 98 % was achieved in September 2006. Starting from 2002 the water cut stabilized at an average of 85%. Figure 4-12 shows the production and workover history of well A8. The green line represents the daily oil production, the red line shows the daily gas production and the blue line illustrates the water cut. Workovers performed are marked with red circles.

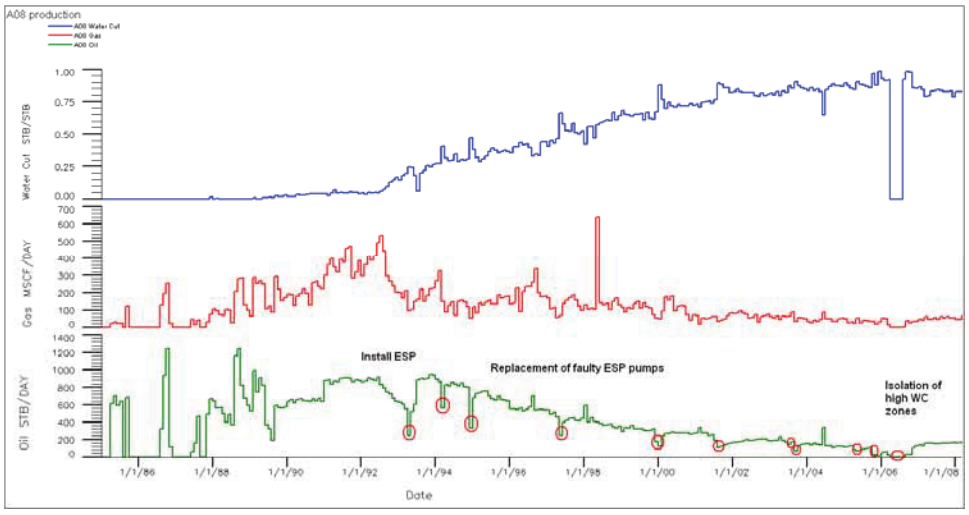

Figure 4-12: Well A8: production and workover history

4.3.2.4 Well A11

The production started in April 1985, continuous production commenced in October 1987. The oil production increased continuously until the maximum oil production rate of 1365 STB/day was achieved in August 1991. Afterwards the rate decreased continuously. The water cut increased continuously starting from October 1987. The maximum water cut of 84.2 % was achieved in November 2007. Figure 4-13 shows the production and workover history of well A11. The green line represents the daily oil production, the red line shows the daily gas production and the blue line illustrates the water cut. Workovers performed are marked with red circles.

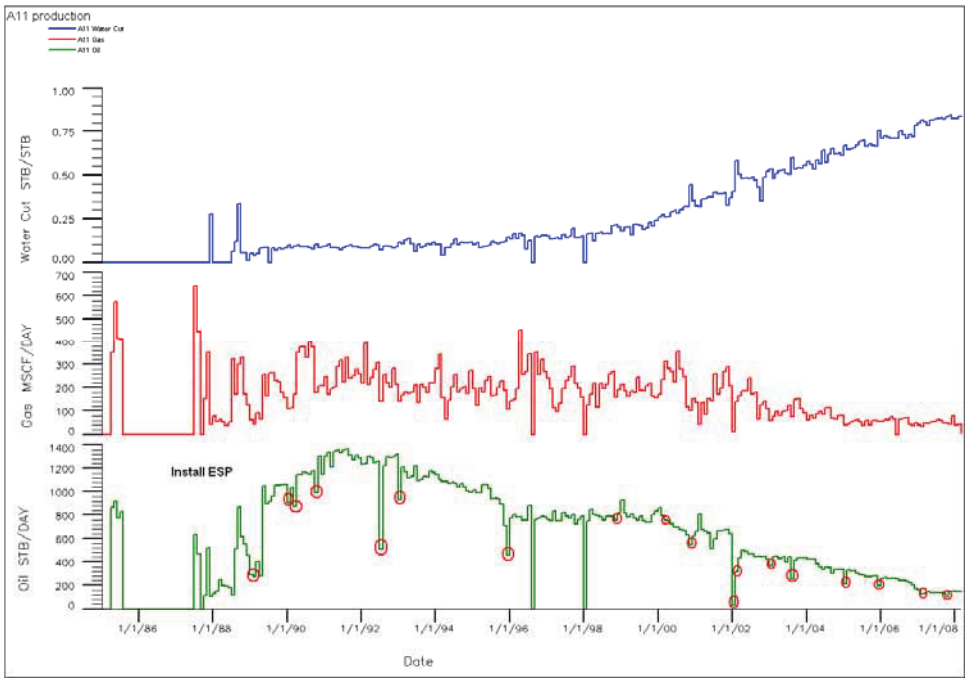

Figure 4-13: Well A11: Production and workover history

4.3.2.5 Well A14

The well started production in October 1985 and continuous production commenced in June 1987. The maximum oil production rate of 1248 STB/day was achieved in September 1988. Afterwards the production rate decreased continuously. The water cut increased continuously after commencement of continuous oil production. It reached a rather constant level with an average water cut of 96 % after 2000. The maximum water cut of 98 % was achieved in August 2005. Figure 4-14 shows the production and workover history of well A14. The green line represents the daily oil production, the red line shows the daily gas production and the blue line illustrates the water cut. Workovers performed are marked with red circles.

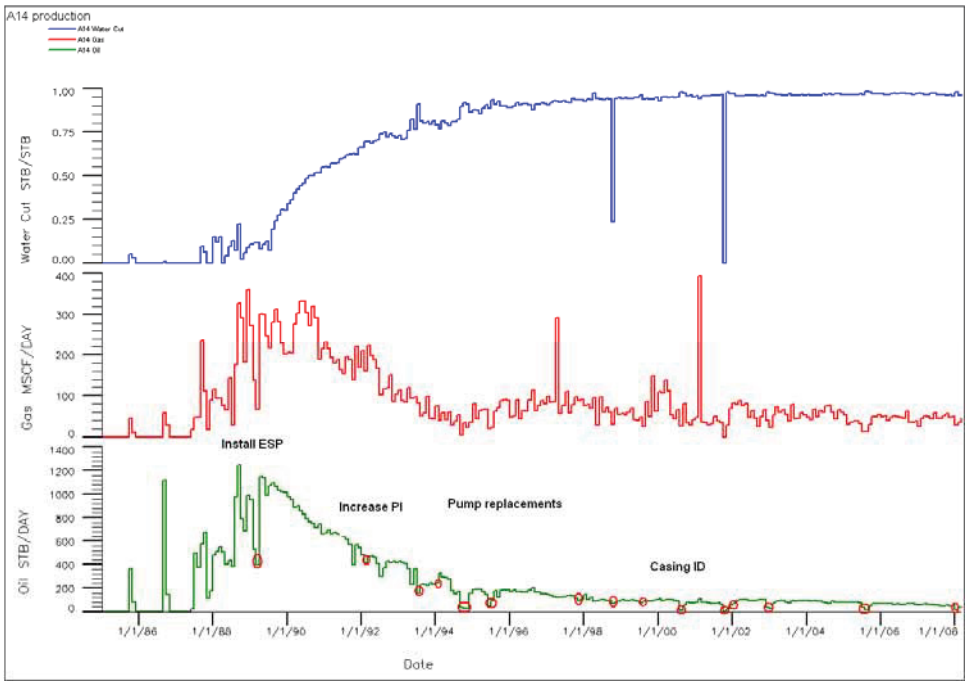

Figure 4-14: Well A14: production and workover history

4.3.2.6 Well A15

The well started to produce in August 1986, continuous production commenced in October 1987. The maximum oil production rate of 825 STB/day was achieved in March 1990. At the beginning of continuous oil production the water cut was at 50 %. After a rapid decrease it started to increase continuously since summer 1988. The maximum water cut of 93.6 % was achieved in November 1999. This peak water cut was above the average water cut of 65% between 1988 and 2004. Figure 4-15 shows the production and workover history of well A15. The green line represents the daily oil production, the red line shows the daily gas production and the blue line illustrates the water cut. Workovers performed are marked with red circles.

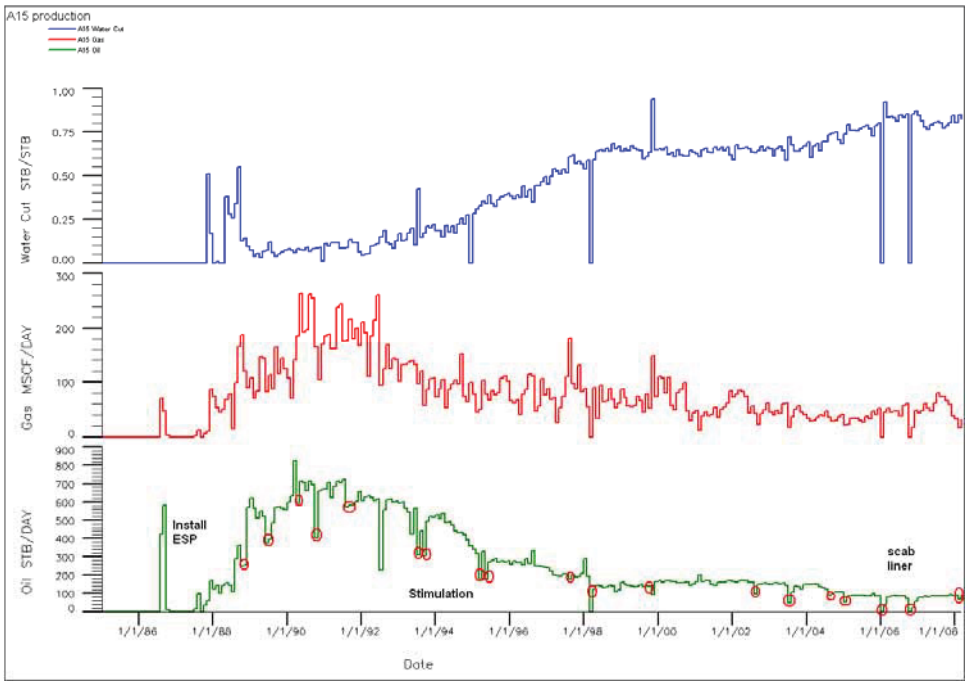

Figure 4-15: Well A15: production and workover history

4.4 Grid Geometry and Upscaling

The reservoir zonation applied in this work is based on the reservoir zonation that was used in previous studies by OMV (1989)[28] and Zueitina Oil Company (1998)[39]. In these studies, the Facha Member was divided into six zones named Facha A (top) to Facha F (bottom), which were divided into a different number of subzones by OMV and ZOC. The author proposed a subdivision of the Facha Member into 15 subzones, primarily based on the responses of the neutron and density logs.

The Facha F is the oldest reservoir unit of the Facha Member and conformably overlies the Kheir Formation. Facha F was divided into five subzones called Facha F1 (top) to Facha F5 (bottom).

Facha F is conformably overlain by Facha E, which can be considered as a transition zone from the basal limestone facies to the dolomitic facies near the top of the reservoir section. Facha E has been divided into two subzones, Facha E1 on top and Facha E2 at the bottom.

Facha E is overlain by Facha D, which is a tight layer with an average thickness of 13 ft.

Facha C is the best reservoir unit in the Hakim Field. Therefore it was divided into five subunits in this work. Facha A and Facha B each consist of a thinly developed dolomite layer on top of a laterally persistent anhydrite zone. The dolomites of the Facha A and Facha B are therefore not in communication with the reservoir units below them.

Table 4-5: Layer Mapping – Geological model and Upscaled Dynamic Model

Zone	Layer Index Simulation Model	Layer Index Geological Model	
		Top	Base
Facha A	1	1	1
Facha A Anhydrite	2	2	2
Facha B	3	3	3
Facha B Anhydrite	4	4	4
Facha C1	5	5	7
Facha C2	6	8	9
Facha C3_1	7	10	11
Facha C3_2	8	12	13
Facha C4_1	9	14	15
Facha C4_2	10	16	17
Facha C5_1	11	18	19
Facha C5_2	12	20	21
Facha C5_2	13	22	23
Facha D	14	24	29
Facha E1_1	15	30	35
Facha E1_2	16	36	41
Facha E1_3	17	42	47
Facha E2	18	48	55
Facha F1	19	56	71
Facha F2	20	72	80
Facha F3	21	81	92
Facha F4	22	93	125
Facha F5	23	126	149

The geological model consists of 231*274*149 equal to 9.4 million total blocks from which around 5.4 million are active. Most of the inactive blocks are cut away due to the different orientation of the model boundary (according to seismic cube) and the grid orientation (according to the main fault direction).

The upscaled model consisted of 49x100x23 equal to total 112,700 blocks from which 77,973 blocks are active.

Each of these coarse cells in the simulation model represents a column of thinner cells in the geo-cellular model. A large cell in the simulation model must have the same bulk volume as the corresponding set of small cells in the geo-cellular model. In addition, the reservoir properties of all the small geo-cellular cells that are combined to form a simulation cell must be represented in some manner. This "upscaling" was done by calculating volume-weighted averages of the properties in the geo-cellular model and applying these averages to the simulation cells.

For porosity, horizontal permeability, initial water saturation and irreducible water saturation the upscaled properties were determined by volume weighted arithmetic average of the small blocks. The vertical permeability was calculated by the corresponding harmonic average.

Figure 4-16, Figure 4-17, Figure 4-18 and Figure 4-19 present a cross-sectional view of the geomodel on top and the upscaled model on the bottom. The cross-sections show porosity, permeability, initial water saturation and irreducible water saturation.

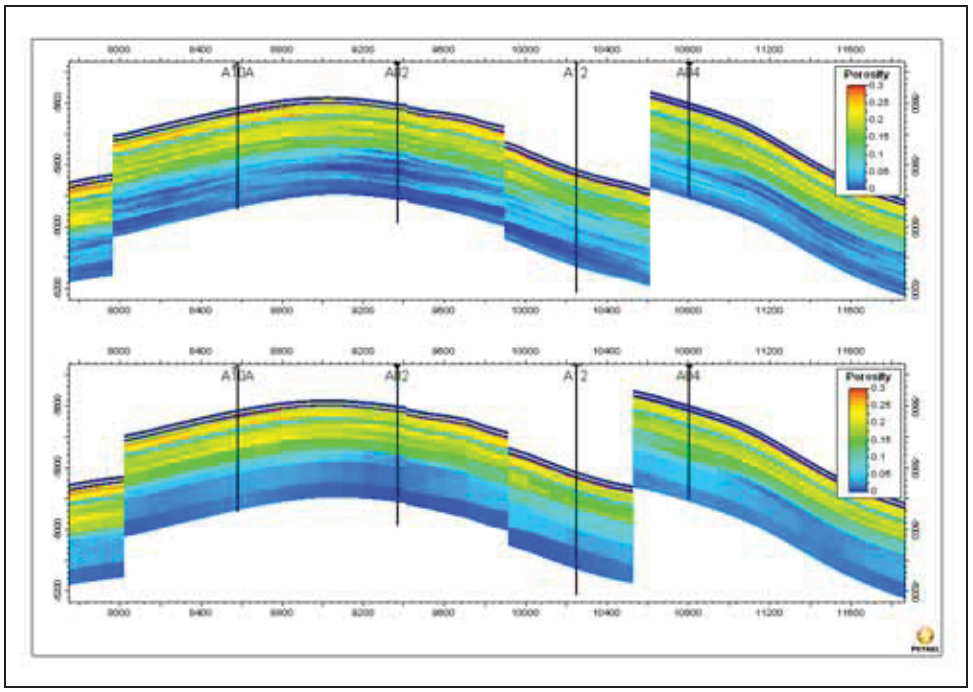

Figure 4-16: Cross-sectional view presenting porosity; geological model on top, upscaled simulation model on bottom

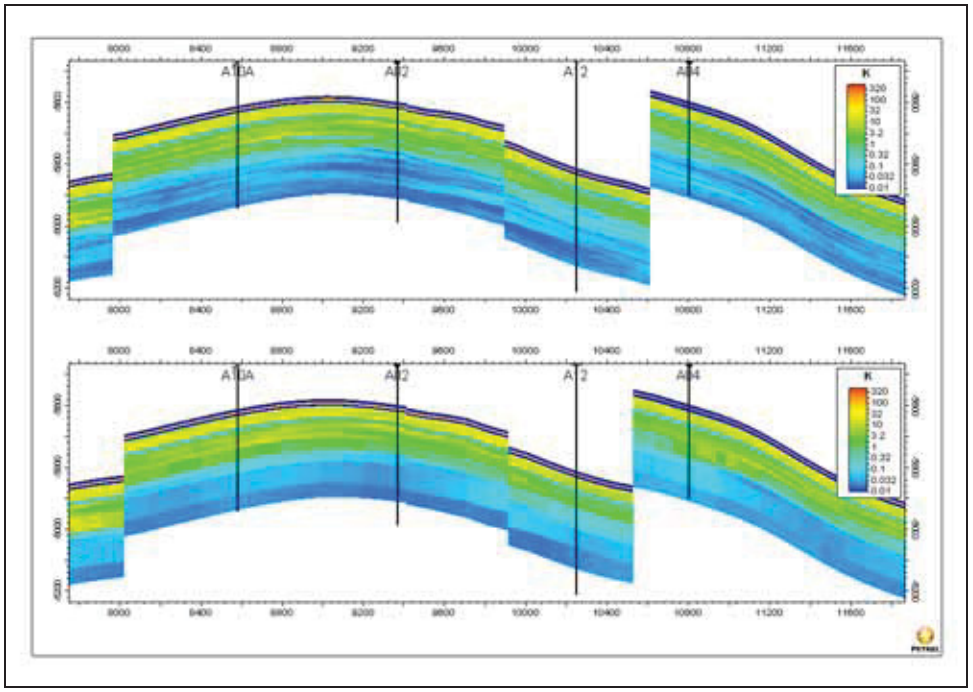

Figure 4-17: Cross-sectional view presenting permeability; geological model on top, upscaled simulation model on bottom

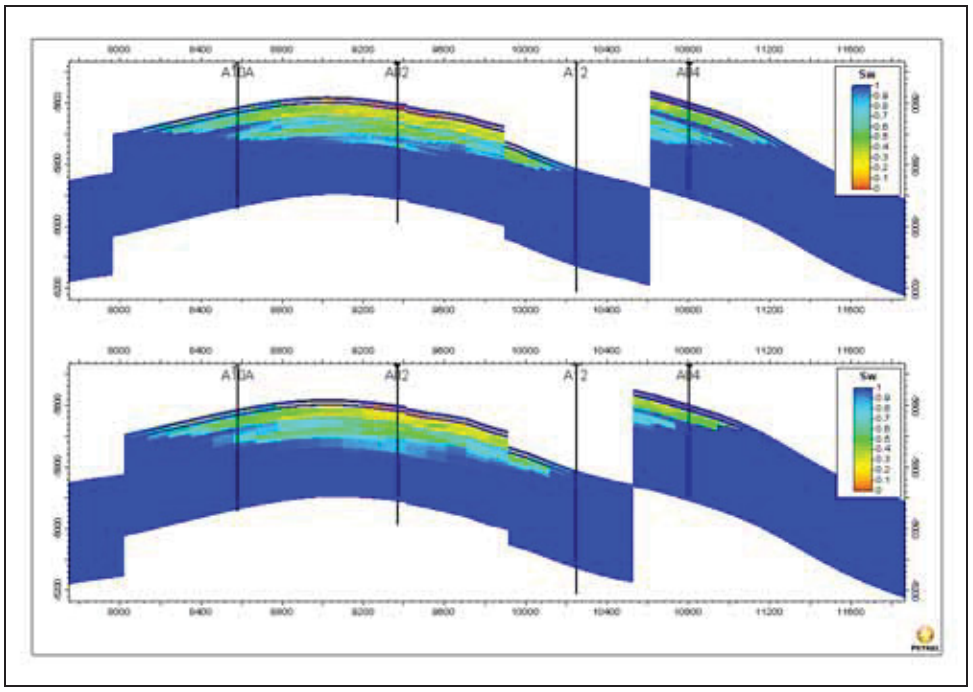

Figure 4-18: Cross-sectional view presenting initial water saturation; geological model on top, upscaled simulation model on bottom

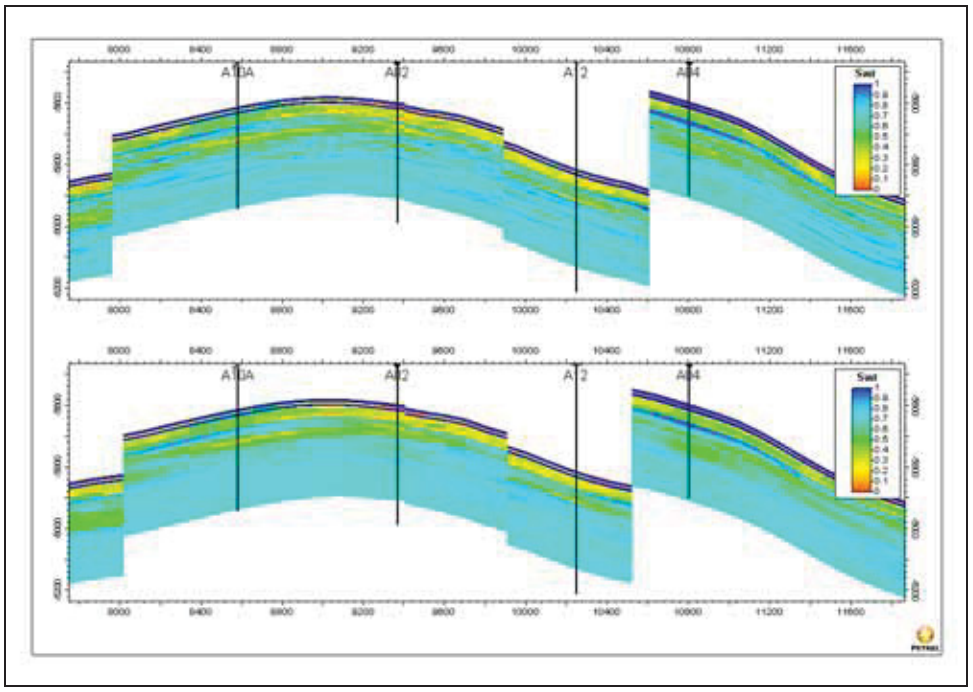

Figure 4-19: Cross-sectional view presenting irreducible water saturation; geological model on top, upscaled simulation model on bottom

4.5 Initialization

To types of initialization can be applied:

1. Equilibrium initialization based on capillary pressure function, having laterally changing threshold pressures.
2. Non-equilibrium initialization on the basis of the modeled saturation distribution from geo-cellular model.

The first approach for every grid block a capillary pressure function is defined, with higher threshold values in areas where the WOC is shallower, and based on these functions and the fluid densities the vertical saturation profile is calculated by the simulation software.

In the second approach the initial saturation values for every grid block are defined; i.e. exactly the same value as in defined in the geo-cellular modeling is used in the simulation grid block. The simulation software calculates the corresponding pseudo capillary pressure in order to stabilize the initialization.

The author decided to use the second approach from the main reason that by applying exactly the same initial saturation distribution, the initial volumes in place will be exactly the same for the simulation model as for the geo-cellular one.

Table 4-6 presents the original fluids in place for the entire reservoir as well as for the two separated parts. Figure 4-20 presents the initial water saturation distribution of the dynamic model. Note as from the mentioned initialization approach mentioned above the values corresponds to both the geo-cellular as well as the simulation model.

Table 4-6: Original Fluids in Place of the Model

	Oil [MMSTB]	Gas [MMscf]	Water [MMSTB]
Entire Field	150.5	63,258.3	1,747.7
Hakim North	13.7	25,794.1	406.3
Hakim South	136.7	37,464.2	1,341.3

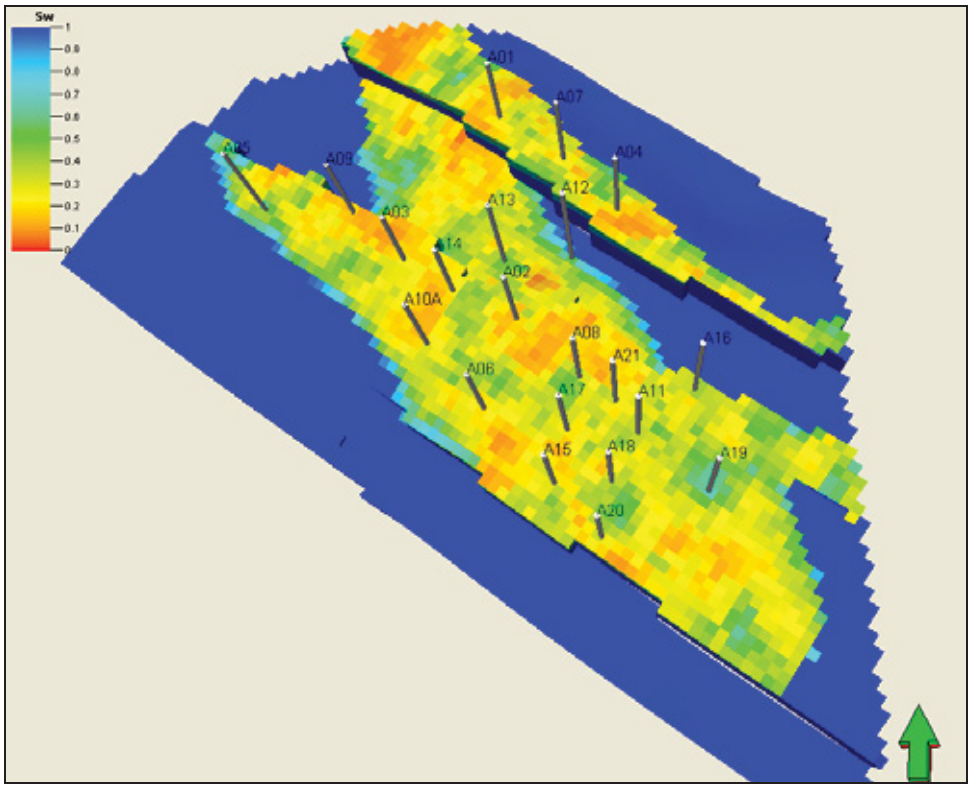

Figure 4-20: Initial Water Saturation Distribution

4.6 Saturation Table Scaling

Non-equilibrium initialization procedure has been applied in order to initialize the model; hence the water saturation as resulting from the upscaling process has been assigned to each simulation block.

From the SCAL analysis normalized relative permeability curves have been derived and endpoint scaling was used; i.e. the relative permeability curves are scaled for every block according to the defined critical water saturation and irreducible oil saturation. The critical water saturation was determined on the geological model and equals the initial water saturation above the water oil contact.

4.7 History Matching

4.7.1 Objectives of the Simulation Study

The main objectives of the study were:

- To develop 3D mathematical models for North and South Hakim fields
- To determine OOIP, movable oil distribution and locate unswept and/or bypassed oil
- To Maximize the reserve by investigating various depletion strategies

According to these objectives, the reservoir simulation work had been carried out in three phases:

Phase 4.a: Dynamic model construction

Phase 4.b: History Matching

Phase 4.c: Predictions

4.7.2 Simulation Software Tools

The Geo-model construction and property population as well as the simulation model grid building and upscaling was performed using PETREL. All simulation runs performed in context of this history matching work were performed using ECLIPSE 100.

4.7.3 History Matching Workflow

The entire work was performed in a strictly integrated manner; i.e. right from the beginning when the first geo-model realization was available dynamic runs were performed in order to gain understanding of the reservoir and consequently guide the modeling process; hence already the geo-model was conditioned to the available dynamic data.

This process as depicted in Figure 4-21 is called dynamic conditioning. The motivation to perform this rather time intensive workflow is that right from the

beginning the observed the dynamic response of the model significantly improves the understanding of the reservoir behavior. It helps to resolve data conflicts very early in the study, as in the dynamic model all input (both static input like structural information, petrophysical properties …. as well as dynamic data like SCAL, PVT …) is compiled together.

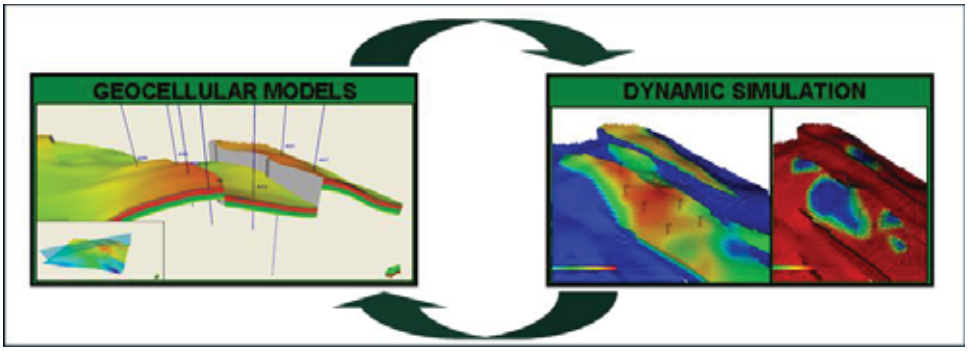

Figure 4-21: Conditioning of the Geo-model to dynamic data

The most important benefit of "dynamic conditioning" is that it is the only true measure of the geo-models quality and leads finally to a model that provides an optimum basis for the detailed history match. During the dynamic conditioning a geo-cellular model was derived which provided already a sufficiently good field match.

For the detailed History Matching process the following data was available in order to match the model:

- Produced and Injected Fluids (from January 1985 until February 2009)
- Oil
- Water
- Gas
- Well Pressure Measurements
- Salinity of Produced Water (since May 1997 continuously measured)
- Initial Brine Salinity 115,000 ppm
- Fresh Water Injection
- RFT – Vertical Pressure Distribution
- PLT – Individual Perforation Inflow

Sufficient and good quality data was available in order to match the reservoir model. The challenge in the detailed matching was twofold, once strong water injection program which was initiated right with the beginning of the continuous production of the field which lead to a strong interaction between the producing and injecting wells, and secondly wide parts of the field are totally swept already leading to the fact that the entire saturation history in those field has to be modeled and matched.

Table 4-7 presents the cumulative produced and injected fluids for the two parts of the field, Hakim North and Hakim South.

Table 4-7: Cumulative Produced and Injected Fluids (until February 2009)

	Oil Produced	Water Produced	Water Injected
Hakim North	3.5 MMSTB	6.6 MMSTB	9.5 MMSTB
Hakim South	25.5 MMSTB	40.6 MMSTB	54.6 MMSTB

The average salinity map presented in Figure 4-22 indicates that wide parts of the field are already entirely flooded by the injected water.

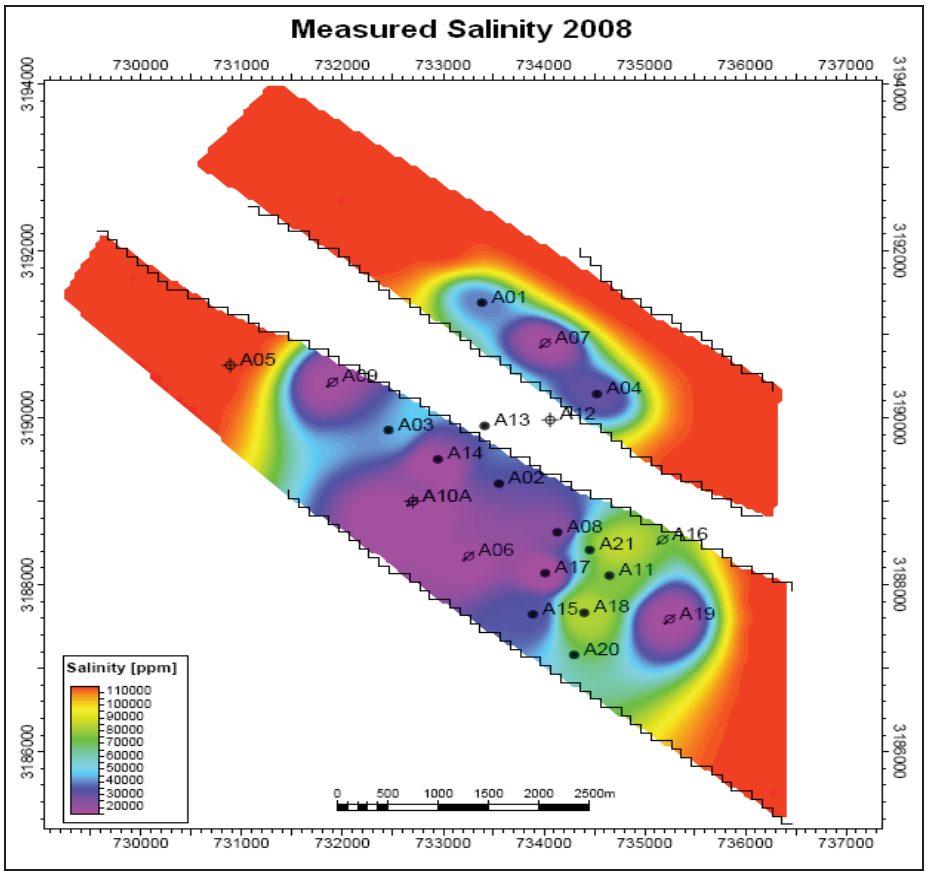

Figure 4-22: Average Salinity Distribution in 2008

For the detailed well by well match the model was operated by net oil rate production control. The only changes introduced during process were moderate permeability modifiers and flow efficiency multipliers for individual perforations.

4.7.4 Updates and Changes on the Simulation Model

The geomodel was conditioned to dynamic data already resulting in a reservoir model that is overall valid and can be seen a field match already. Consequently the changes that had to be introduced to the simulation in order to achieve a well by well match were minor.

During the detailed matching neither structural modifications nor porosity changes were necessary. The only changes applied by the author to the model were flow efficiency multipliers for the individual perforations and permeability multipliers.

Transmissibility values across the faults have been kept unchanged, with the only exception of the main fault separating Hakim North from the Southern area.

4.7.4.1 Relative Permeability Modifications

Four rock regions (or Saturation Region) were used during history matching. The areal distribution of the individual rock regions is shown, Figure 4-23. In vertical direction a stack of simulation cells has the same rock region. The rock regions differ only in the oil water relative permeability curves.

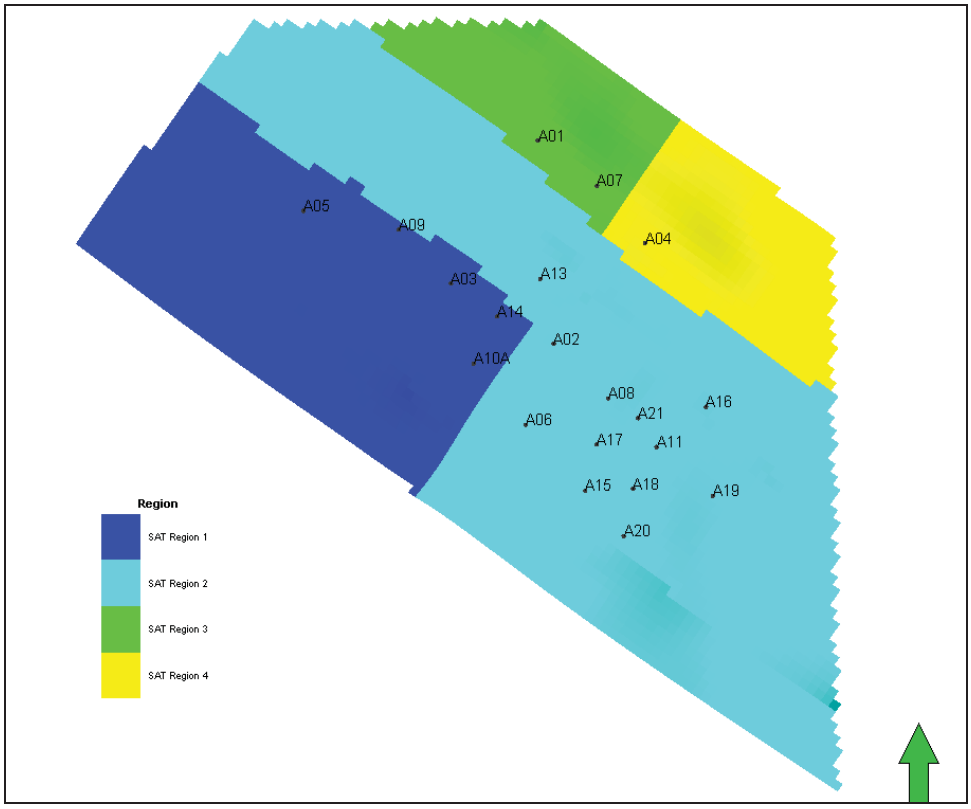

Figure 4-23: Distribution of the four rock regions used

The difference of the individual saturation region is in the shape oil relative permeability curve only. The water relative permeability curve is exactly the same for every region. For the saturation region number 4 the shape of the oil relative permeability curve has been used exactly as determined in the SCAL analysis performed. In case of region number 1, 2 and 3, the shape was slightly adapted in order to improve the match. Figure 4-24 presents the water relative permeability curve and the four different oil relative permeability curves.

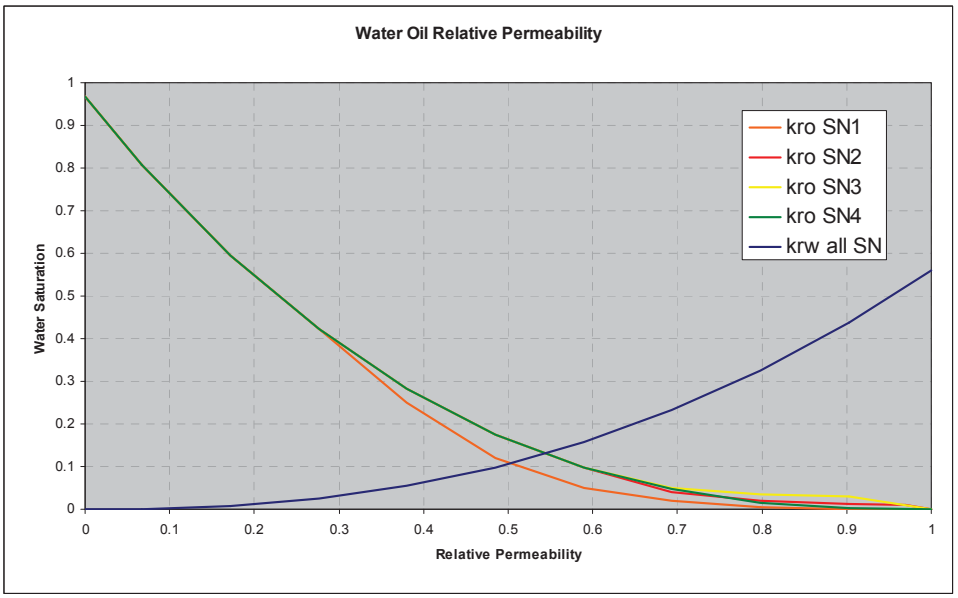

Figure 4-24: Oil water relative permeability curves for the individual rock regions

4.7.4.2 Permeability Alterations in the HM model

To achieve a well by well history match the permeability distribution was changed on two levels:

- Regional changes e.g.: on volume region level
- Local changes in the vicinity of the individual wells.

Aim of all these permeability changes was to optimize the communication between the injectors and the producers to tune the calculated water cut of the wells, to match the historical ones.

The Figure 4-25 below presents the final permeability distribution for each layer.

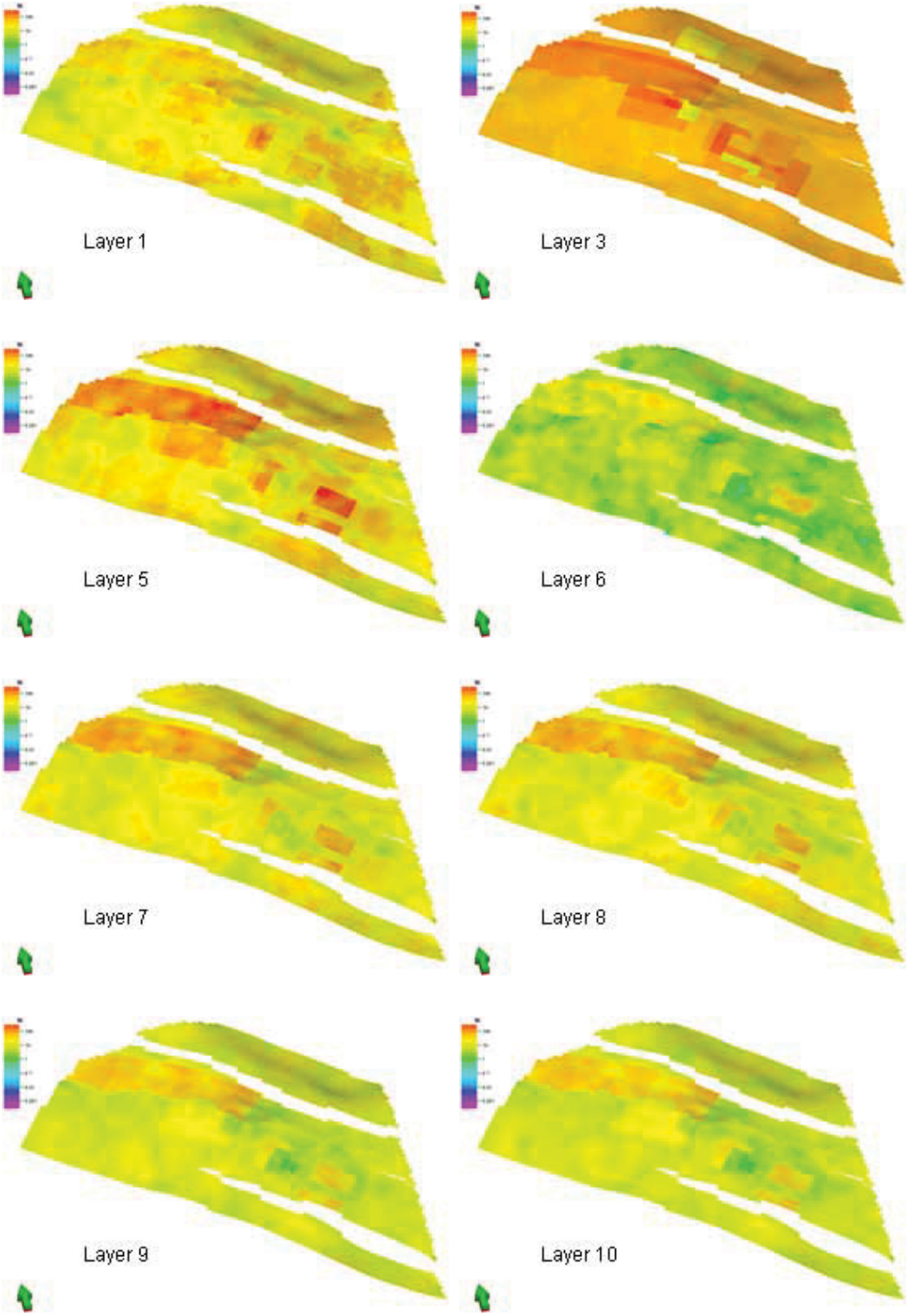
Layer 1
Layer 3
Layer 5
Layer 6
Layer 7
Layer 8
Layer 9
Layer 10

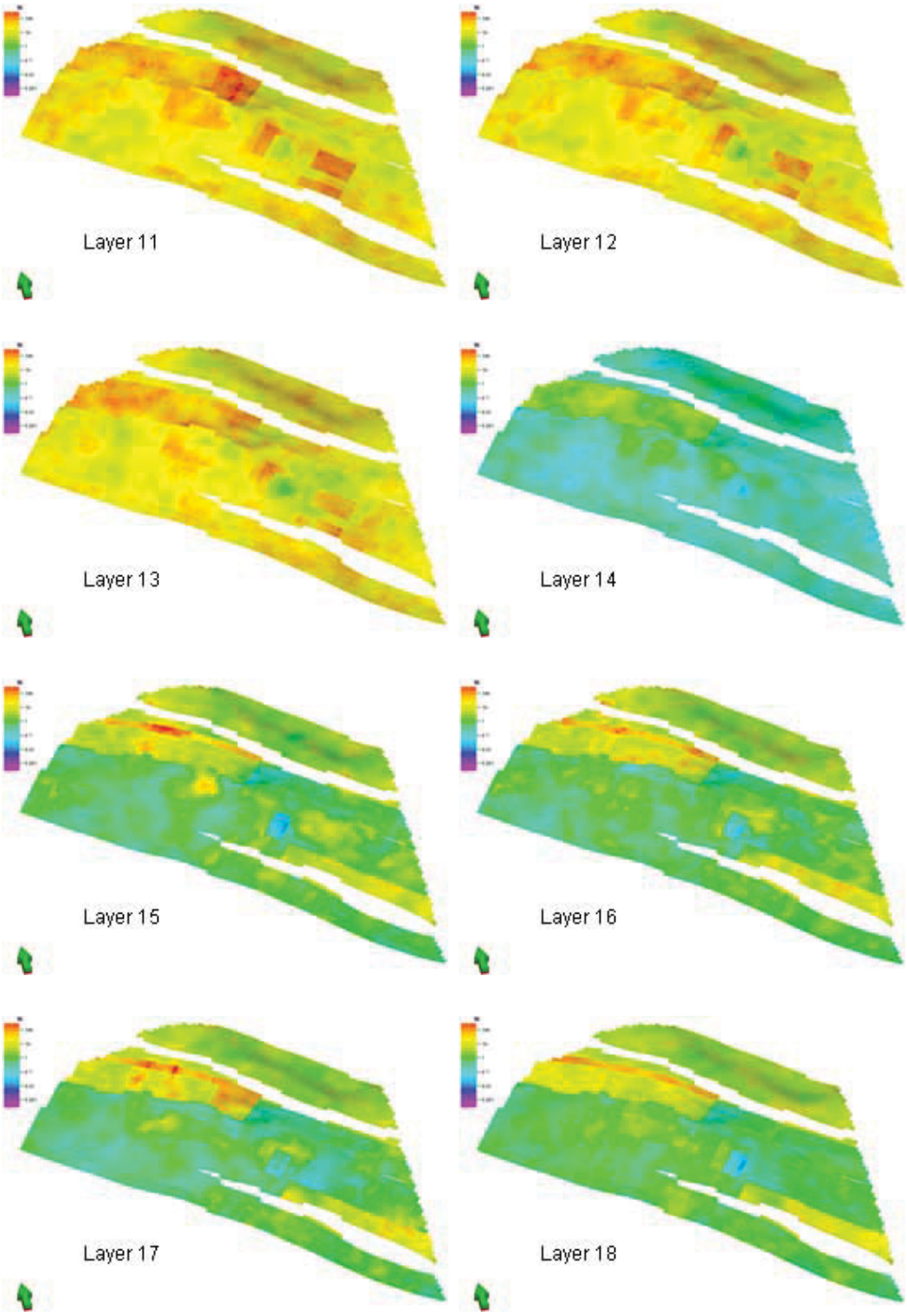
Layer 11
Layer 12
Layer 13
Layer 14
Layer 15
Layer 16
Layer 17
Layer 18

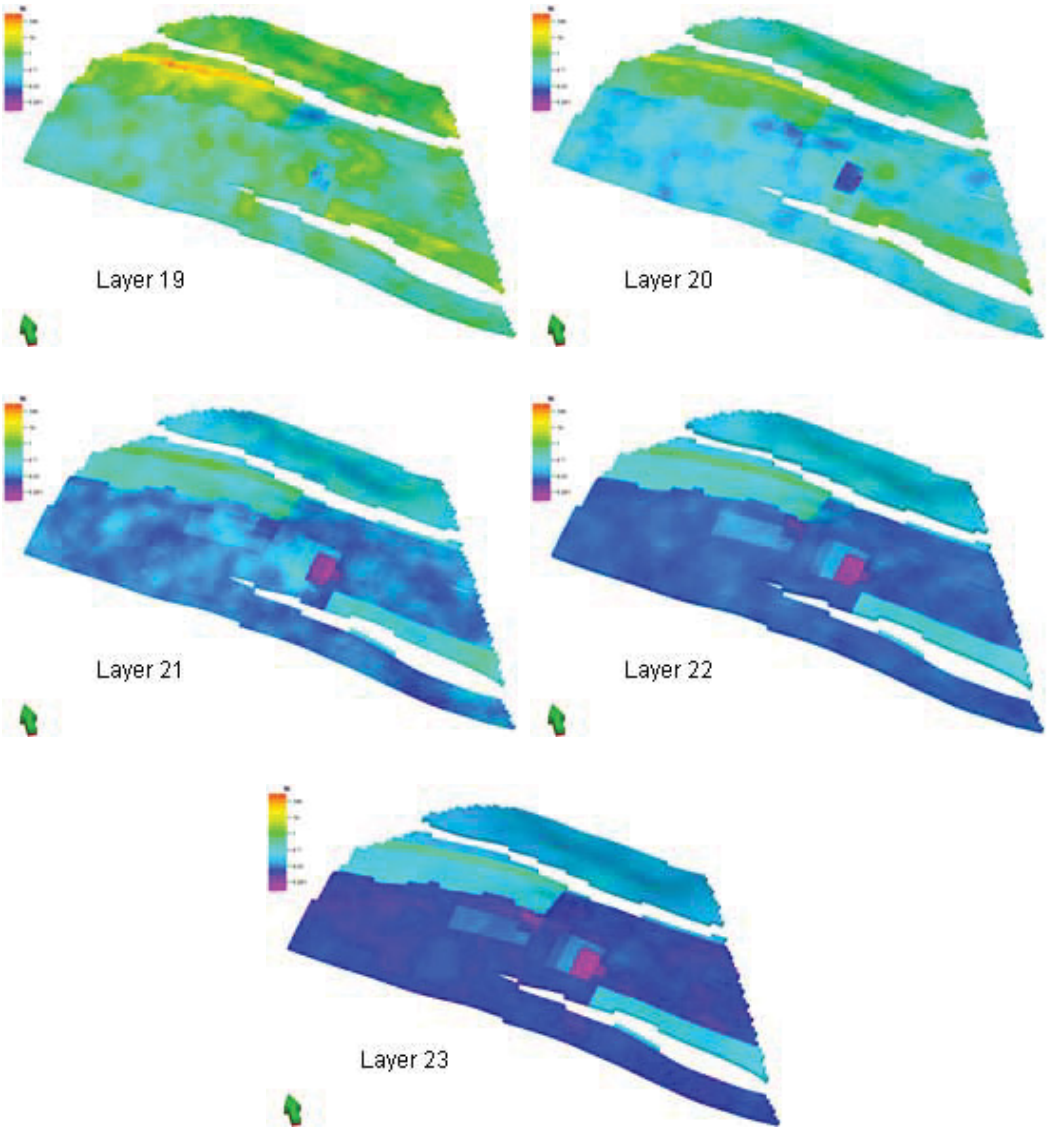

Figure 4-26: Final permeability values for each layer

4.7.4.3 Flow Efficiency Multipliers for Individual Perforations

Flow efficiency multipliers have been used in order to guide production and injection and further calibrate flowing bottomhole pressure. These multipliers were introduced at the date when the well was completed or recompletion was performed. These flow efficiency multipliers were then kept constant for the entire run. The only exception are the wells in Hakim North, were obviously over time the injection/production shifted to the upper layers, probably due to scaling. For these wells the flow efficiency for the zones Facha A, Facha B and Fache C1 was increases when the field was shut-in in 1994.

4.7.4.4 Aquifer Parameters

To model additional edge aquifers in the reservoir model 6 boundaries with corresponding Fetkovich analytical aquifer were defined. Figure 4-27 shows the analytical aquifer boundaries added to the reservoir model.

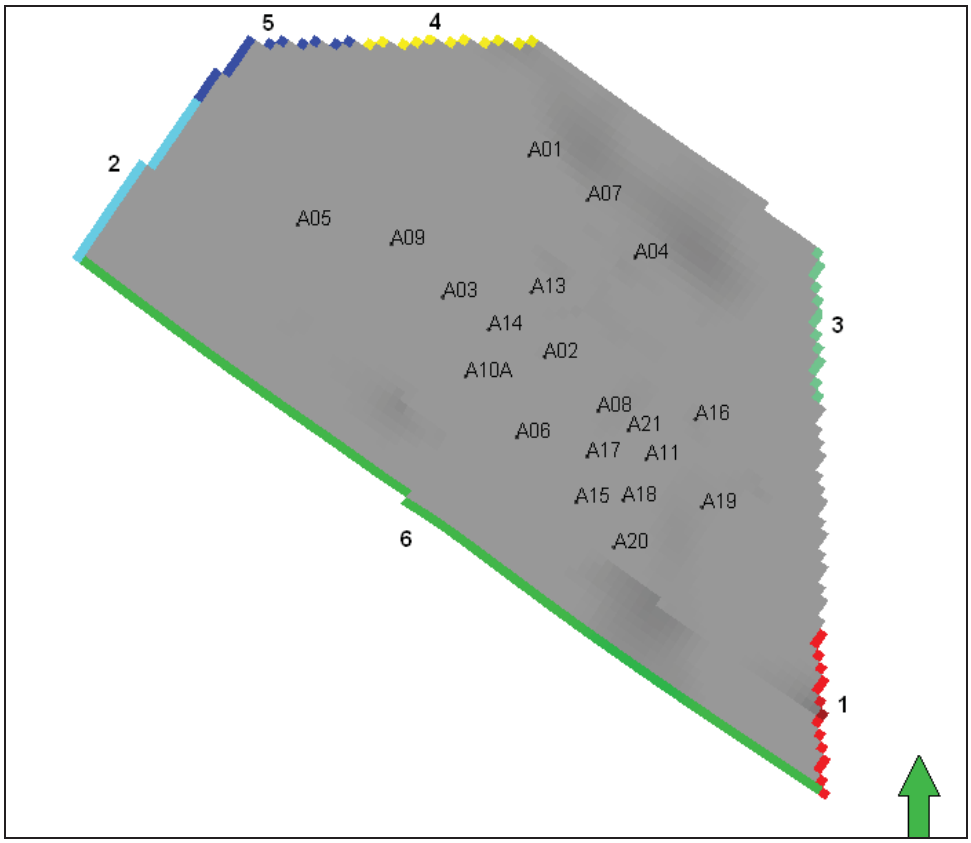

Figure 4-27: Top view of the reservoir model with the individual analytical aquifer boundaries (colored blocks)

The main portion of the water influx entered the reservoir across the boundary 5 which is connected to the graben area. Around 68% of the total water influx enters into this region as no water injection is performed in the graben. From the other boundaries the influx is very minor or even negative as in case of boundary 2 and 6 the high injection volume pushed water into the analytical aquifer.

Table 4-8: Fetkovich Analytical Aquifer Parameters and Results of the History Matched Hakim Model.

Hakim: Summary of Analytical Aquifer Data and Cum. Water Inflow at End of History Match Period			
Boundary	VINIT	AQUIJW	Cum. Water Inflow
	[STB]	[STB/day/psi]	[MMSTB]
Bound1	5E+9	5	0.91
Bound2	5E+12	10	-0.43
Bound3	5E+9	50	1.21
Bound4	5E+9	10	1.80
Bound5	5E+10	100	5.38
Bound6	5E+12	10	-0.91
		Sum	7.96

The total amount of water inflow from all six analytical aquifers is 7.96 MMstb. The cumulative water injection over the history period is 66.30 MMSTB and 49.11 MMSTB have been produced.

4.7.5 Results of History Match

Table 4-9 summarizes the key data of the simulation model.

Table 4-9: Summary of the Basic Simulation Model Data

Basic Data of History Match Model – Hakim North and South	
Start of Simulation Period	1985/01/01
Start of Production	1985/04/01
End of HM period	2009/02/28
Block size	100 m x 100 m
Number of simulation layers	23
Number of active blocks	77,973
OOIP entire Field	150.5 MMstb
OOIP Hakim North	13.7 MMSTB
OOIP Hakim South	136.7 MMSTB
Initial reservoir pressure North	2540 psia @ 5700 ftSS
Initial reservoir pressure South	2678 psia @ 5700 ftSS
Aquifer model	Fetkovich type
Number of active wells	19
Production control	well rate, monthly average
Average time step	15 days

As already written in the introduction the main objective of this phase of the work is, beside the assessment of the original oil in place, to determine the movable oil distribution and locate unswept and/or bypassed oil.

In both Hakim South as well as Hakim North significant water injection using fresh water is performed the key aspect to achieve the objectives is to model the injector/producer communication as close as possible. To understand and assess the distribution of the injection water in the reservoir and consequently assess the swept/unswept areas and the bypassed oil two crucial calibration data are available. As the injected water is fresh water this is on one hand side, the salinity measurements of the produced water and additionally the water breakthrough in all the production wells. At the end of the history all wells produce water already.

Figure 4-28 presents a map generated from the measured salinity values at 2008 on top and the calculated salinity distribution in this year. The map was generated based on the individual well measurements. The calculated salinity values are the average block values, averaged over the Facha A, Facha B and the Fache C zones.

From this Figure an excellent agreement can be seen in the salinity values. In the Hakim North the injected water of A7 reached both producers relatively early and a big portion of the produced water is the injected one.

In the graben area no decrease of the salinity of the produced water (well A13) was observed. This can be seen also from the calculated salinity distribution, as no injection water entered in to the graben area and consequently the entire water production of A13 is reservoir brine.

The area including the producers A3, A14 and A2 is nearly entirely swept. This becomes obvious from the low measure salinity and the high water cuts. Again the very close agreement in the calculated salinity can be seen.

The area having the biggest remaining production potential is located between the two injectors A6 and A19. The average front of the injected water is delimited by A8, A17 and A15 towards North West and A11 and A18 towards South East. Again the calculated salinity reproduces the measurements very close.

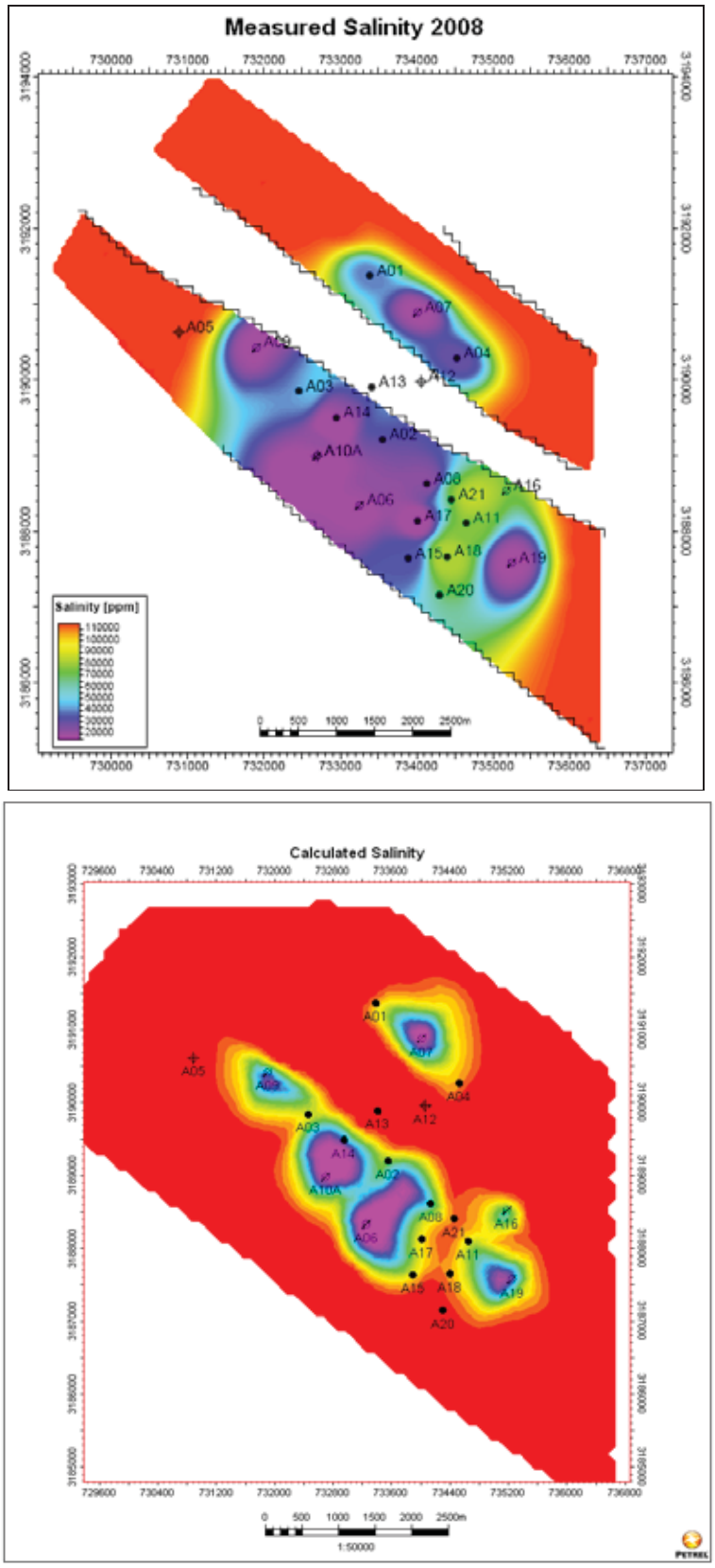

Figure 4-28: Salinity distribution in 2008 – map of measured one, bottom calculated one

In terms of water production and water breakthrough a good match could be achieved for all wells, except for well A14 and A15.

A14 which are located in the already entirely swept area of the water breakthrough.The water cut trend could be matched very well. The well produces since the year 2000 at very high water cut of more than 95% and in the last years at an average of 96%. Figure 4-29 presents the water cut and the oil production rate for the well.

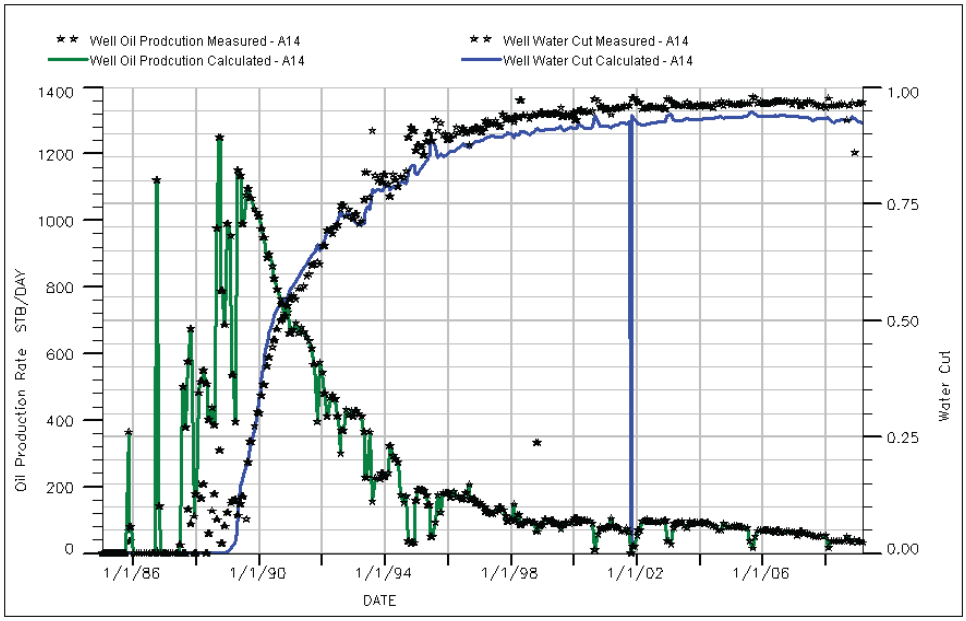

Figure 4-29: Oil production and Water Cut for well A14

The calculated water cut in the last years is on an average 93%, which basically agrees well with the 96% measured one. But when considering the water production rate the difference is significant. This discrepancy results mainly from the applied well target which is the oil production rate. At the end the well produces 30-40 STB/day which is then used as target production for the well calculation. Based on this rate the water production is calculated. From block saturation point of view the vicinity of the well is very close at the irreducible oil saturation value and only very minor inaccuracy in this data causes the mismatch.

In case of A15 the strong interference between the individual neighboring wells can be observed. Figure 4-30 presents the water cut and the oil production rate for the well A15. The water cut of this well is influenced from the production well

A18 and especially of A17 and in addition from the two injectors A6 and A19.

The decrease in the water cut after 1998 is due to the fact that injection by A19 pushes oil from the South towards A15. During the time when well A17 is shut in July 2004 until October 2006 one can see the increase in the well A15. To model the measured behavior of this well more exactly is seen to be beyond the model resolution.

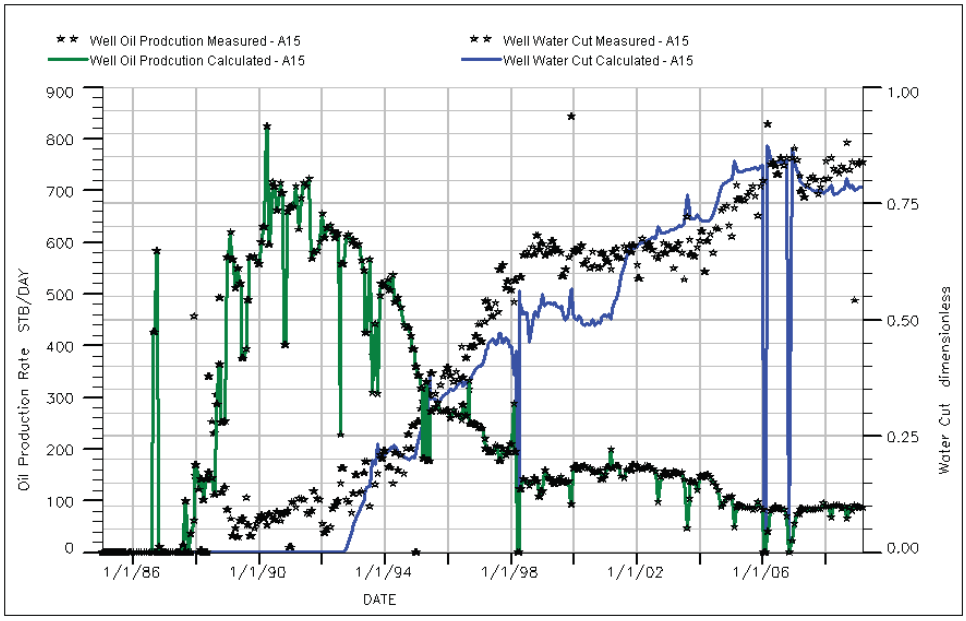

Figure 4-30: Oil production and Water Cut for well A15

Figure 4-31, Figure 4-32, Figure 4-33 and Figure 4-34 below present the combined, or group oil production rate, liquid production rate, water and water injection rate, respectively for Hakim North. All plots show the measured values by stars and the calculated one by continuous lines.

For Hakim South Figure 4-35 presents the comparison of the measured to calculated RFT data. Figure 4-36, Figure 4-37, Figure 4-38, Figure 4-39 compare again the group oil production rate, liquid production rate, water and water injection rate, respectively for Hakim South.

4.7.5.1 Hakim North

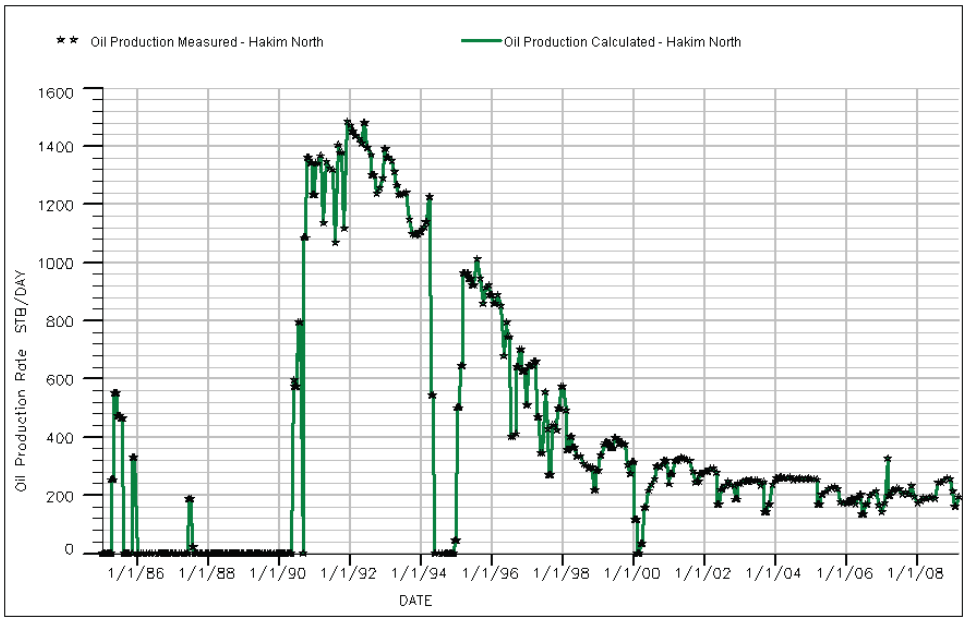

Figure 4-31: Oil production rate for Hakim North

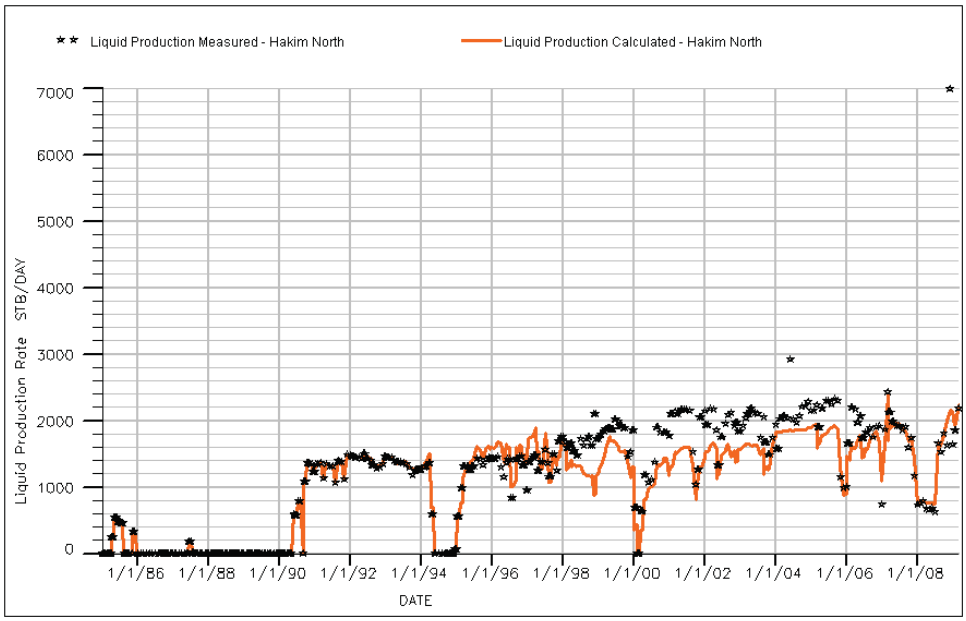

Figure 4-32: Liquid production rate for Hakim North

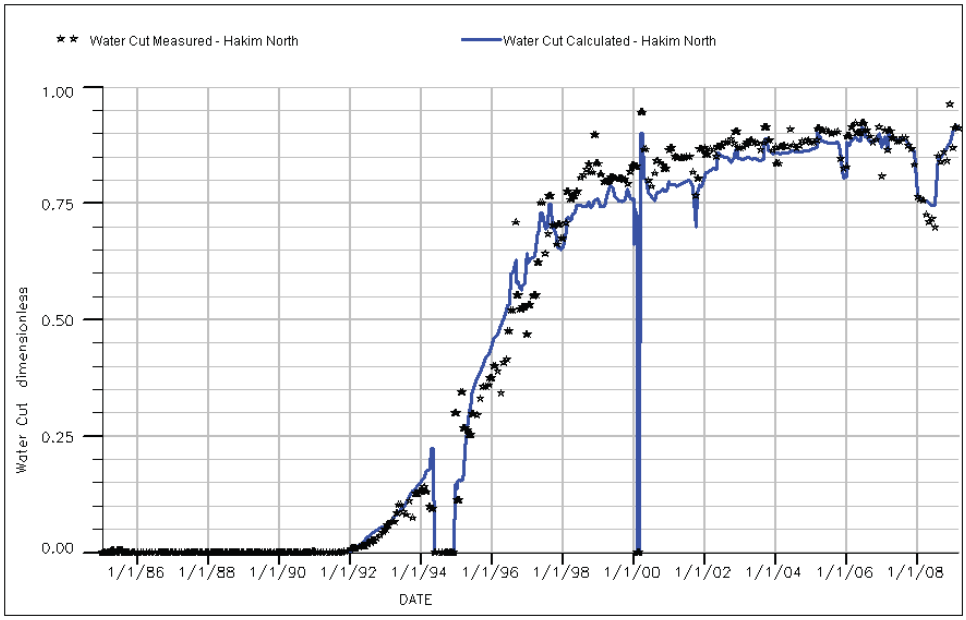

Figure 4-33: Water Cut for Hakim North

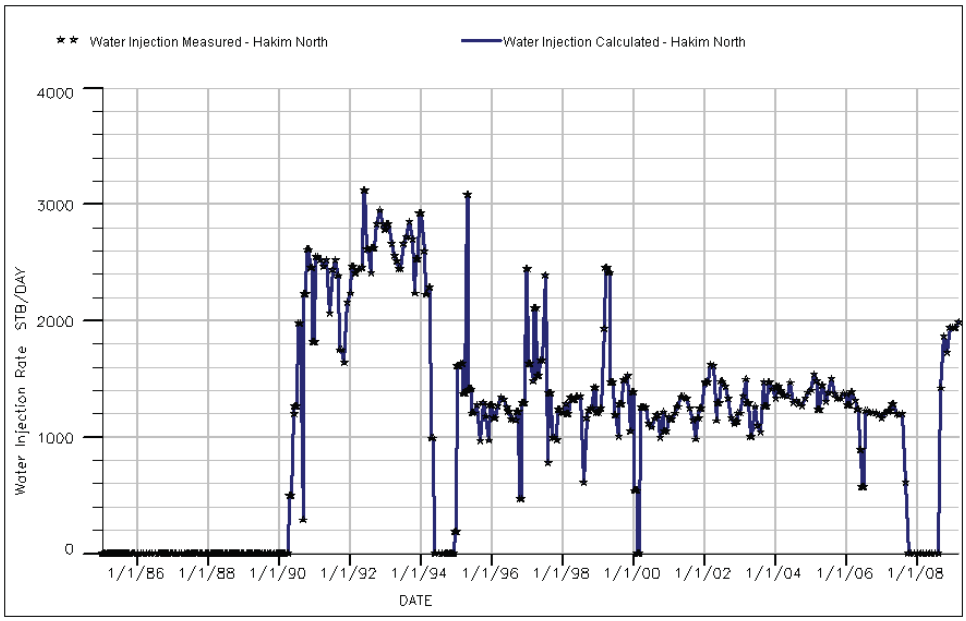

Figure 4-34: Water injection rate for Hakim North

4.7.5.2 Hakim South

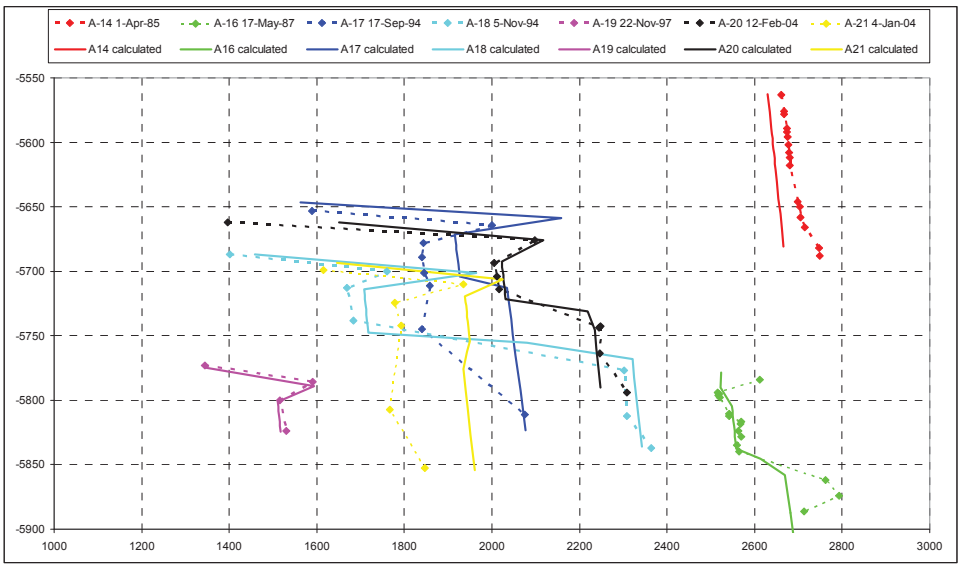

Figure 4-35: Comparison of RFT – Measured values dotted lines, Calculated in continuous lines

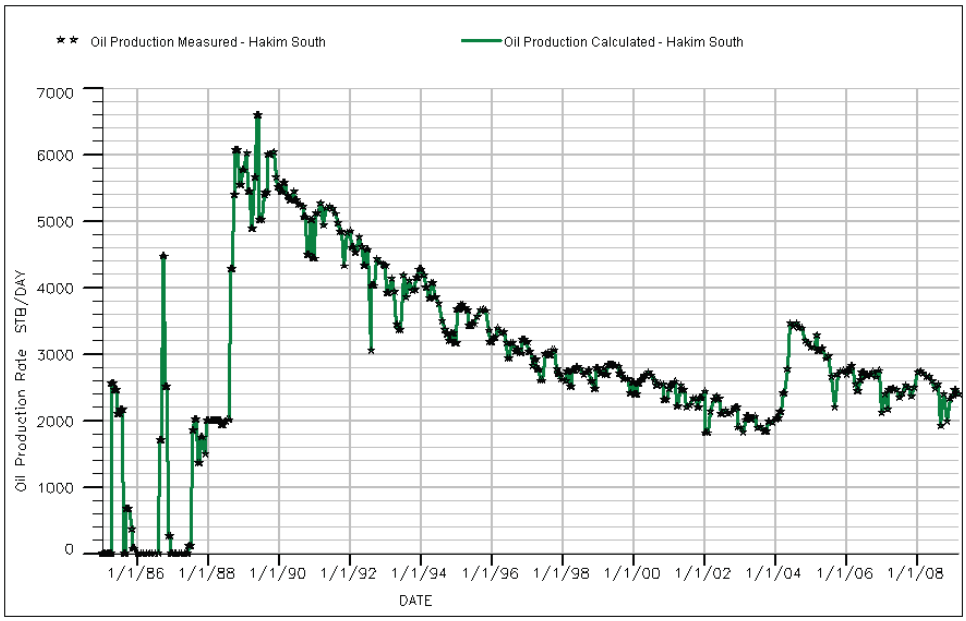

Figure 4-36: Oil production rate for Hakim South

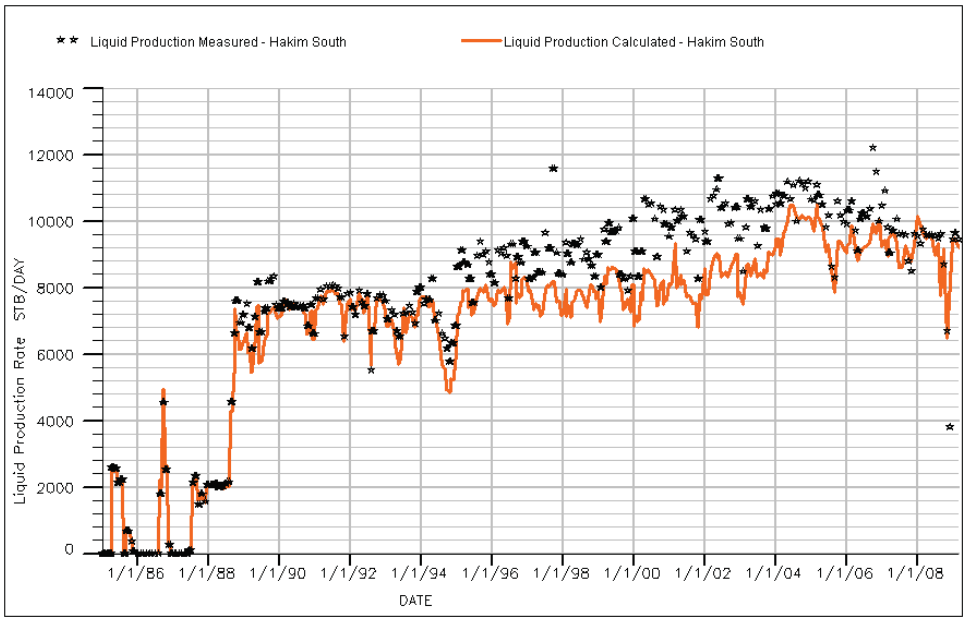

Figure 4-37: Liquid production rate for Hakim South

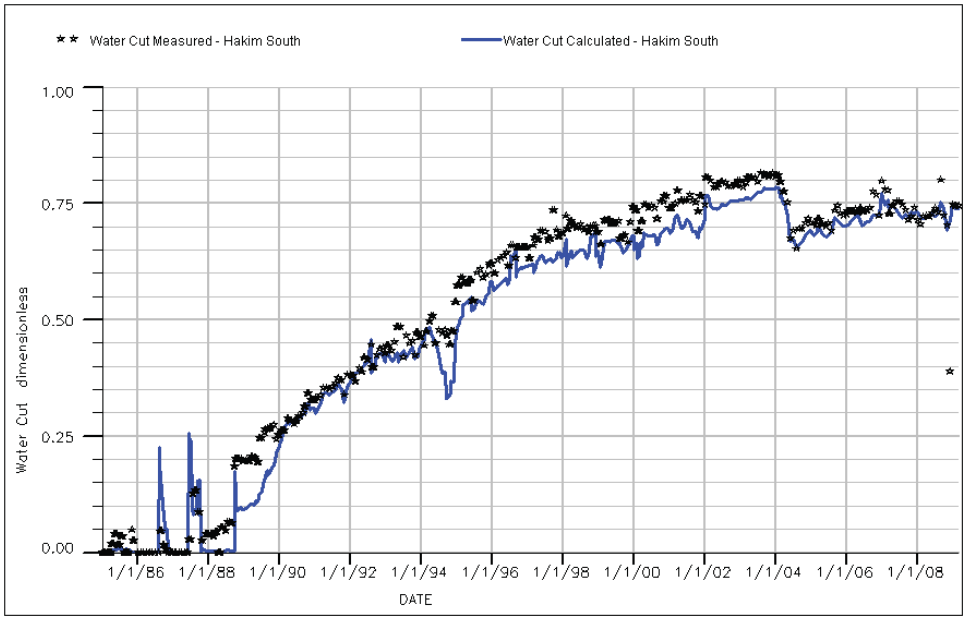

Figure 4-38: Water Cut for Hakim South

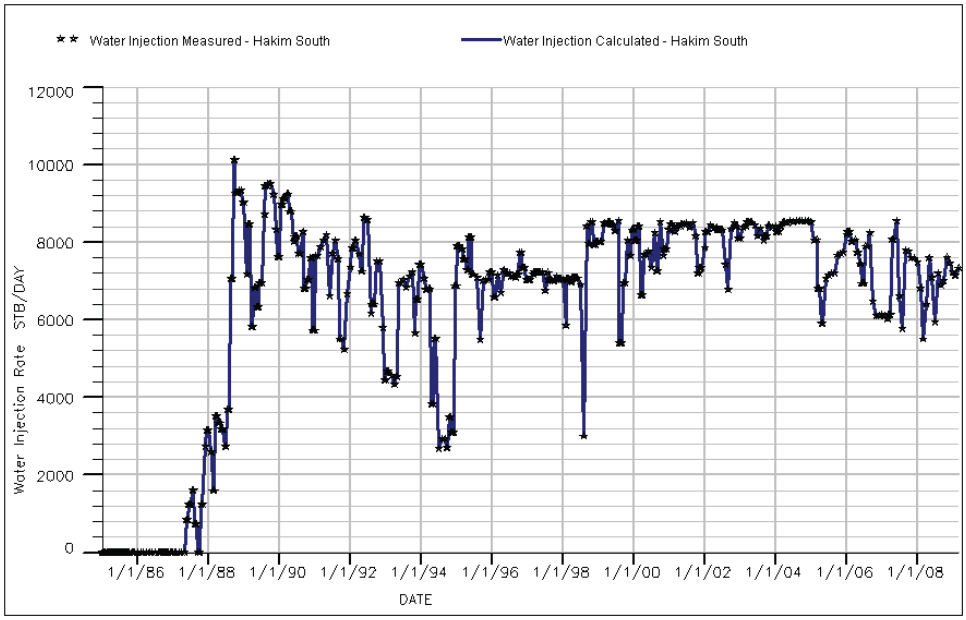

Figure 4-39: Water injection rate for Hakim South

4.7.5.3 Moveable Oil Distribution Plots

Figure 4-40 presents the initial movable oil distribution. The unit of the movable oil quantity is reservoir barrel per square meter [rbbl/m²]. Figure 4-41 is the corresponding picture of the moveable oil distribution at the end of the historical period in February 2009.

From the distribution plot at the end of the history period it becomes obvious that some areas in the field are entirely swept. In the Hakim North area the entire are from A1 over A7 to A4 and southeast wards is watered out already, no significant oil production potential is left in that area anymore. The last remaining oil is North West of A1.

In the graben area the situation is similar and significant amount of produceable oil volume is left in the area close to A1.

In the main part of Hakim South the area A5, A9, A3, A14 to A2 is also significantly watered out. And the main potential for production is left in between the main active producers in that are A6 and A19, hence in the area around A21 and A20. this area is delimited by the wells A8, A17, A15 and A11 and A18 which produce at high water cut and in case of A17 are already shut in. North of

A21 and along the fault towards A13 good potential of remaining, bypassed oil can be seen.

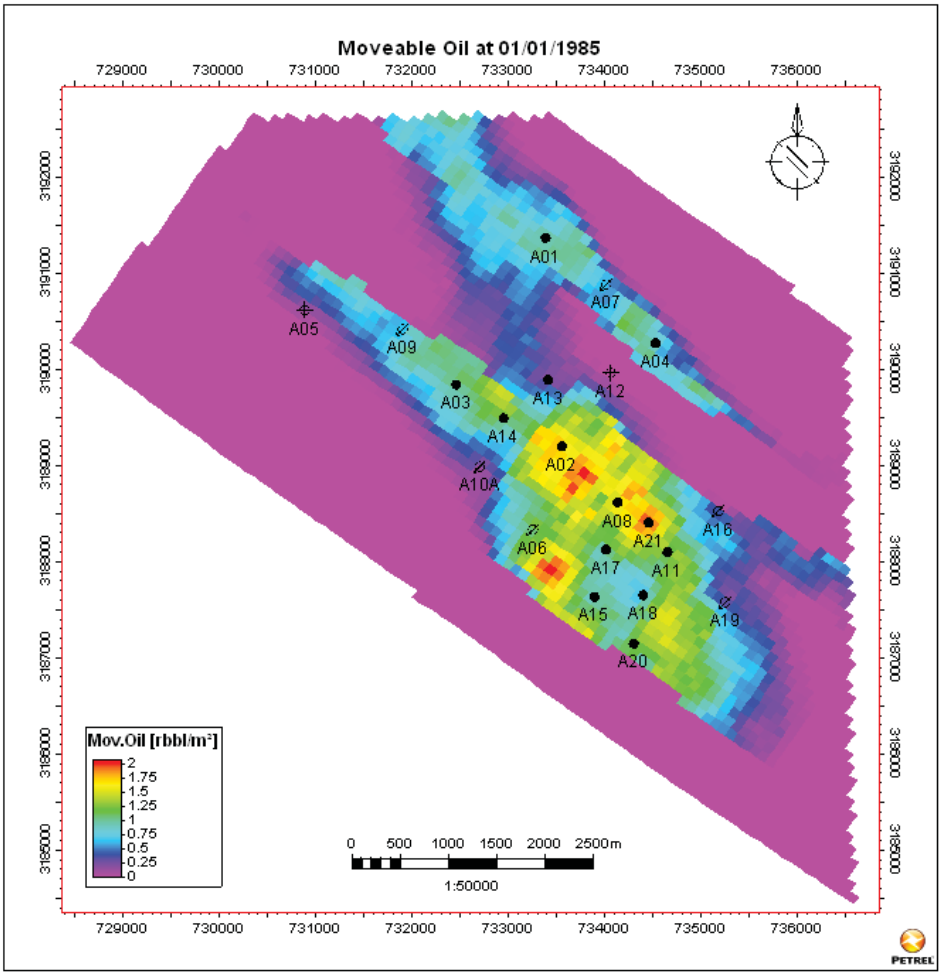

Figure 4-40: Initial moveable oil distribution

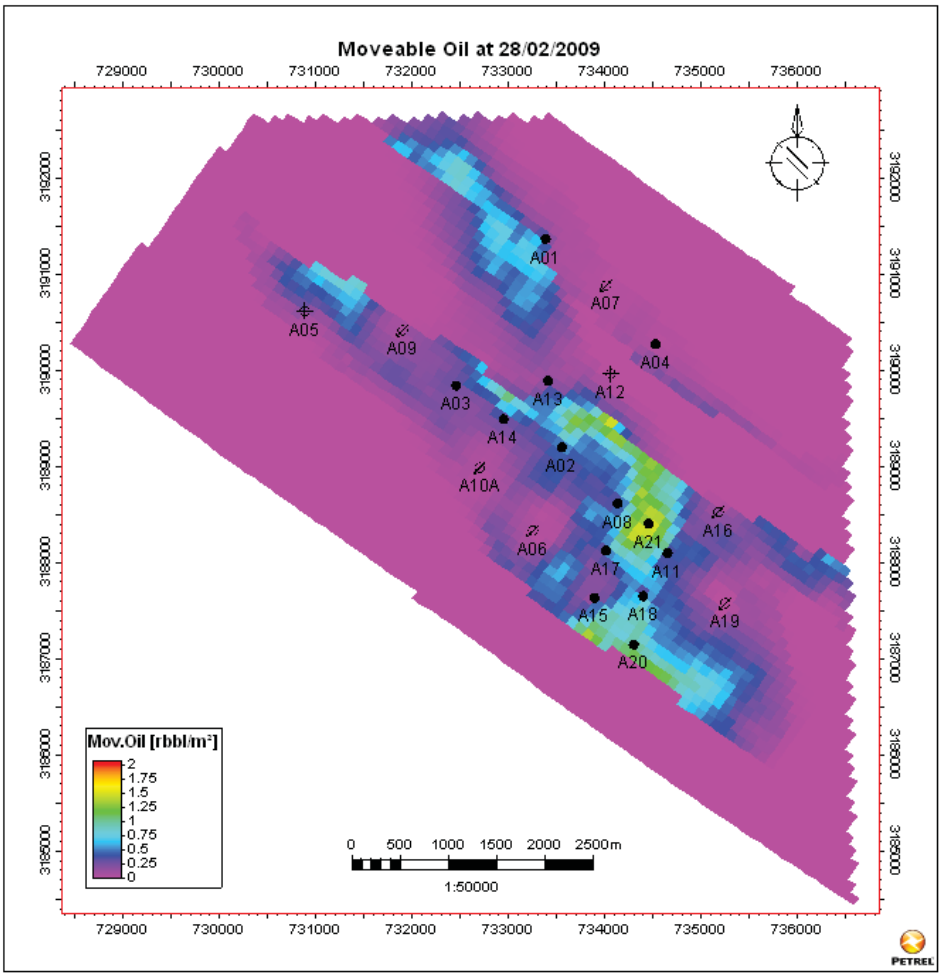

Figure 4-41: Moveable oil distribution at the end of the historical period

Chapter 5

5 Comparison of Independent and Commingled Production

This master thesis should assess the benefits of an optimized reservoir zone production and injection for each separated reservoir unit for such a type of reservoir compared to simple commingled production; i.e. to assess the possible improvement of production optimization technique like Intelligent Well Completion Techniques.

To assess the possible improvement of a production optimization technique, Intelligent Well Completion Techniques have been setup, assuming the possibility of controlling the inflow of individual perforations over time. For example, Intelligent Well Completions are available for the Facha A, Facha B and Facha C zones.

An intelligent completion controls the production from different well intervals by means of downhole-chokes. This functionality was introduced into the simulation model by flow efficiency modifiers for the individual perforations using 'WPIMULT' keyword in the ECLIPSE software.

The following six wells have been considered as candidates for intelligent completions: A2, A3, A8, A11, A14 and A15

In the first group of runs every well was tried to be optimized in a standalone manner; i.e. for every well one run set-up was optimized with changes applied to solely one of these wells mentioned above. Optimization was done by introducing the flow efficiency multipliers over time for the individual perforations and trying to minimize water production of the considered well. The measured well oil production was considered as target. Hence not oil production was optimized, but with the given produced oil the goal was to optimize the water production.

All the changes, assumed action of Intelligent Well Completion Techniques, determined in the six individual set-ups were then combined into one run deck. As the well spacing is relatively small in the reservoir and water injection and production rates are significantly interference between the individual wells especially in the thinner zones Facha A and Facha B can be neglected. The run should assess the interference as well as the cumulative gain of applying the technology to six wells simultaneously.

5.1 Single Well Optimization Set-up for Well A2

Figure 5-1 presents the water cut performance of the well. The blue line represents the water cut without intelligent completions; i.e. the original set-up, the history matched model. The well is completed as the real well in the field producing from the individual zones in a commingled way. The red line presents the result when intelligent completions are used. The flow efficiency of the individual perforations is changed over the run in order to minimize the water cut. Multiple runs have been performed by author in order to maximize the reduction in the water production. The graph presents the result with the highest gain in the production performance.

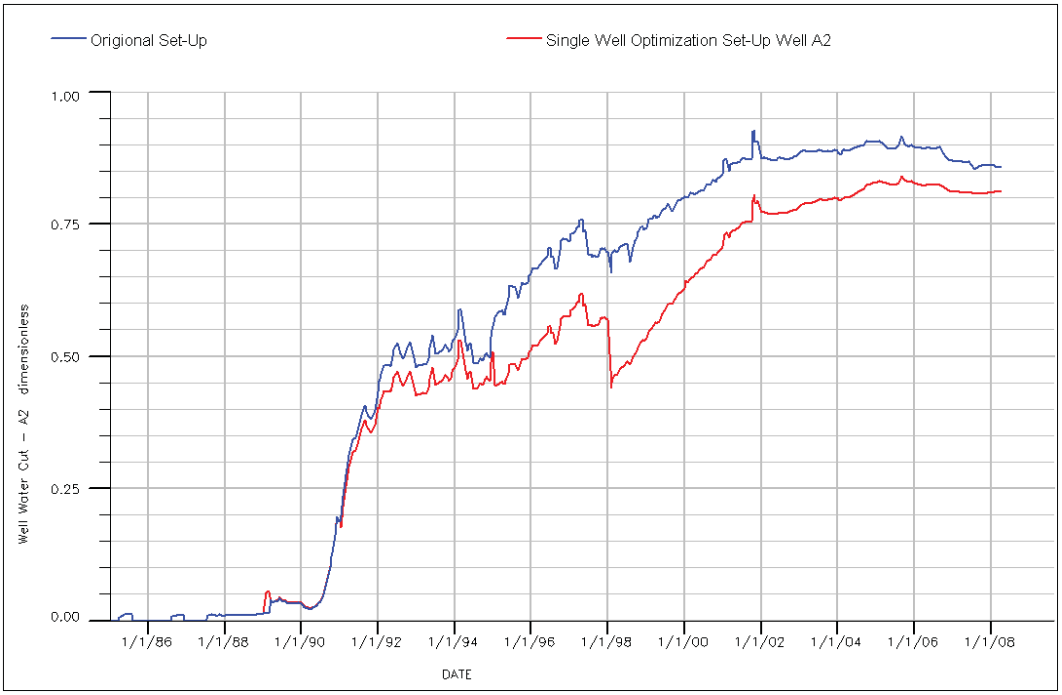

Figure 5-1: Comparison of the Water Cut for well A2; blue line not optimized commingled production, red line optimized set-up using intelligent completion

One can see already from Figure above that the improvement in the water production is significant. Table 5-1 compares the water production for the given well. The original set-up using the existing commingled production resulted in a water production of 6.73 MM STB. The optimized set-up using intelligent completions lead to a total water production of 3.76 MM STB. Hence the reduction in the cumulative water production was 2.97 MM STB equal to 44%.

Table 5-1: Comparison of the cumulative water production for the original set-up with the optimized one for well A2

Well A2 Water Production			
Original Set-Up [MM STB]	Optimized Set-Up [MM STB]	Absolute Difference [MM STB]	Relative Difference [%]
6.73	3.76	2.97	44.09

When comparing the overall field performance (Figure 5-2) no substantial gain can be seen. This is due to the fact that the individual wells strongly interact with each other. The runs set-up was optimized in a way that water production in well A2 was optimized in a way that the flow efficiency of perforations where the

water broke through from the injectors was reduced. Consequently the pressure in the vicinity of the well in those optimized layers was less reduced compared to the original set-up (no intelligent completions) resulting in higher water production by the neighboring wells in this zone. Hence the gain of less water production by the well A2 was compensated by higher water production from the neighboring wells.

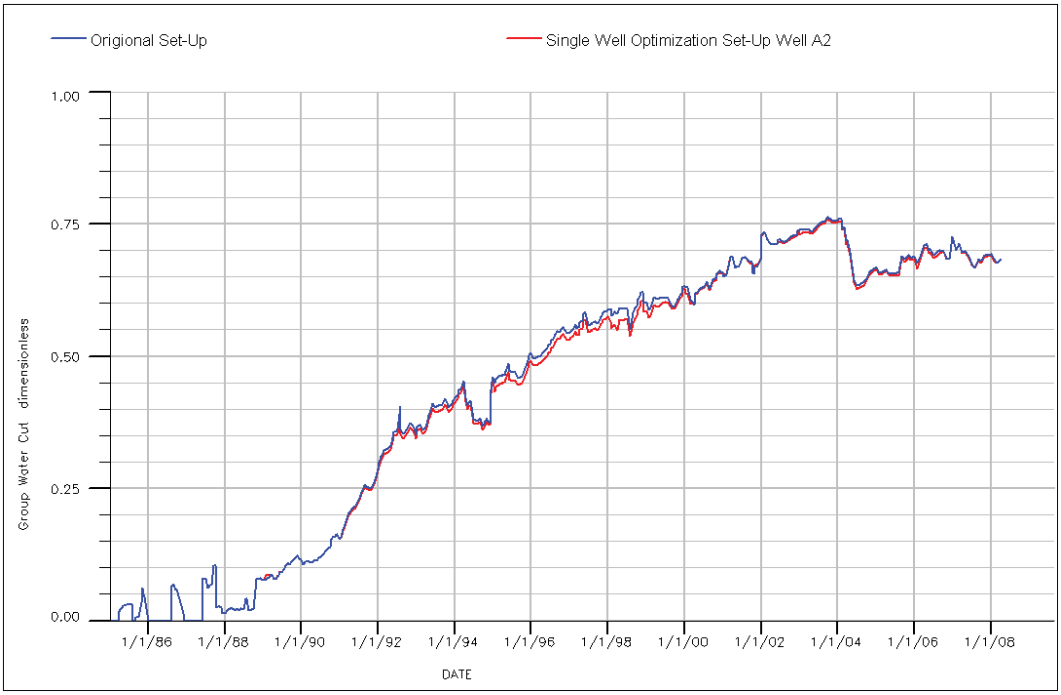

Figure 5-2: Comparison of the Water Cut for the entire field; blue line not optimized commingled production, red line optimized set-up using intelligent completion for well A2 only

5.2 Single Well Optimization Set-up Well A3

Figure 5-3 presents the water cut performance of the well. Again the blue line represents the water cut without intelligent completions; i.e. the original set-up, the history matched model. The red line presents the result when intelligent completions are used.

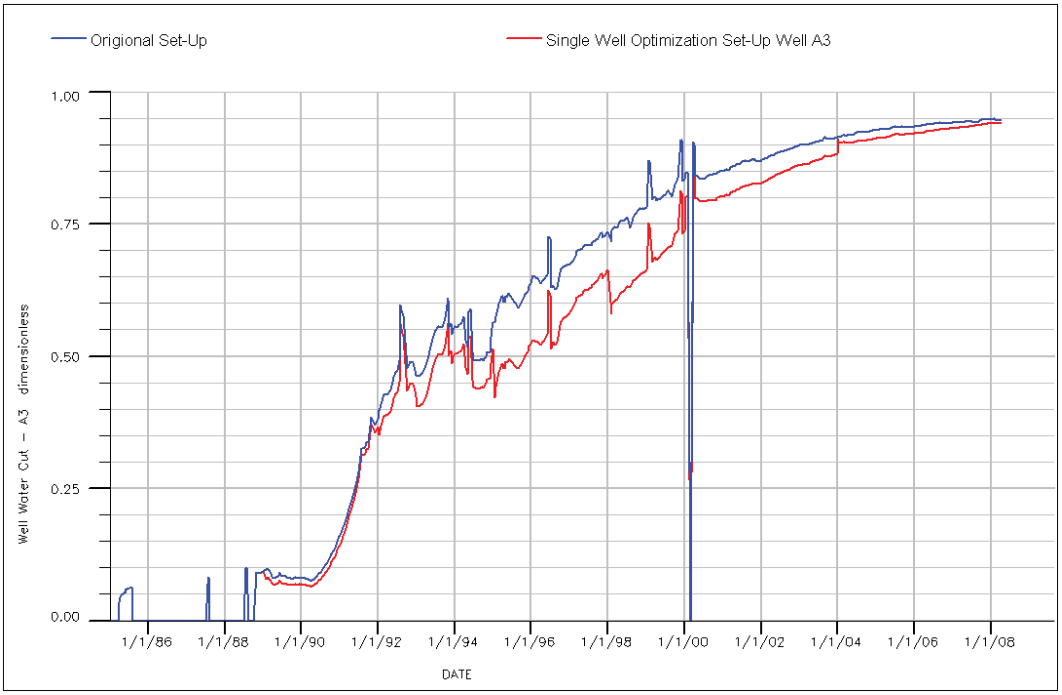

Figure 5-3: Comparison of the Water Cut for well A3; blue line not optimized commingled production, red line optimized set-up using intelligent completion

The reduction in the water production is again significant. Table 5-2 presents the calculated cumulative water production of the optimized run and the original set-up. The reduction is 1.1 MM STB of water equal to 25%.

Table 5-2: Comparison of the cumulative water production for the original set-up with the optimized one for Well A3

Well A3 Water Production			
Original Set-Up [MM STB]	Optimized Set-Up [MM STB]	Absolute Difference [MM STB]	Relative Difference [%]
4.44	3.34	1.10	24.79

In case of the field performance (Figure 5-4) also in this run no substantial improvement could be observed. Again the improvement in the water production of well A2 is compensated by neighboring wells.

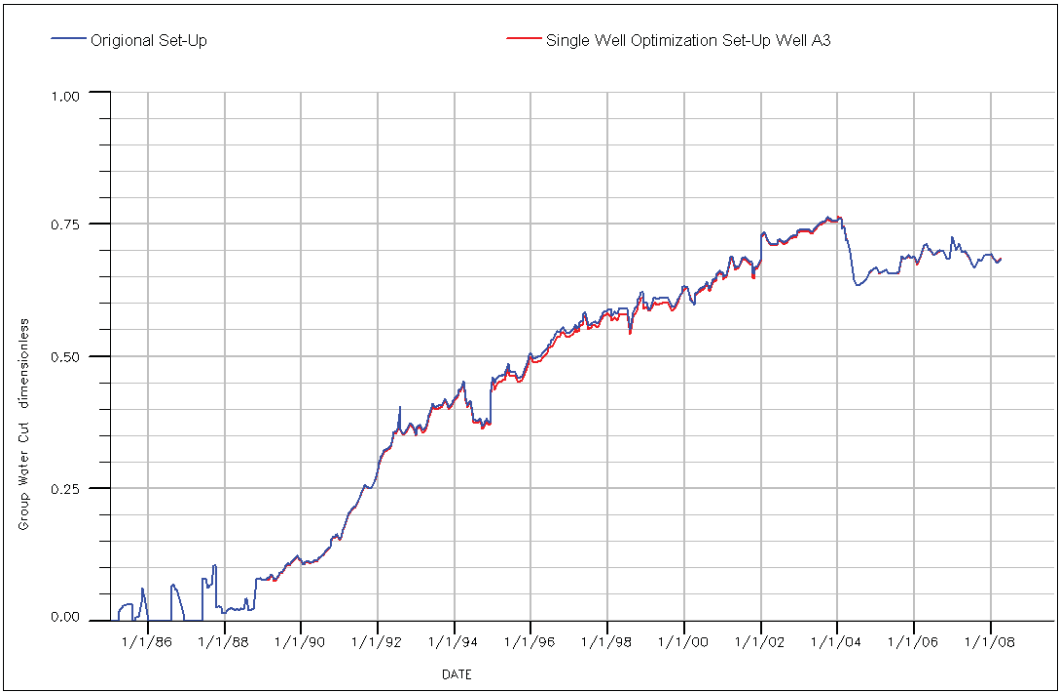

Figure 5-4: Comparison of the Water Cut for the entire field; blue line not optimized commingled production, red line optimized set-up using intelligent completion for well A3 only

5.3 Single Well Optimization Set-up Well A8

Figure 5-5 presents the water cut performance of the well for the optimized run and the original set-up. The coloring scheme is the same as in the previous sections above.

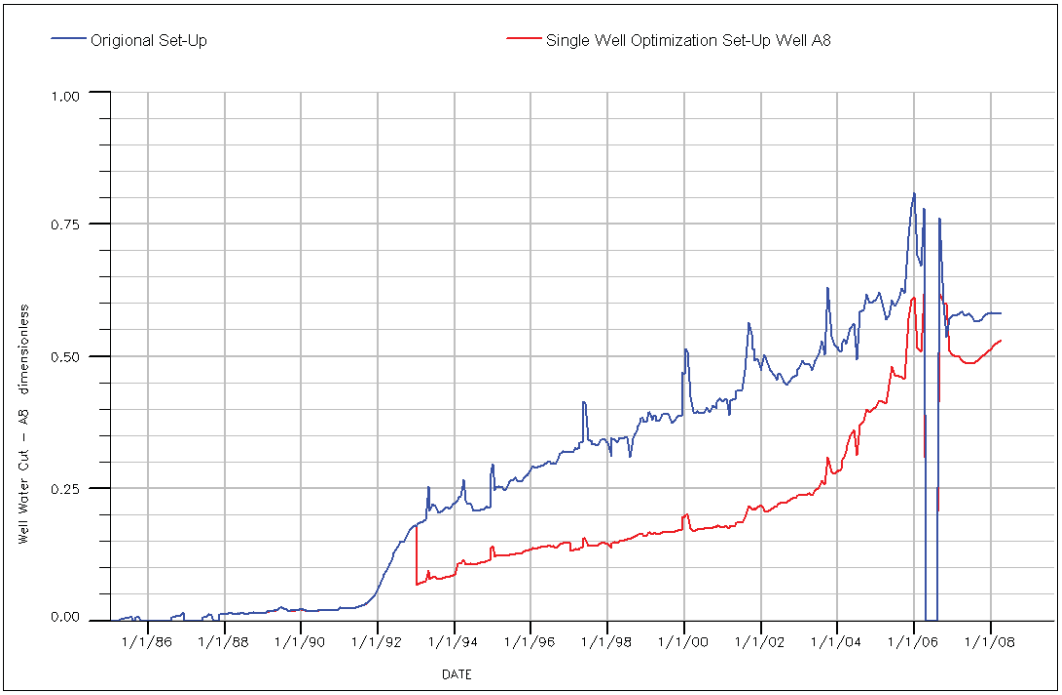

Figure 5-5: Comparison of the Water Cut for well A8; blue line not optimized commingled production, red line optimized set-up using intelligent completion

The reduction in the water production is again significant. Table 5-3 presents the calculated cumulative water production of the optimized run and the original set-up. The reduction is 0.6 MM STB of water equal to 56%

Table 5-3: Comparison of the cumulative water production for the original set-up with the optimized one for Well A8

Well A8 Water Production			
Original Set-Up [MM STB]	Optimized Set-Up [MM STB]	Absolute Difference [MM STB]	Relative Difference [%]
1.11	0.49	0.62	55.84

When comparing the field performance (Figure 5-6) nearly no improvement can be seen by optimizing only well A2.

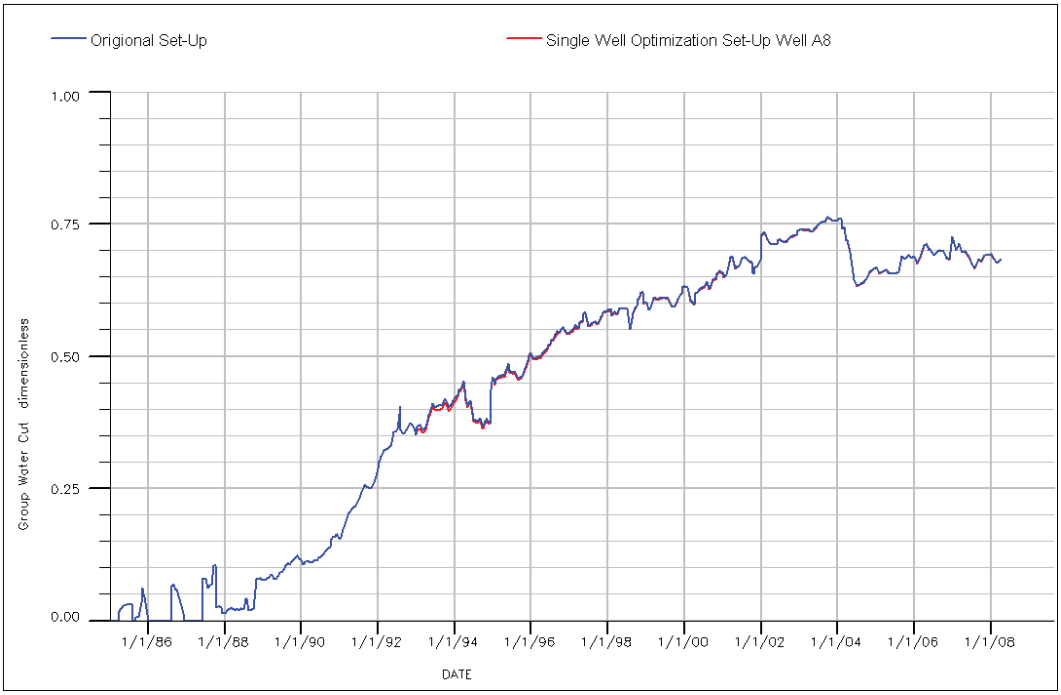

Figure 5-6: Comparison of the Water Cut for the entire field; blue line not optimized commingled production, red line optimized set-up using intelligent completion for well A8 only

5.4 Single Well Optimization Set-up Well A11

Figure 5-7 presents the water cut performance of the well for the optimized run and the original set-up. The coloring scheme is the same as in the previous sections above.

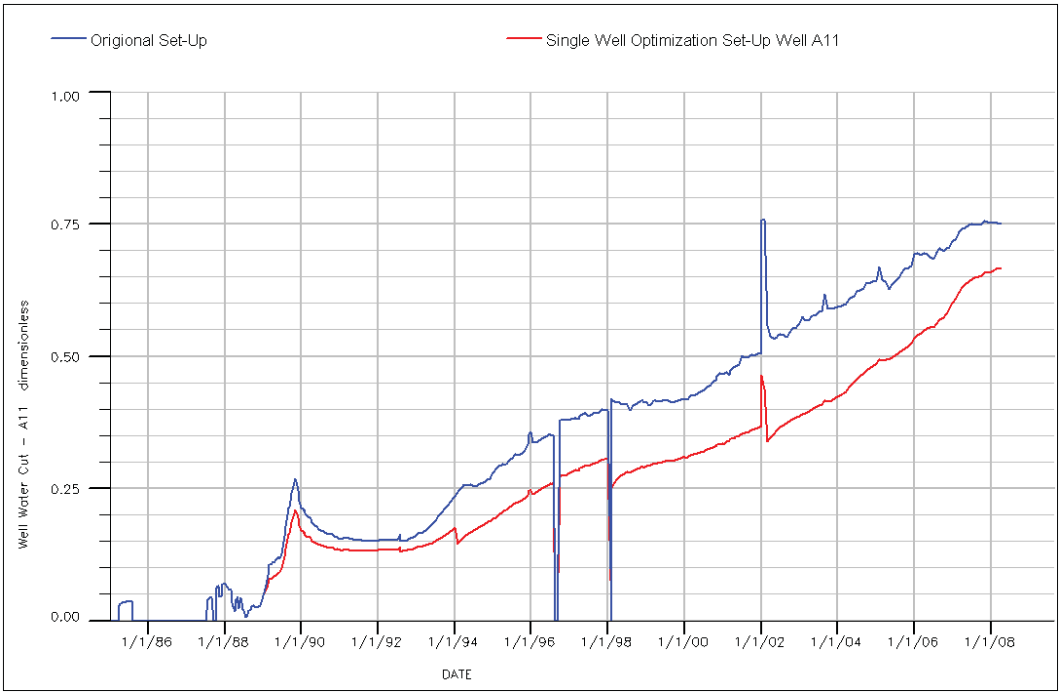

Figure 5-7: Comparison of the Water Cut for well A11; blue line not optimized commingled production, red line optimized set-up using intelligent completion

The reduction in the water production is again significant. Table 5-4 presents the calculated cumulative water production of the optimized run and the original set-up. The reduction is 1.2 MM STB of water equal to 40%

Table 5-4: Comparison of the cumulative water production for the original set-up with the optimized one for Well A11

Well A11 Water Production			
Original Set-Up [MM STB]	Optimized Set-Up [MM STB]	Absolute Difference [MM STB]	Relative Difference [%]
3.05	1.84	1.21	39.59

When comparing the entire field performance (Figure 5-8) the improvement is insignificant.

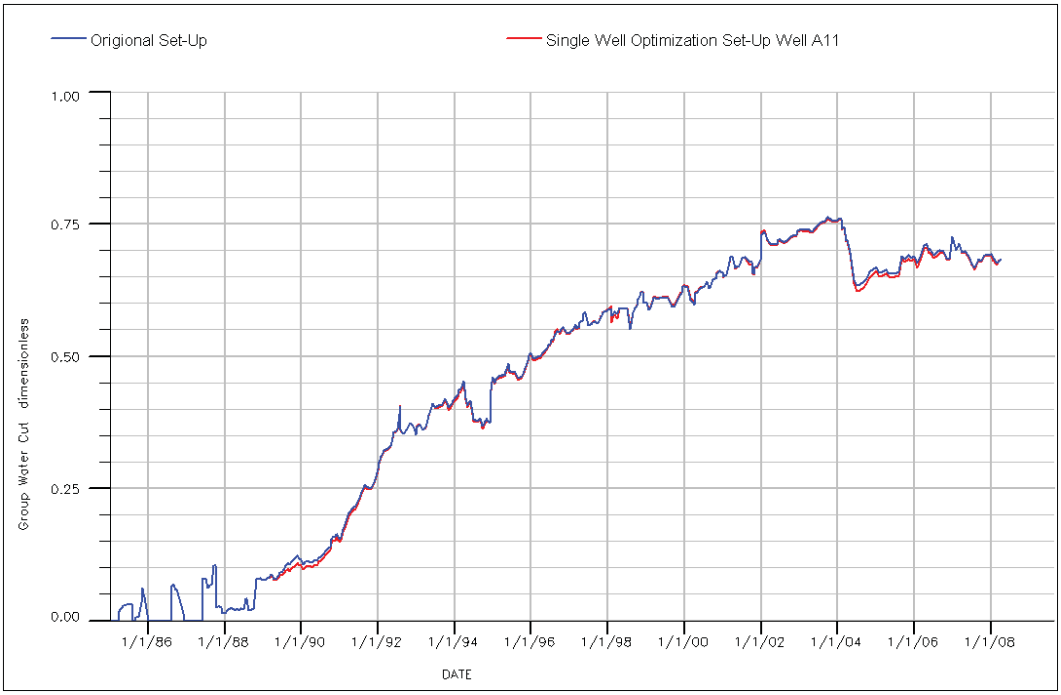

Figure 5-8: Comparison of the Water Cut for the entire field; blue line not optimized commingled production, red line optimized set-up using intelligent completion for well A11 only

5.5 Single Well Optimization Set-up Well A14

Figure 5-9 presents the water cut performance of the well for the optimized run and the original set-up. The coloring scheme is the same as in the previous sections above.

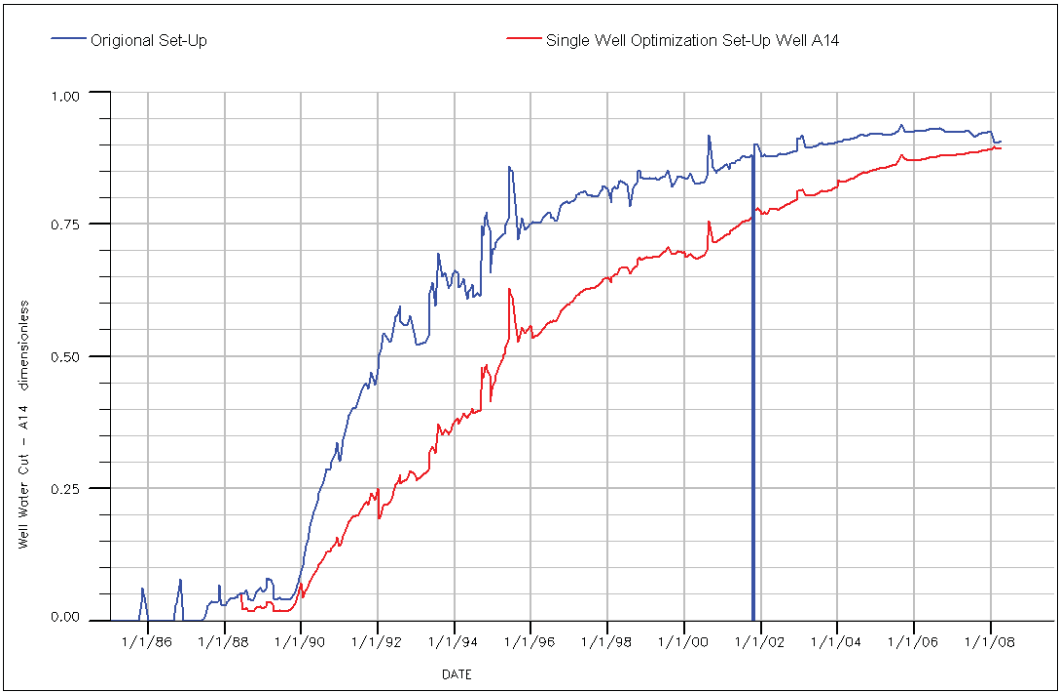

Figure 5-9: Comparison of the Water Cut for well A14; blue line not optimized commingled production, red line optimized set-up using intelligent completion

The reduction in the water production is again significant. Table 5-5 presents the calculated cumulative water production of the optimized run and the original set-up. The reduction is 2.0 MM STB of water equal to 54%

Table 5-5: Comparison of the cumulative water production for the original set-up with the optimized one for Well A14

Well A14 Water Production			
Original Set-Up [MM STB]	Optimized Set-Up [MM STB]	Absolute Difference [MM STB]	Relative Difference [%]
3.66	1.67	1.99	54.33

In case of the field performance (Figure 5-10) also in this run no substantial improvement could be observed. Again the improvement in the water production of well A14 is compensated by neighboring wells.

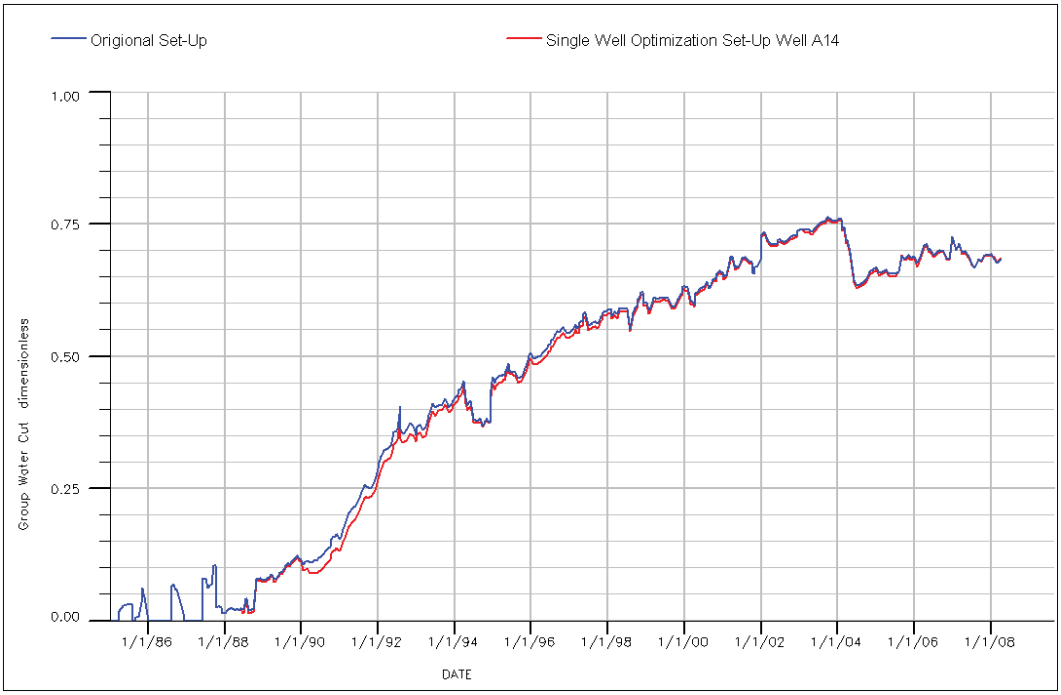

Figure 5-10: Comparison of the Water Cut for the entire field; blue line not optimized commingled production, red line optimized set-up using intelligent completion for well A14 only

5.6 Single Well Optimization Set-up Well A15

Figure 5-11 presents the water cut performance of the well for the optimized run for well A15 and the original set-up. The coloring scheme is the same as in the previous sections above.

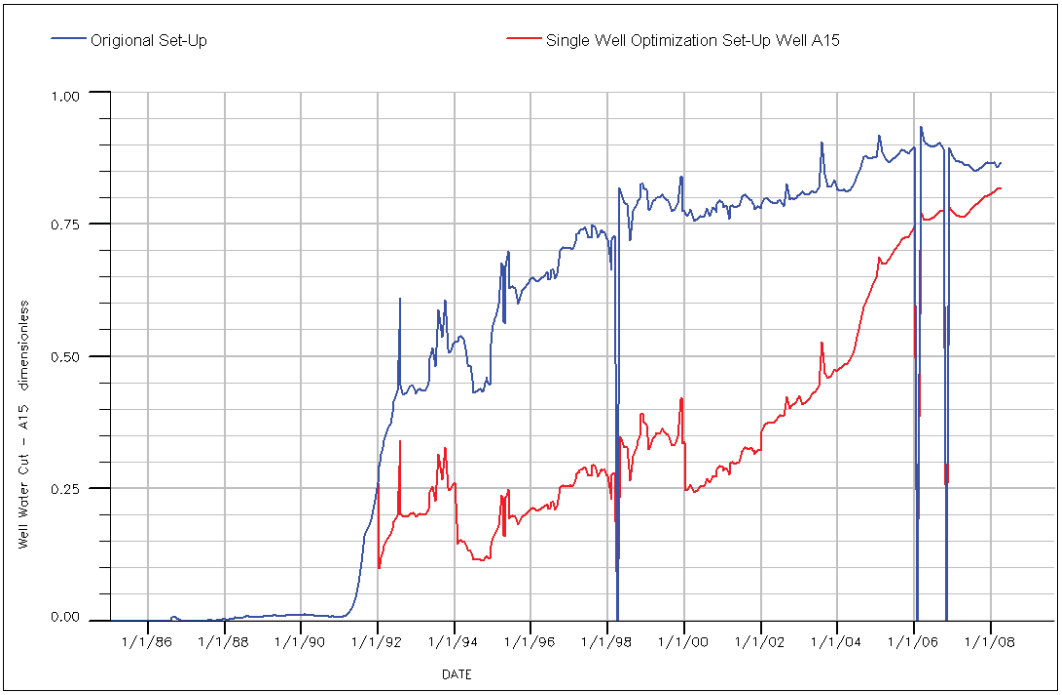

Figure 5-11: Comparison of the Water Cut for well A15; blue line not optimized commingled production, red line optimized set-up using intelligent completion

The reduction in the water production is again significant. Table 5-6 presents the calculated cumulative water production of the optimized run and the original set-up. The reduction is 0.8 MM STB of water equal to 76%.

Table 5-6: Comparison of the cumulative water production for the original set-up with the optimized one for Well A15

Well A15 Water Production			
Original Set-Up [MM STB]	Optimized Set-Up [MM STB]	Absolute Difference [MM STB]	Relative Difference [%]
3.22	0.76	2.46	76.27

In case of the field performance (Figure 5-12) also in this run no substantial improvement could be observed. Again the improvement in the water production of well A15 is compensated by neighboring wells

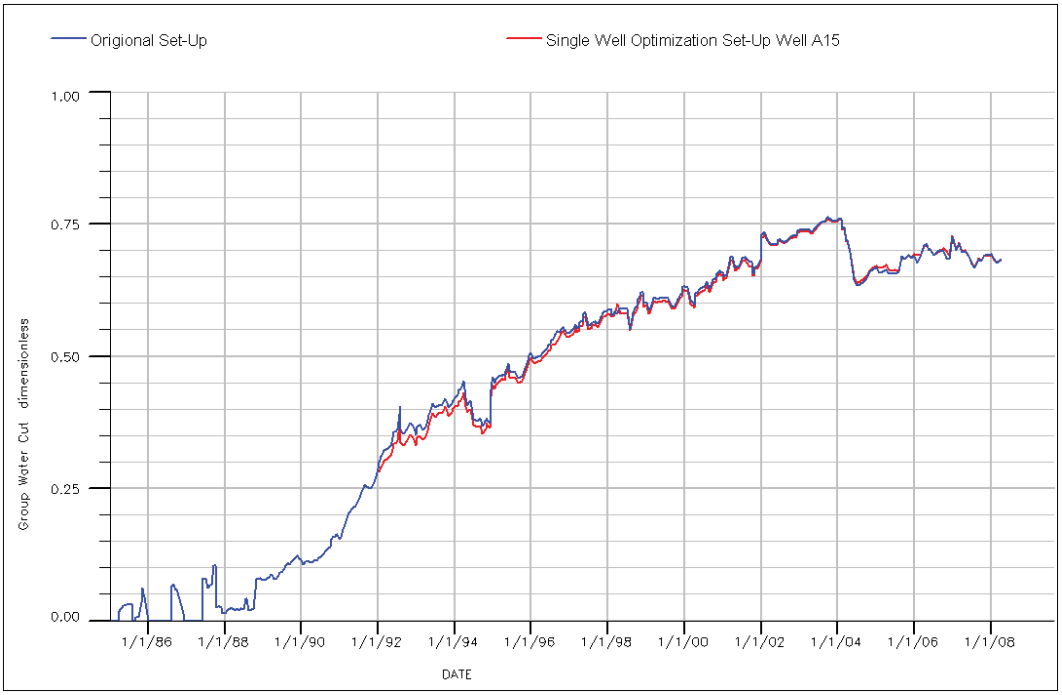

Figure 5-12: Comparison of the Water Cut for the entire field; blue line not optimized commingled production, red line optimized set-up using intelligent completion for well A15 only

5.7 Combined Optimization Set-Up

From the runs using intelligent completion for single wells only it becomes obvious that possible gain in the production performance of the individual wells are compensated by worse performing neighboring wells to a wide extend. Consequently a standalone optimization of the wells is questionable to deliver the desired results.

The run set-up presented in this section uses intelligent completion for all six wells mentioned above: A2, A3, A8, A11, A14 and A15. Figure 5-13 presents the water cut performance of the field. The blue line represents the water cut without intelligent completions; i.e. the original set-up, the history matched model. The wells are completed as the real wells in the field producing from the individual zones in a commingled way. The red line presents the result when intelligent completions are used. The flow efficiency of the individual perforations is changed over the run in order to minimize the water cut.

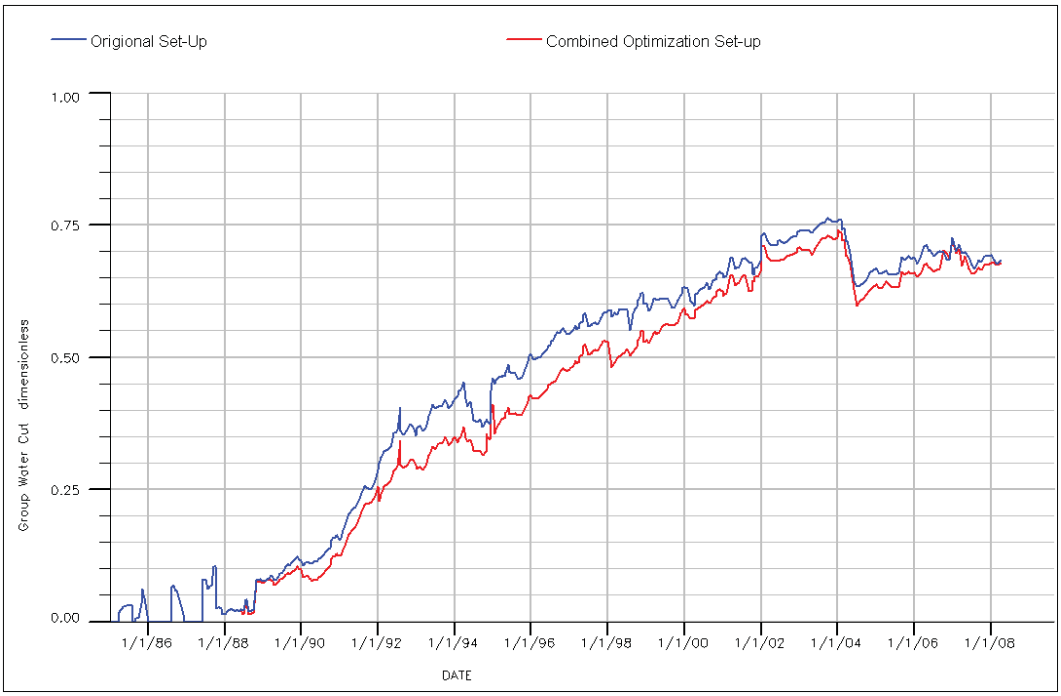

Figure 5-13: Comparison of the Water Cut for the entire field; blue line not optimized commingled production, red line optimized set-up using intelligent completion for wells A2, A3, A8, A11, A14 and A15

The overall improvement is significant. Table 5-7 presents the cumulative water production for the original set-up in comparison to the results obtained when intelligent completions are used for the six wells simultaneously.

Table 5-7: Water production comparison between original set-up and combined optimization set-up

Hakim South Water Production			
Original Set-Up [MM STB]	Optimized Set-Up [MM STB]	Absolute Difference [MM STB]	Relative Difference [%]
27.29	22.88	4.41	16.15

The reduction in the water production is 4.4 MM STB equal to 16%.

From the six runs using intelligent completion only for one individual well a theoretical gain in the field performance could be calculated. I.e. the reduction in the cumulative field water production for each of the six runs is summed up, leading to a reduction of 2.9 MM STB in the cumulative water production which equals 11%. This is considerable less than the reduction using intelligent completions for all six wells simultaneously; indicating again that the entire field should be considered when trying to optimize the production scheme for individual wells.

Table 5-8: Water production comparison between original set-up and theoretical sum of the six single well optimization set-ups

Hakim South Water Production			
Original Set-Up [MM STB]	Optimized Set-Up [MM STB]	Absolute Difference [MM STB]	Relative Difference [%]
27.29	24.35	2.94	10.77

Up to now only the water production values have been compared and an overall reduction of 16% could be achieved for the best performing set-up.

Figure 5-14: Comparison of the average field pressure; blue line original set-up, red line run using intelligent completion for the six wells simultaneously

Figure 5-14 presents the average field pressure versus time. The blue line is the pressure for the original set-up without using any intelligent completions. The red line is the field pressure when intelligent completions are used for the wells A2, A3, A8, A11, A14 and A15 simultaneously. From that Figure it becomes obvious that the reduced water production has a significant positive influence on the average reservoir pressure. In the later period of the field life the pressure is about 200 psi higher and would led to higher recovery of the field or less injection would be required to maintain the pressure.

5.8 Completion Optimization using TPPM

Abrahem, Heinemann and Mittermeir developed advanced tool to optimize the history matching process called target pressure and phase method (TPPM). A detailed work on this method is given in the Abraham's Dissertation[1].

The method determines flow efficiencies for individual perforations automatically to achieve desired production rates of individual wells; I.e. the inflow for a given well is optimized by applying flow efficiency multipliers for the perforations in order to produce exactly the target rates, both water and oil. If the method fails and the calculated water cut is still higher as the target then the method tries to reduce the water cut to the possible lowest value.

This option can be used to determine multipliers assuming intelligent completions automatically. When for the considered wells the target production is not the measured oil and water production but rather the measured oil production and zero water production TPPM tries for the well to reduced the water production to a minimum. I.e. for every time interval the flow efficiency factors for every perforation are calculated achieving the lowest water cut for the given well. By means of TPPM the optimum multipliers which have been worked out in multiple runs using ECLIPSE as presented in the previous sections could be determined by a single run automatically.

Figure 5-15, Figure 5-16, Figure 5-17, Figure 5-18 and Figure 5-19 present the automatically determined perforation status for the wells A2, A3, A8, A14 and A15, respectively. The pink color indicates when a peroration is open and blue when it is shut-in. The X-Axis presents the simulation time and the Y-Axis the individual layers. Note Layer 2 and 3 are the sealing anhydrites and consequently not perforated.

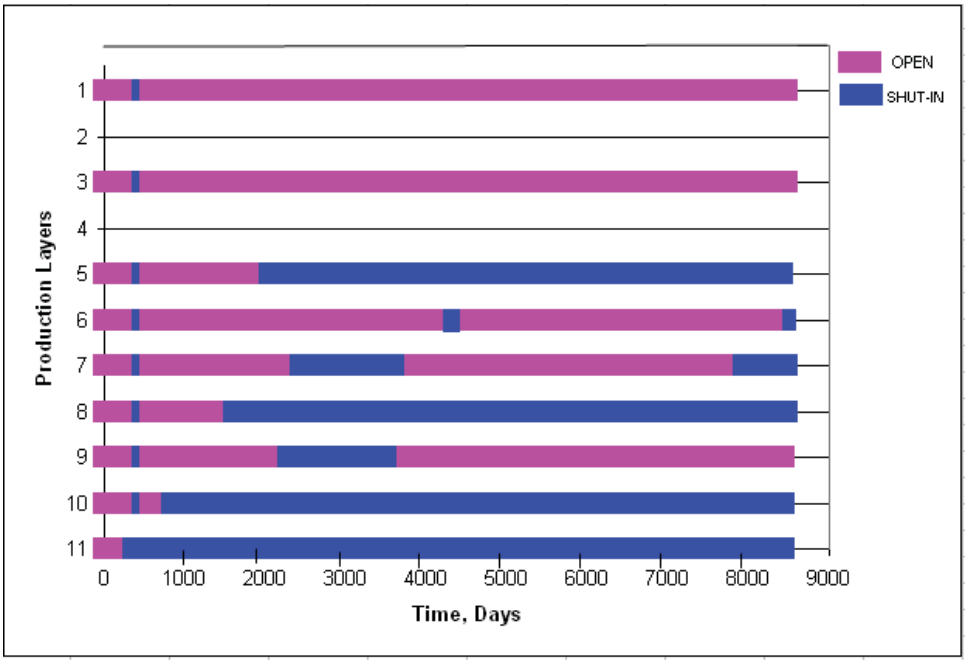

Figure 5-15: Automatically determined perforation status for well A2

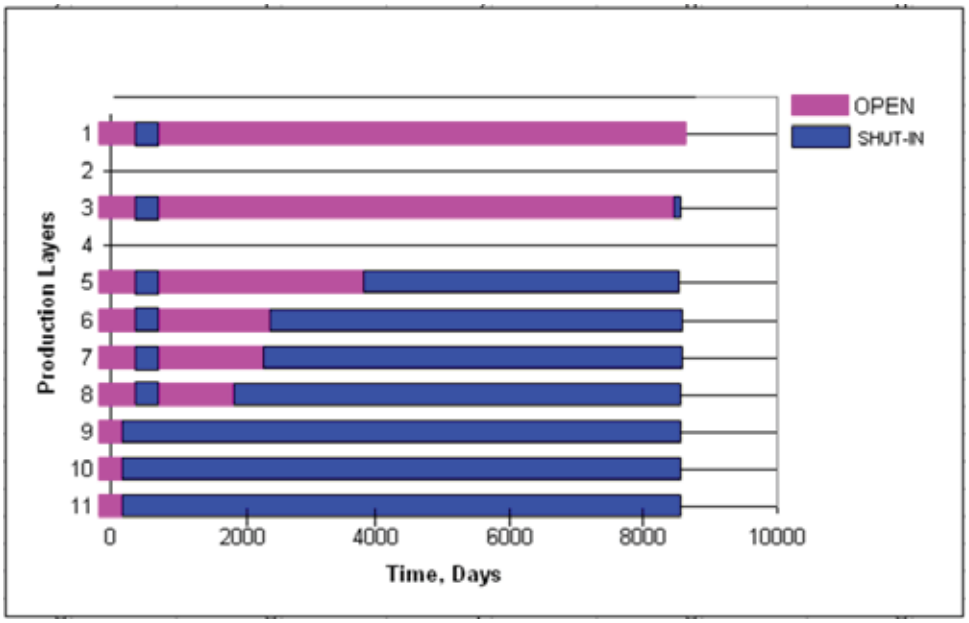

Figure 5-16: Automatically determined perforation status for well A3

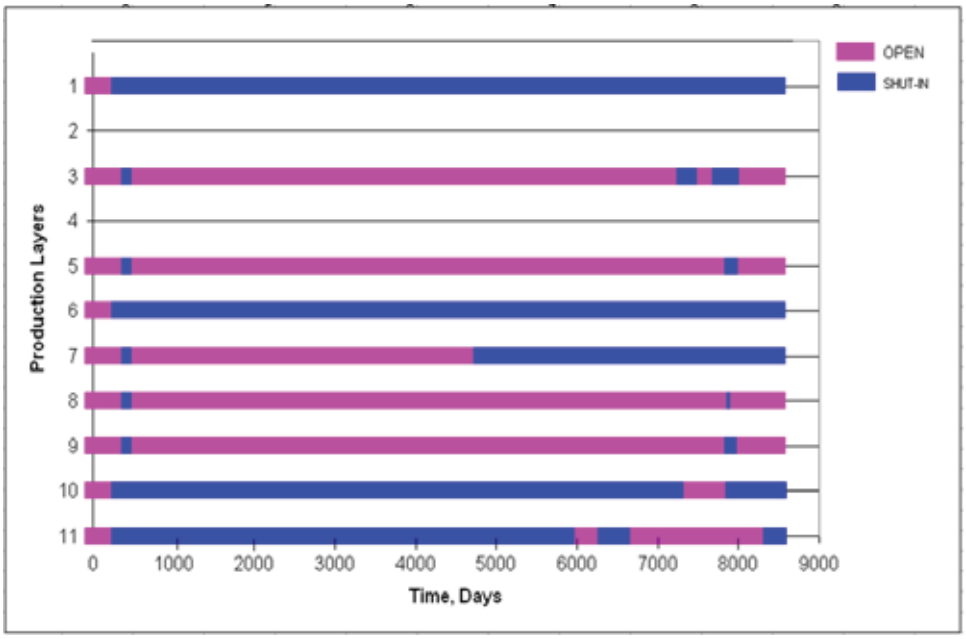

Figure 5-17: Automatically determined perforation status for well A8

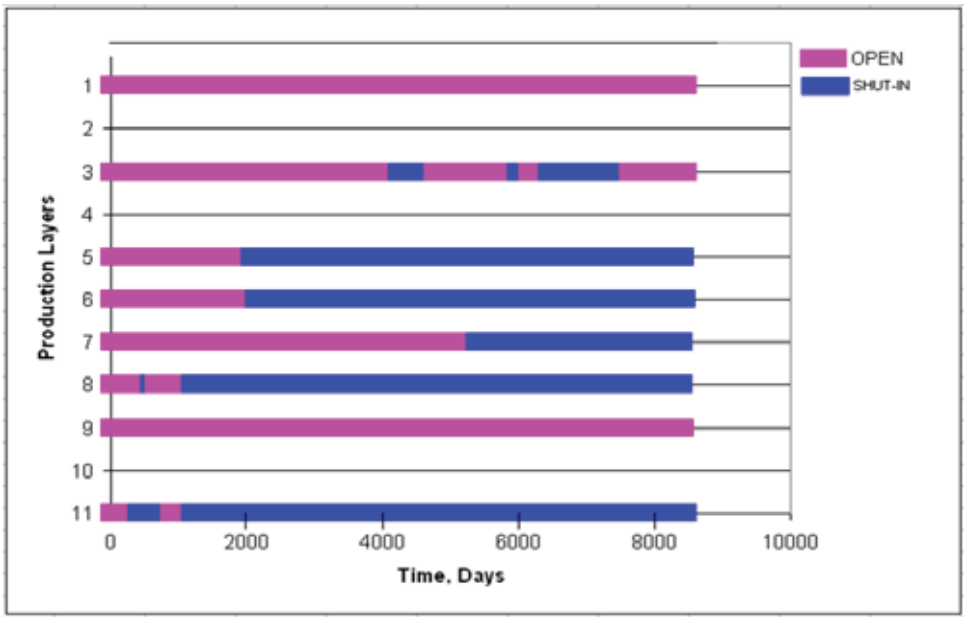

Figure 5-18: Automatically determined perforation status for well A14

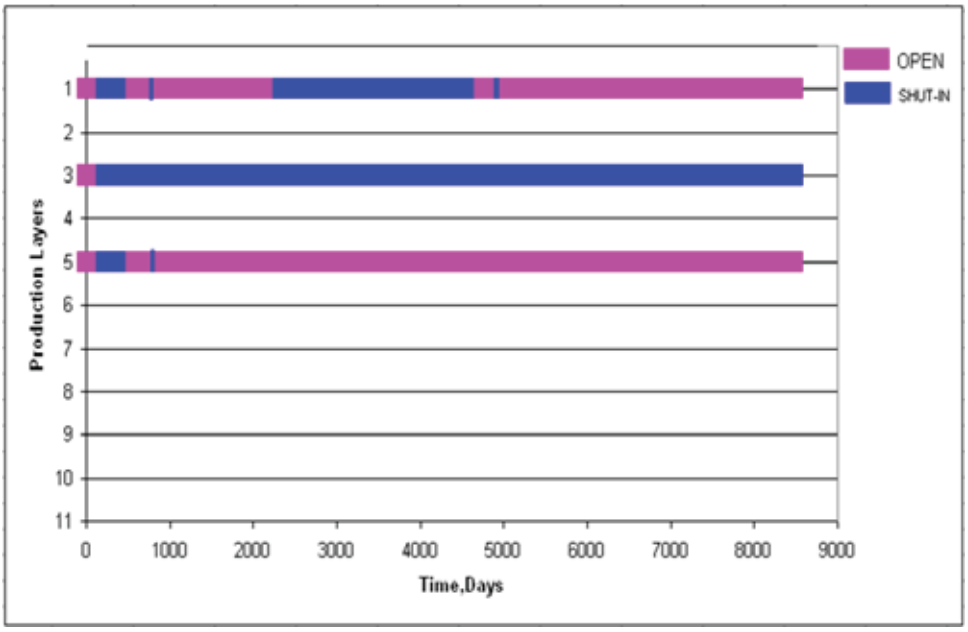

Figure 5-19: Automatically determined perforation status for well A15

The reduction in the water production in the TPPM run is presented in Table 5-9. The water production calculated when the target pressure and phase method is applied is reduced by 5.1 MM STB equal to 19%. These automatically calculated flow efficiency multipliers can be also transferred as ECLIPSE input; hence the method produces the WPIMULT keywords automatically.

Table 5-9: Water production comparison between original set-up and TPPM run

Hakim South Water Production			
Original Set-Up [MM STB]	TPPM Set-Up [MM STB]	Absolute Difference [MM STB]	Relative Difference [%]
27.29	22.16	5.13	18.8

TPPM turned out not only to produce better results in terms of perforation inflow optimization due to its automatism is by far more convenient and faster than the manual tuning of the ECLIPSE input. This benefit will increase with the size (number of wells to optimize and number of separated pools) of the field to optimize.

Chapter 6

6 Summary and Conclusions

A realistic dynamic reservoir model for the Hakim field was build. The work performed included the careful examination of the static geological model, the production history; gathering and quality check all PVT and SCAL data. The model was successfully history matched.

Based on the history matched model the benefits of intelligent well completion technologies have been assessed. This was done using ECLIPSE by means of manually introduced flow efficiency multipliers to optimize perforation inflow and consequently minimize water production form the field. In addition to that the newly developed Target Pressure and Phase Method was successfully applied to determine flow efficiency multipliers automatically.

Based on the work presented in this thesis the following conclusions can be drawn:

1. Intelligent Well Completion Techniques could be applied to Libyan fields improving reservoir production performance.
2. The applicability and possible advantages of such techniques should not be investigated on a well by well basis, but rather in the context of the full complexity of the field operations. Interaction of between wells close to each other should not be underestimated; i.e. the performance improvement of a certain well optimized in a standalone way can lead to a decreased performance of neighboring wells and the gain in the production might be compensated.
3. The goal of these operations is not solely to increase oil production and decrease the water-cut but additionally to improve the ultimate recovery of the considered field, too.

4. During the regulation of the perforation inflow rates it is essential to consider the influence on the sweep efficiency, too.
5. The target pressure and phase method (TPPM)[1] developed by Abrahem, Heinemann and Mittermeir seems to be an optimal method to define depletion based on Intelligent Well Completion Technology.

Chapter 7

7 Nomenclature

3D	=Three dimensions/dimensional
c	=Compressibility
μ	=Viscosibility, Pa.s/Pa
kr	=Relative permeability, fraction
p	=Pressure, psia
q	=Production of phase p, m 3 /s
rw	=Well radius, m
λ	=Mobility, 1/m 3 .Pa.s
μ	=Viscosity, Pa.s
ρ	=Mass density, kg/m 3
$\overline{\rho}$	=Mass density at standard conditions, kg/m 3
ϕ	=Porosity, fraction
γ	= specific gravity of fluid.
B	=Formation volume factor
S	=Saturation, fraction
WI	=Production index
RI	=Resistivity Index
DLE	=Differential Liberation Experiment
FVF	=Formation Volume Factor
GOR	=Gas Oil Ratio
WOC	=Water Oil Contact
BHP	=Bottomhole Pressure
rb	=reservoir barrel
STB	=Stock Tank Barrel

STO	=Stock Tank Oil
SCF	=Standard Cubic Feet
PLT	=Production Logging Tool
RFT	=Repeated Formation Tester
TPPM	=Target Pressure and Phase Method

Chapter 8

8 References

1. Abraham, F.A.S., 2009, “A New Approach to History Matching of Water Driven Oil Reservoirs”; Dissertation, May 2009

2. Ahlbrandt, T.S., 2001, The Sire Basin province of Libya–Sirte-Zelten total petroleum system: U.S. Geological Survey Bull. 2202-F, Washington, D.C., 33 p.

3. Adam Anderson, Integrations Intelligent well System with other Completion Technology.

4. Amado, L.C.N, Ganzer, L. And Heinemann, Z.E.: "Finite Volume Discretization of Fluid Flow Equations on General Perpendicular Bisection Grids ", Paper Presented at the 1994 fifth Intl. Forum on Reservoir Simulation, Muscat, Oman, Dec. 10-04

5. Aziz, K. and Settari, A.:Petroleum Réservoir Simulation, Applied Science Publishers, 1979.

6. Anderson, W., G.: “Wettability Literature Survey- Part 1: Rock/Oil/Brine Interactions and the Effects of Core Handling on Wettability,” paper SPE 13932, *JPT* (October 1986), 1125-1144.

7. Anderson, W., G.: “Wettability Literature Survey- Part 2: Wettability Measurement," *JPT* (Nov.1986) 1246-1262.

8. Anderson, W., G.: “Wettability Literature Survey- Part 3: “The Effects of Wettability on Electrical Properties of Porous Media," paper SPE 13934, *JPT* (December1986) 1371-1378.

9. Anderson, W., G.: “Wettability Literature Survey- Part 5: “The Effects of Wettability on Relative Permeability," paper SPE 16323, *JPT* (November 1987) 1453-1468.

10. Baker Hughes, Advantages of All-Electric Intelligent Well Completion Systems, June 18th 2008 - Galveston, Texas.

11. Brent Emerson, Optimizing Production through Expandable, Intelligent Multi Lateral Wells.

12. Craft and Hawkins, Applied Petroleum Reservoir Engineering, text book.

13. Craig, F.F: The Reservoir Engineering Aspects of Waterflooding, Monograph Series, SPE; Richardson, TX (1971) 3.

14. Cuiec, L.: " Rock/Crude-Oil Interactions and Wettability: An Attempt To Understand Their Interrelation," paper SPE 13211 presented at the 1984 SPE Annual Technical Conference and Exhibition, Houston, Texas, 16-19 September.

15. Carlos Glandt, Case Studies Team EPT-AWS "Smart Well Technology in Shell"

16. Dake, L.P.: The Practice of Reservoir Engineering, Elsevier, Amsterdam, 1994.

17. Donaldson, E.C., Thomas, R.D., and Lorenz, P.B.: "Wettability Determination and Its Effect on Recovery Efficiency," *SPEJ* (March 1969) 13-20.

18. Dr. Guy Vachon, Baker Oil Tools, Intelligent well systems advance toward maturity,

19. Farhad Ebadi, Mark Reynolds, Dr. David Davies, Prof. Patrick W.M.Orbett, Reservoir Management & Improved Recovery. Institute of Petroleum Engineering. Heriot-Watt University, Edinburgh U.K

20. Field Evaluation of Oil/Water Monitoring Devices for Commingled Production, Dennis Murphy, Process Specialist, Area Energy LLC, and Parviz Mendizadeh, Consultant, Production Technology.

21. Gant, P.L., Anderson, W.G.: "Core Cleaning for Restoration of Native Wettability," SPE Formation Evaluation (March 1988), 131-138.

22. Heinemann Z. E.: "Petroleum Recovery," study textbook series, Volume 3, Department Petroleum Engineering, Leoben, Austria, 2005.

23. Heinemann Z. E. ,Reservoir Simulation Part 1, April 2005.

24. Heinemann Oil GmbH: 3D Reservoir Characterization and Geologic Modeling and Reservoir Simulation Study South & North Hakim Fields

25. Hallett, D., 2002, Petroleum geology of Libya: Elsevier Science B.V., Amsterdam, The Netherlands, 503 pp.

26. Hassan S. Hassan, Petroleum Geology of Libya overview, Univ. of South Carolina

27. Iraj.Ershaghi, Overview of Intelligent Well Completion and Smart Well Technologies, University of Southern California PTTC Workshop March 27, 2003.

28. OMV, Simulation Study on North and South Hakim, 1989.

29. PHH Petroleum Consultants LTD: Reservoir Simulation Study North and South Hakim Fields, April 1994.

30. Patrick Schorn, President, Schlumberger Completions, Intelligently Using Intelligent Completions, JPT • APRIL 2008

31. Roohi, M., 1996, A geological view of source-reservoir relationships in the western Sirt Basin, *in* Salem, M.J., El-Hawat, A.S., and Sbeta, A.M. *eds*., Geology of the Sirt Basin, v. 2: Elsevier Science B.V., Amsterdam, The Netherlands, p. 323–336.

32. Rusk, D. C., 2001, Libya: Petroleum potential of the underexplored basin centers—A twenty-first-century challenge, *in* Downey, M.W, Threet, J.C., and Morgan, W.A., *eds.,* Petroleum provinces of the twenty-first century: American Assoc. Petroleum Geologists, Mem. 74, p. 429–452.

33. Stephen Dyer, Yasser El-Khazindar, Angel Reyes, Michael Huber, Ian Raw, and David Reed, Schlumberger, Intelligent completions for better reservoir management, Article Published Jan 5, 2009.

34. Timo Jokela, Intelligent Completions Current and Future Direction, Schlumberger Completions, June 2007.

35. T. Graf,SPE, S.P.Graf,SPE, P. Evbomoen,SPE and C. Vmadia,SPE, Schlumberger. "A Rigorous Well Model to Optimize Production from Intelligent Wells and Establish the Back-Allocation Algorithm" , SPE-99994,

36. Van Baak, J.H.(2004): "Multi-Zone flow allocation in smart wells" Msc thesis report TU Delft, Dept. of Geotechnology, Report nr.TA/PW/04-23

37. Wennekers, J.H.N., Wallace, F.K., and Abugares, Y.I., 1996, The geology and hydrocarbons of the Sirt Basin, a synopsis, *in* Salem, M.J., Mouzoughi, A.J., and Hammuda, O.S., *eds.*, Geology of Sirt Basin, v. 1: Elsevier Science B.V., Amsterdam, The Netherlands, p. 3–56.

38. Zueitina Oil Company: Reservoir Simulation Study South Hakim Field Concession NC74A, January 2000.

39. Zueitina Oil Company: Geological and Petrophysical Report, March 1998.